CANADIAN THESES

THÈSES CANADIENNES

NOTICE

The quality of this microfiche is heavily dependent upon the quality of the original thesis submitted for microfilming. Every effort has been made to ensure the highest quality of reproduction possible.

If pages are missing, contact the university which granted the degree.

Some pages may have indistinct print especially if the original pages were typed with a poor typewriter ribbon or if the university sent us an inferior photocopy.

Previously copyrighted materials (journal articles, published tests, etc.) are not filmed.

Reproduction in full or in part of this film is governed by the Canadian Copyright Act, R.S.C. 1970, c. C-30.

AVIS

La qualité de cette microfiche dépend grandement de la qualité de la thèse soumise au microfilmage. Nous avons tout fait pour assurer une qualité supérieure de reproduction.

S'il manque des pages, veuillez communiquer avec l'université qui a conféré le grade.

La qualité d'impression de certaines pages peut laisser à désirer, surtout si les pages originales ont été dactylographiées à l'aide d'un ruban usé ou si l'université nous a fait parvenir une photocopie de qualité inférieure.

Les documents qui font déjà l'objet d'un droit d'auteur (articles de revue, examens publiés, etc.) ne sont pas microfilmés.

La reproduction, même partielle, de ce microfilm est soumise à la Loi canadienne sur le droit d'auteur, SRC 1970, c. C-30.

THIS DISSERTATION HAS BEEN MICROFILMED EXACTLY AS RECEIVED

LA THÈSE A ÉTÉ MICROFILMÉE TELLE QUE NOUS L'AVONS REÇUE

Experimental Investigations on Shallow Strip Anchor Plates in Sand

Mustafa Abumengel

A Thesis

in

The Department

of

Civil Engineering

Presented in Partial Fulfillment of the Requirements
for the Degree of Master of Engineering at
Concordia University
Montréal, Québec, Canada

March, 1987

ISBN 0-315-35556-5

Abstract

Experimental Investigations
on Shallow Strip Anchor Plates in Sand

Mustafa Abumengel

This thesis presents the experimental results on shallow strip anchors in sand. The objective of this investigation is to study the effect of anchor's inclination, embedment ratio, and size on its load-displacement behaviour.

Model anchors of different sizes were tested at various depths of embedment and inclination angles vary from 0 to 90 degrees with respect to the vertical. The tests were proceeded by applying the pull out forces at a constant rate of displacement.

It was found that the ultimate pullout capacity increases with the increase in angle of inclination, embedment ratio, and height of the anchor plate. The test results were compared well with the theoretical model proposed by Foriero (1985) for anchor inclination at angles ranging from 0 to 60 degrees with respect to the vertical, where as for a 90 degree inclination, the present test results show fair agreement with the theory proposed by Meyerhof (1973) and Neely et. al. (1973).

The present test results were also compared with the other available theories where a conclusion can be drawn.

ACKNOWLEDGEMENTS

The author wishes to express his most sincere appreciation and gratitude to Dr. A.M. Hanna, the supervisor of this thesis for his valuable guidance, suggestions, and encouragement throughout this work.

The assistance of all the technicians in the Civil Engineering Department is gratefully acknowledged.

The continuous encouragement and untiring moral support of my mother, my girlfriend Debby, and my best friend M. Abukhader are greatly appreciated.

The author is grateful to the National Science and Engineering Council of Canada for the financial assistance.

I dedicate this thesis to the memory of my brothers Mahmod and Mehdi.

TABLE OF CONTENTS

NOTATIONS

D	Depth of anchor plate from ground surface to the top of the plate
H	Height of anchor plate
B	Width of anchor plate
A	Area of anchor plate
h	Height of retaining wall
α_v	Load inclination with respect to the vertical axis
e_{max}	Maximum voids ratio
e_{min}	Minimum voids ratio
e	Voids ratio of soil deposit
E_p	Passive force on retaining wall
G	Specific gravity of solid particles
K_b, K_c	Uplift coefficients for shallow anchors
K_p	Passive earth pressure coefficient
$K_{p\gamma}$	Passive earth pressure coefficient due to weight component
K_s	Coefficient of punching shear resistance
K_{pr}	Passive earth pressure coefficient for rough wall
K_{ar}	Active earth pressure coefficient for rough wall
P_s	Side friction resistance
Q_u	Ultimate pull-out capacity

R.D Relative density

γ Initial unit weight of sand

ϕ Angle of shearing resistance of soil

δ Average mobilized angle of shearing resistance on the assumed friction planes

LIST OF FIGURES

LIST OF TABLES

CHAPTER I

INTRODUCTION

Anchors or buried structures, form an important component of many civil engineering projects. These structures are usually subjected to pullout forces.

The resistance of soil subjected to compression is reasonably well understood, while soil resistance to uplift is still uncertain.

Anchors have been widely used to support structures such as anchored bulkheads, sheet piles, wherein the anchors are subjected to horizontal pullout forces (Figure 1.1-a). Anchors may be subjected to vertical pullout forces mainly due to a horizontal load above the ground level resulting from wind loading; tension in cables spanning between towers, or any other similar external loading. There are some other cases where anchors could be subjected to inclined pullout forces as in suspension bridge cables and cable roofs (Fig. 1.1-b).

Anchors are also used to support floating equipment in shallow and deep water. Anchors may be used singly or in groups which depend upon the magnitude of applied loads, the ground conditions and details of the structure. Size and type of anchors vary greatly where they could be made of steel plates, deadman block, piles, injections etc. (see figures 1.1-c, 1.1-d).

At present still there is no reliable method for determining uplift resistance of soil anchor plates. The recommendations contained in the civil engineering code of practice are based on classical passive retaining wall theory which are valid only for anchor plates at shallow depths. The development of a dependable method requires understanding of the relative importance of the many variables associated with pullout resistance of soil

anchors. In accordance with this need, this experimental investigation is undertaken to study the effect of the important variables on the anchor capacity. The variables considered are: anchor's depth of embedment, inclination and size, and corroborate the results of this study via comparison with published data as well as laboratory testing of a small scale anchor plate.

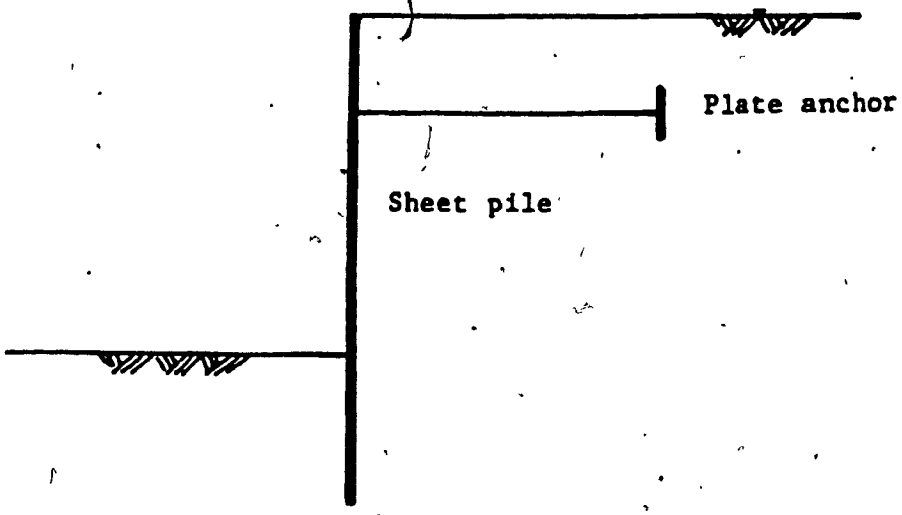

(a) Vertical anchors subjected to horizontal pullout force

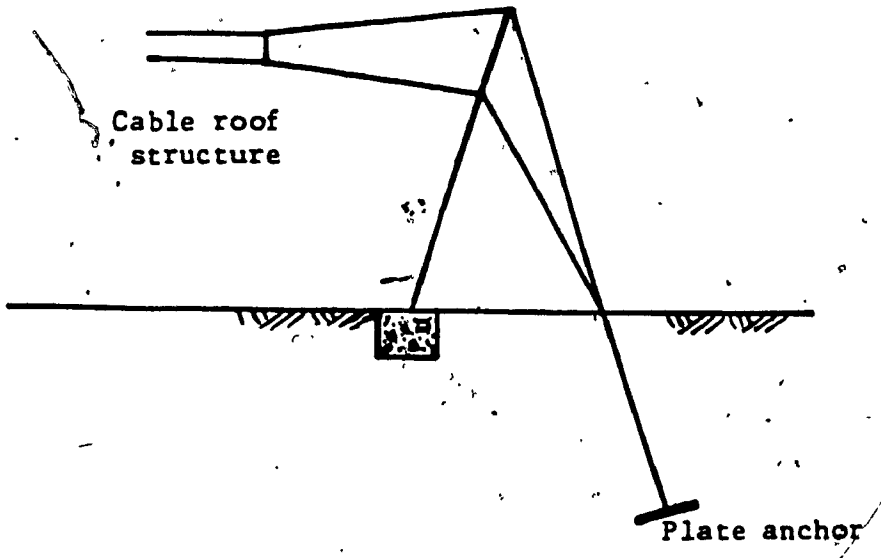

(b) Inclined anchor subjected to inclined pullout force.

Figure 1.1: Types of anchor plates

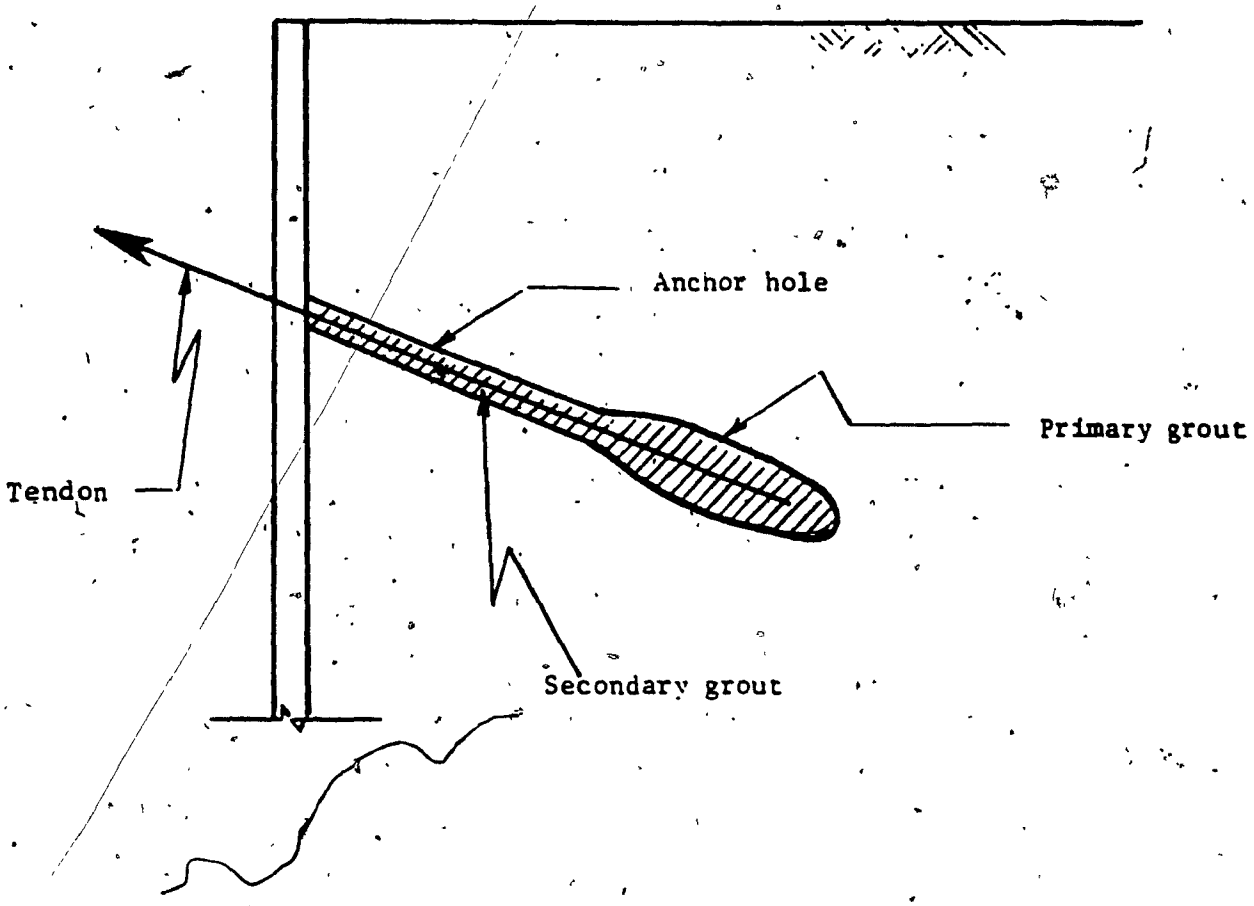

Figure 1.1-c: Ground anchor

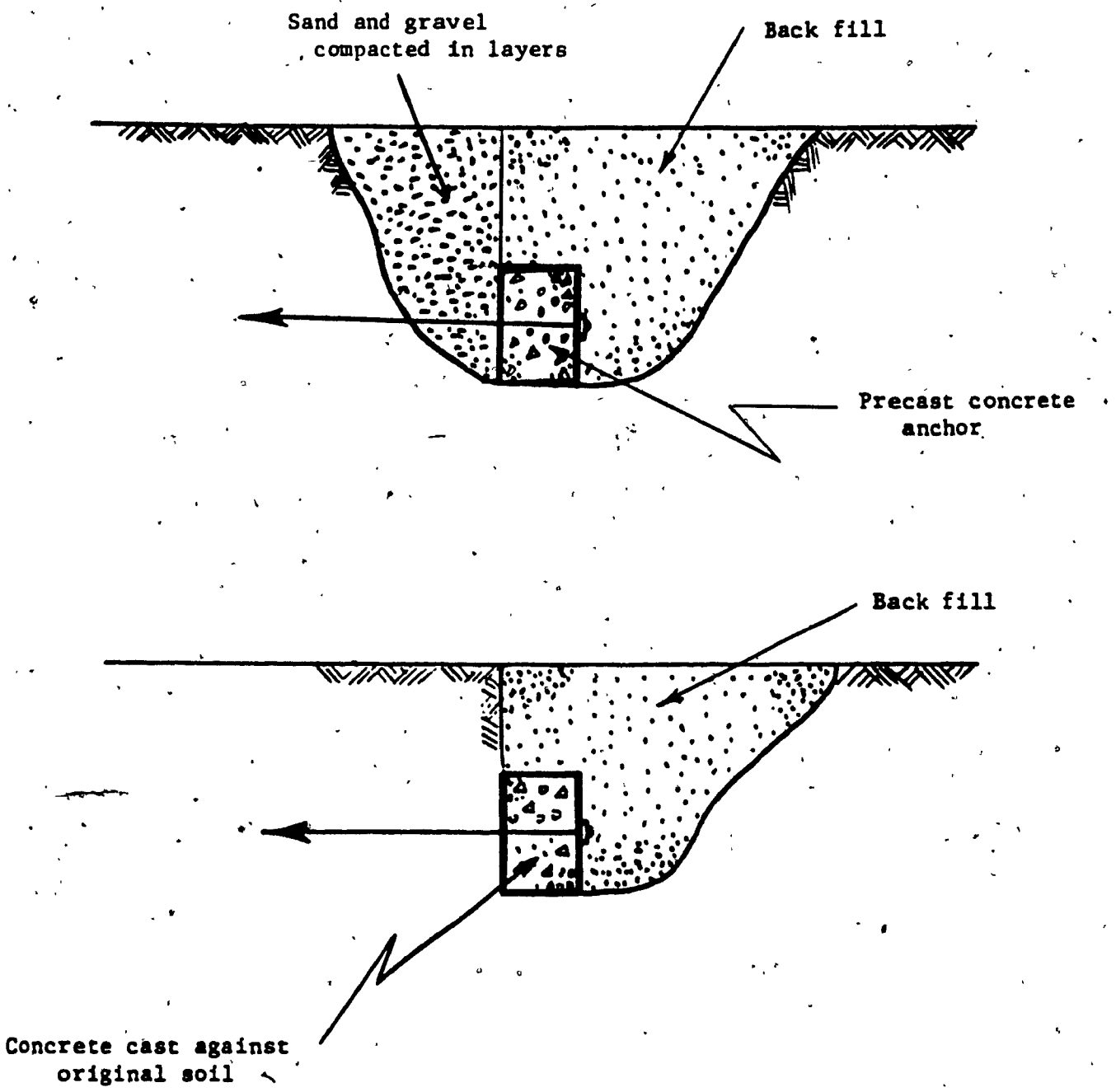

Figure 1.1-d: Concrete block anchors

CHAPTER II

LITERATURE REVIEW

Buchholz (1930), was first to carry out model tests to investigate the behaviour of anchorages in sand, however, his study was limited to vertical steel anchorage plates subjected to horizontal loading.

Buchholz has found that the critical embedment ratio is the ratio beyond which the failure pattern does not reach the soil surface, he defined this ratio as H/h = 7.0, where (H) is the depth from the soil surface to the bottom edge of the anchor, and (h) is the height of the anchor plate, he also found that the results obtained from slightly dampened sand did not vary significantly from those obtained from completely dry sand in identical conditions (Figures 2.1-a, 2.1-b) show some of his test results.

Terzaghi (1943), evaluated the resistance of vertical anchors, assuming passive and active pressure to be developed in front of and behind the anchor plate respectively. This approach was adopted in the British civil engineering code of practice.

Referring to Figure 2.2-a, 2.2-b, Terzaghi suggested that the net resistance of a vertical anchor is

$$Q_u = P_p - P_a \qquad (1)$$

where:

P_p = the passive pressure trust in front of the anchor

P_a = the active pressure trust on the back of the anchor

P_p/unit width = $0.5\ \gamma K_{p_r} H^2$

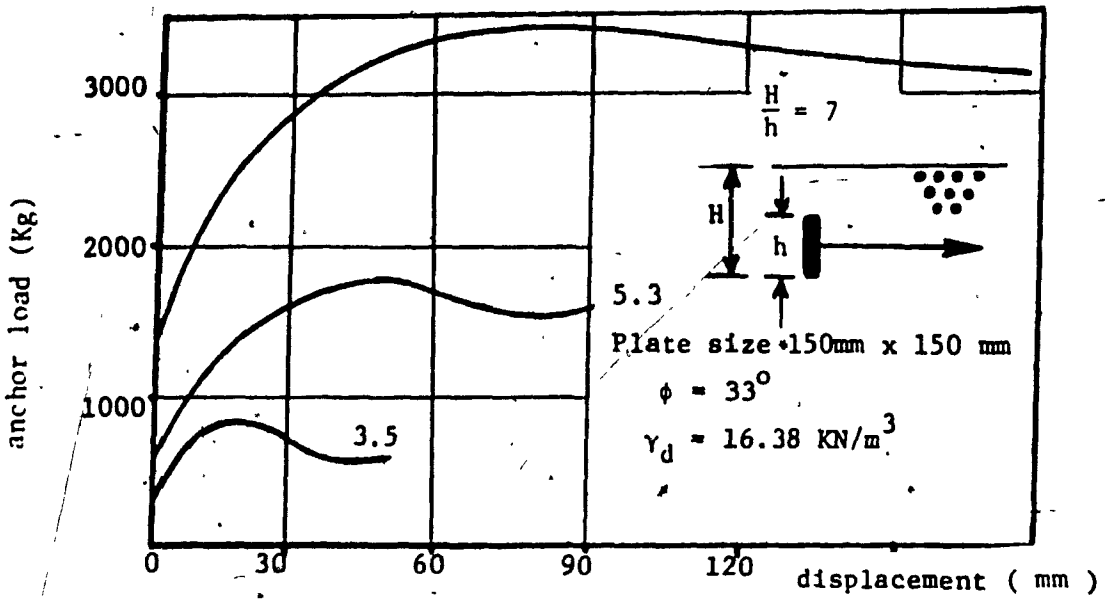

Figure 2.1-a: Typical load displacement curves for 150mm square anchor (Buchholz-1930)

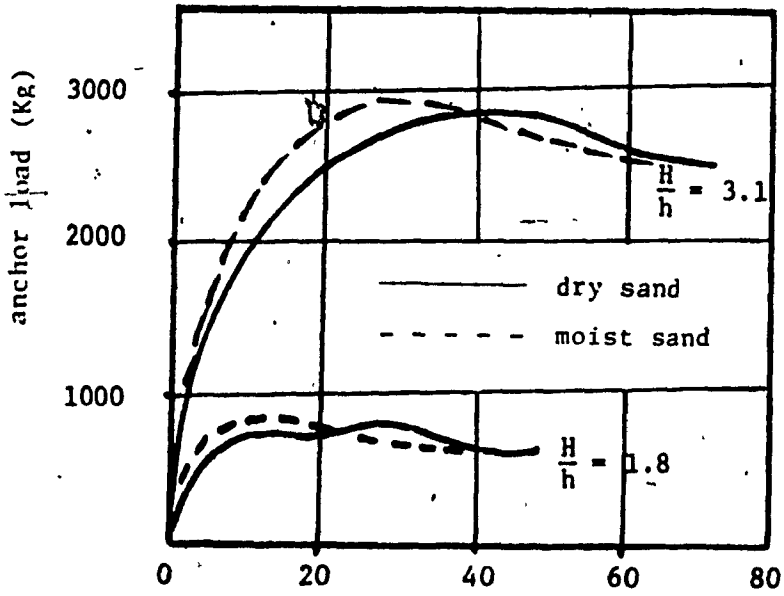

Figure 2.1-b: Typical load displacement curves for 300 mm square anchor (Buchholz-1930)

P_a/unit width = $0.5\ \gamma K_{ar} H^2$

K_{Pr}, K_{ar} is the passive and active earth pressure coefficients for rough wall.

$$K_{Pr} = \frac{\cos^2 \phi}{[1 - \sqrt{(\frac{\sin(\phi + \delta)\sin\phi}{\cos\delta})}]^2}$$

$$K_{ar} = \frac{\cos^2 \phi}{[1 + \sqrt{(\frac{\sin(\phi + \delta)\sin\phi}{\cos\delta})}]^2}$$

where:

ϕ = angle of internal resistance

δ = angle of wall friction

γ = unit weight of the soil

If wall friction was considered in conjunction with plane surfaces of failure, extremely high values of (K_{P_r}) will be obtained, especially in case of high (ϕ) values Tschebotarioff (1962).

Terzaghi also stated that the full angle of wall friction used for determining (K_{P_r}) can only be mobilized if the anchor has sufficient dead weight to balance the upward component of the resistance or otherwise restrained from moving upwards. Since only a fraction of (δ) is normally mobilized due to the relatively small weight of the wall,

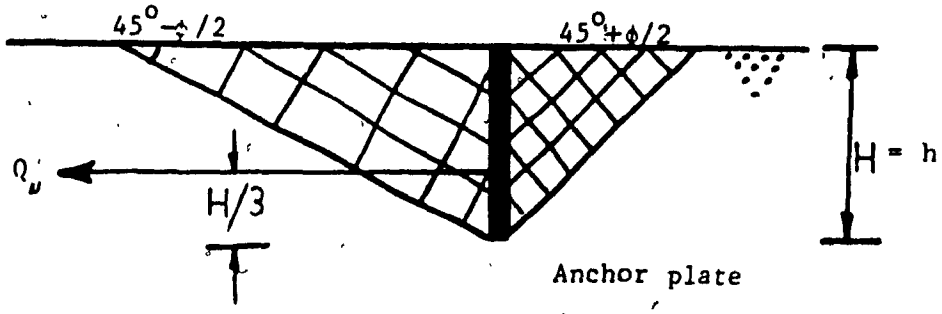

Figure 2.2-a: Shear pattern in sand adjoining an anchor wall (Terzaghi 1943)

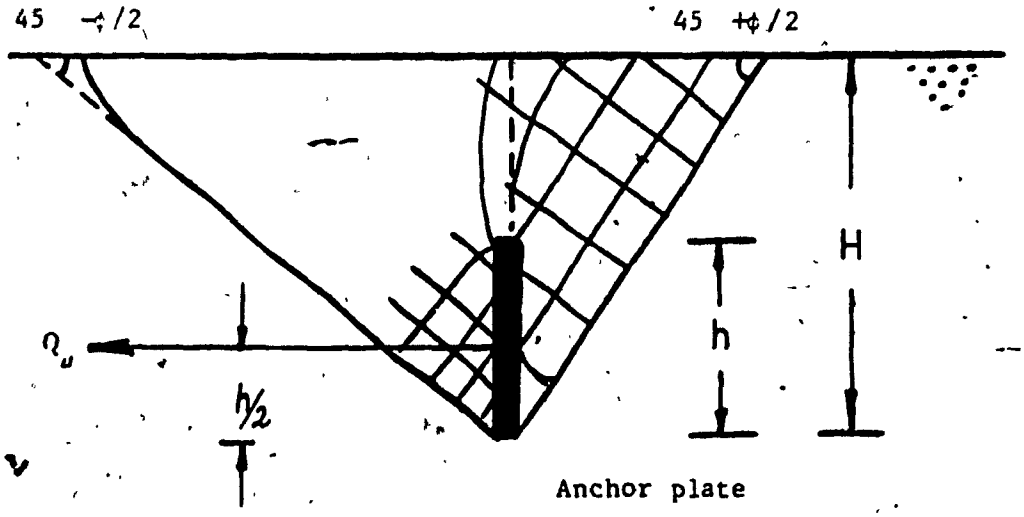

Figure 2.2-b: Shear pattern in sand adjoining an anchor wall whose upper edge is below the surface of the sand (Terzaghi 1943)

Terzaghi assumed that:

$\delta = 0$ degrees

$$K_{Ps} = \frac{\cos^2 \phi}{(1 - \sin\phi)^2} = \tan^2 (45 + \frac{\phi}{2})$$

$$K_{as} = \frac{\cos^2 \phi}{(1 + \sin \phi)^2} = \tan^2 (45 - \frac{\phi}{2})$$

In case of isolated anchor plate Terzaghi suggested that an additional side shear resistance on the side faces of the wedge of soil which the anchor tends to push out, should be included. The sides of the wedge are assumed to form parallel to the tie rod as shown in Figure 2.3.

Hence equation #1 becomes

$$Q_u = (P_p - P_s) - P_a$$

P_s is the side shear resistance.

For cohesionless soils the pressure over the side face of the wedge ($P_s/2$)

$$= \int_0^H K_a \gamma z (H - z) \tan (45 + \frac{\phi}{2}) dz$$

$$= K_a \gamma \tan (45 + \frac{\phi}{2}) \int_0^H (H . z - z^2) dz$$

$$= K_a \gamma \tan (45 + \frac{\phi}{2}) [\frac{H . z^2}{2} - \frac{z^3}{3}]_0^H$$

$$= K_a \gamma \tan (45 + \frac{\phi}{2}) \frac{H^3}{6}$$

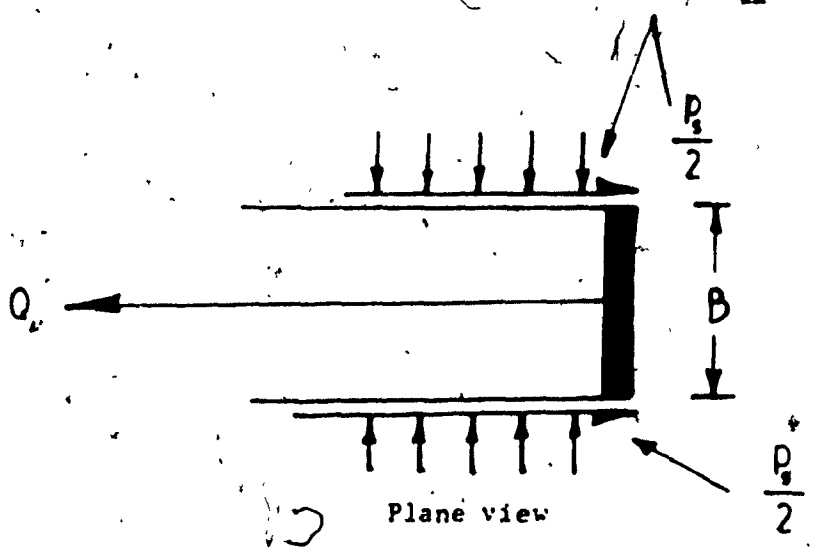

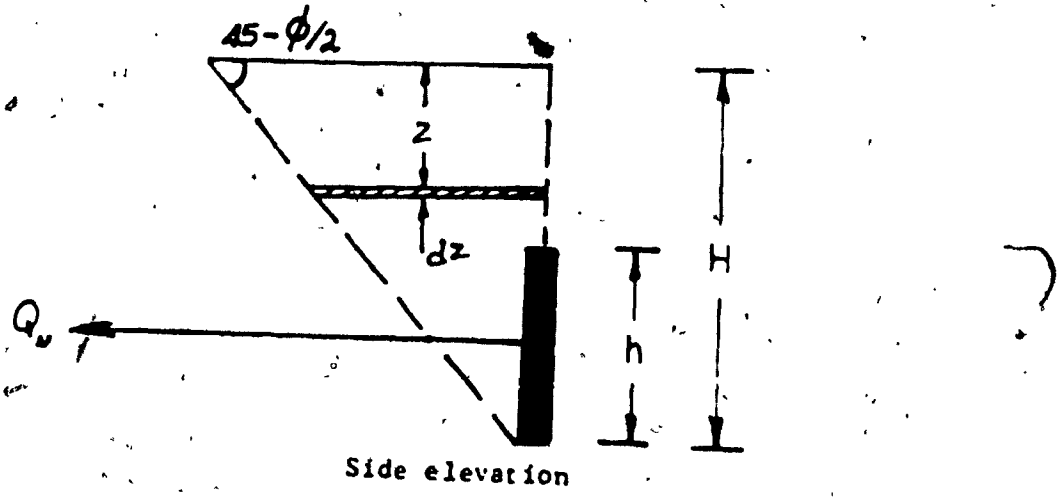

Figure 2.3: Side shear resistance for single anchor plate

Therefore side shear resistance for both sides of soil wedge

$$P_s = 2\,[K_a \gamma \tan (45 + \frac{\phi}{2}) \cdot \frac{H^3}{6}] \tan \phi$$

$$P_s = K_a \gamma \tan (45 + \frac{\phi}{2}) \cdot \frac{H^3}{6}] \cdot \tan \phi \cdot \frac{H^3}{3}$$

Hueckel (1957), carried out large number of tests on vertical and inclined anchor plates buried in sand at an embedment ratio H/h = 2. He included in his research program tests on single square anchors made of different materials (hence different surface roughness) where he found that the surface roughness of plate anchors has no essential influence on the value of the ultimate resistance. Also he found that the ultimate resistance of inclined plates having the rod kept in horizontal direction is smaller than that of verical ones, regardless of their direction of inclination. Some of his test results are shown in Figures 2.4 and 2.5.

Meyerhof (1973), extended his theory of uplift resistance (Meyerhof and Adams 1968), to calculate the ultimate resistance of inclined anchors (Fig. 2.6) in c-ϕ soils. The vertical uplift resistance was given by:

$$Q_u = 2cH + 2P_p \sin \delta + W_o \qquad (1)$$

where:

P_p = the passive earth pressure inclined at average angle (δ) acting downward on a vertical plane through the footing and the soil above it.

By taking the normal component of P_p then

$$P_p \cos \delta = 1/2\, \gamma H^2 K_p$$

by substituting in equation number (1) gives:

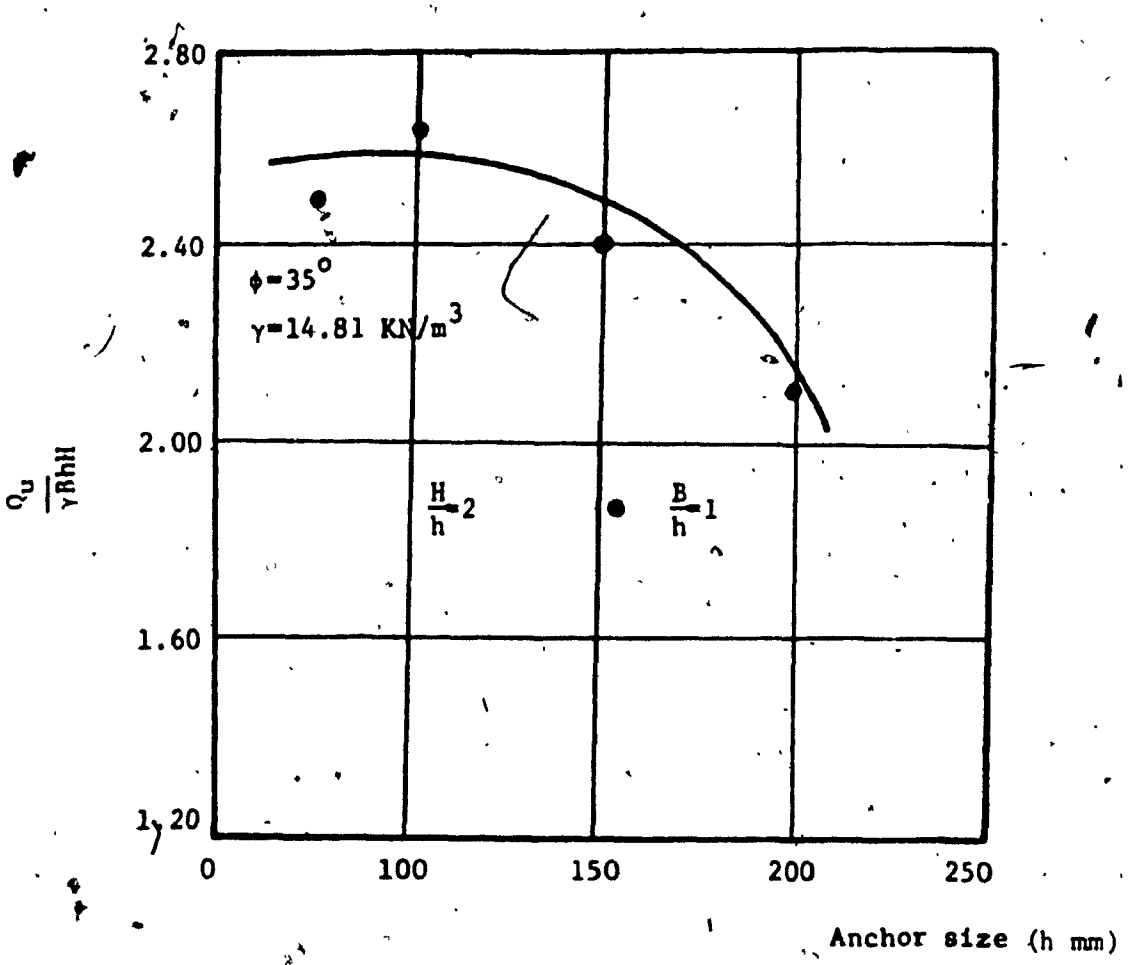

Figure 2.4: Hueckel's test results (1957)

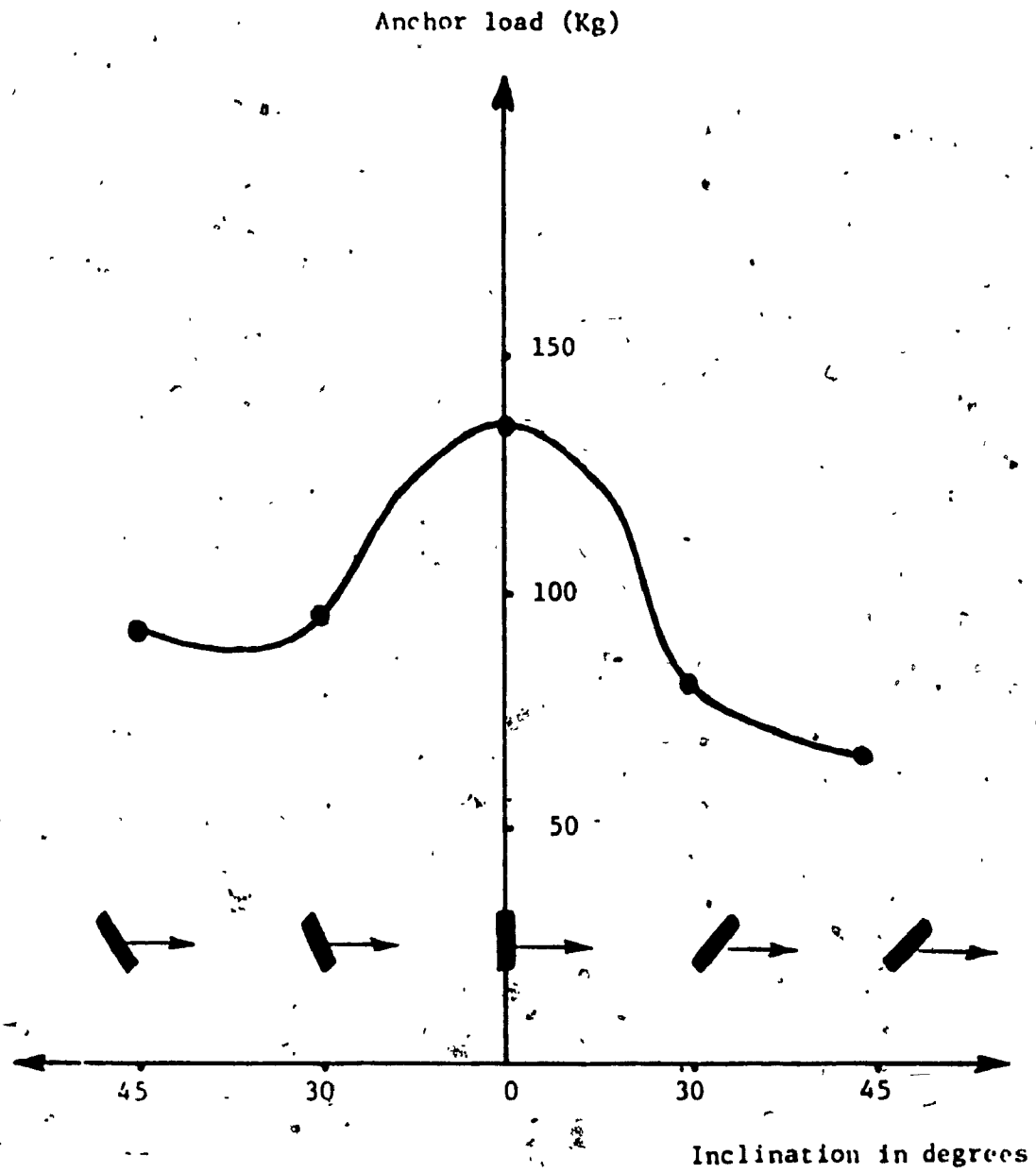

Figure 2.5: Comparison of anchor loads upon plates of various inclinations (Hueckel, 1957)

$$Q_u = 2cH + \gamma H^2 Kp \tan \delta + W_o \qquad (2)$$

Meyerhof found that when an inclined anchor is loaded to failure a similar soil mass of roughly truncated pyramidal shape is displaced upwards, for shallow anchors, a general shear failure was assumed to occur when the failure pattern reaches the soil surface (Figure 2.7-a).

Therefore, as for vertical uplift the ultimate resistance of shallow inclined anchors may be expressed by:

$$Q_u = \left(\frac{cK_cH}{h.} + \frac{\gamma H^2 K_b}{2h}\right) A + W_0 \cos \alpha B \qquad (3)$$

where:

A - area of anchor

α = inclination angle with respect to the vertical

K_b, K_c = uplift coefficients for shallow anchors

h = height of anchor

W_o = weight of anchor and soil mass vertically above the anchor base

In case of shallow strip anchors the coefficients K_b, K_c can be determined from the earth pressure coefficients. For an inclined wall (Caquot and Kerisel 1949).

As a particular case of vertical anchor in sand α_v = 90 degrees.

Equation (1) was given as:

$$Q_u/\text{unit width} = 1/2\ \gamma H^2 K_b$$

For a given angle of shearing resistance (ϕ), values of (K_b) increase as the load

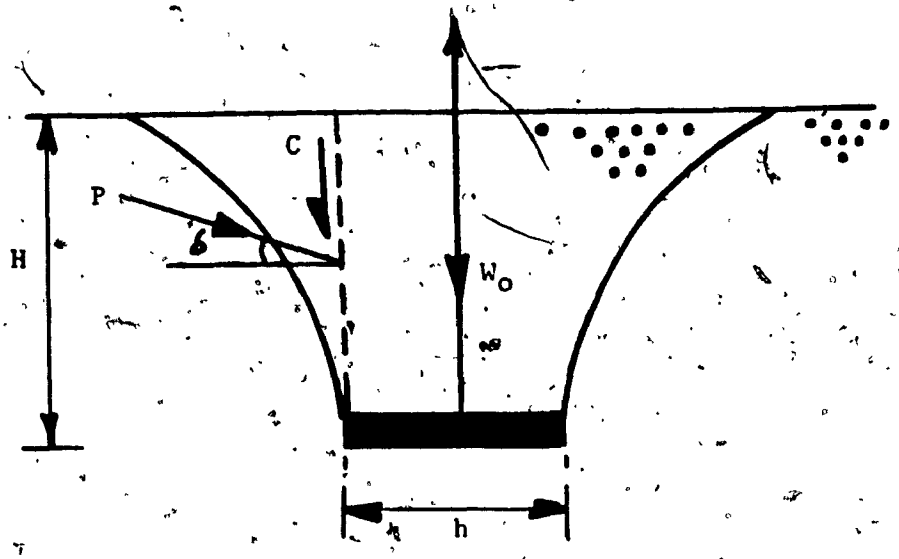

Figure 2.6: Failure of soil above a strip footing under uplift load (Meyerhof and Adams 1968)

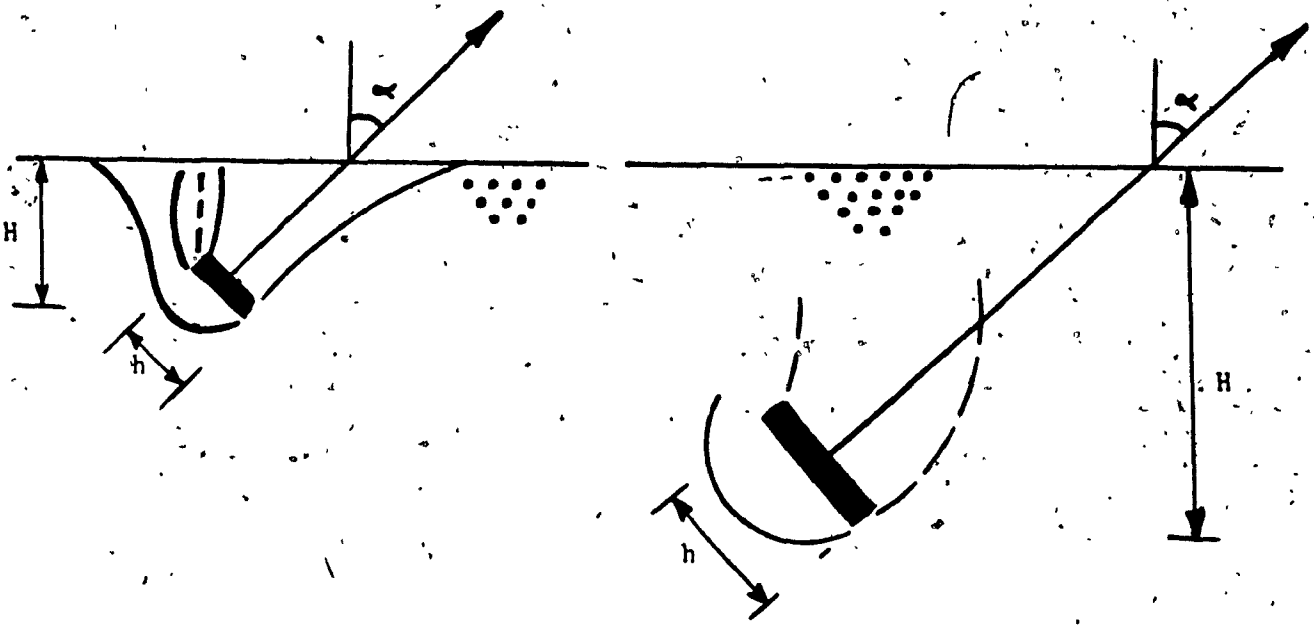

a/ - shallow anchor

b - deep anchor

Figure 2.7: Failure patterns of inclined anchors (Meyorhof 1973)

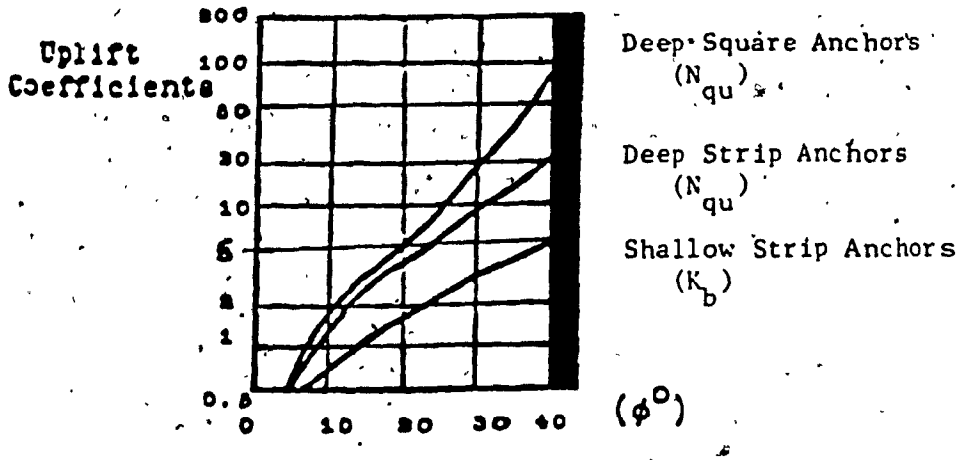

Figure 2.8-a: Uplift coefficients for vertical anchor (Meyerhof 1973)

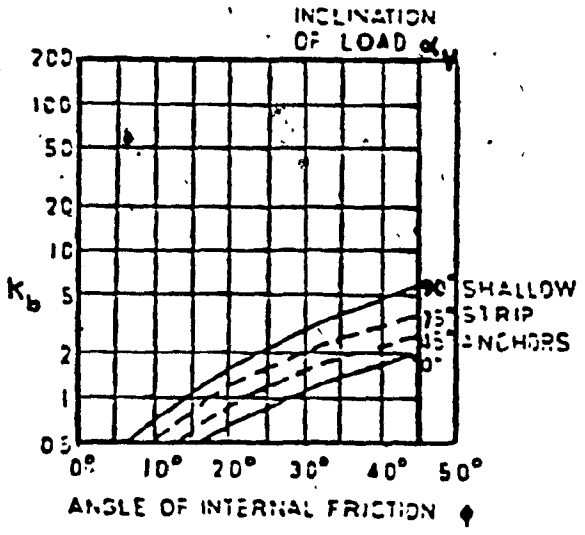

Figure 2.8-b: Theoretical uplift coefficients for anchors (Meyerhof 1973)

inclination (α_v) increases with respect to the vertical (Fig. 2.8-b). In case of deep anchors a local shear failure takes place (Figure 2.7-b). Meyerhof and Adams (1968) showed that for horizontal anchors the critical embedment ratio $(H/h)_{cr}$, where the failure pattern fails to reach the surface is about (4) for loose sand and clay and about (8) for dense sand. Meyerhof, also observed that the critical depth tends to decrease with the increase of load inclination. For deep continuous inclined anchors (Fig. 2.7-b), Meyerhof (1973) found that:

$$Q_u = (cN_{cu} + \gamma H N_{q_u})\, A + W_a \cos \alpha_v$$

N_{cu}, N_{q_u} are the uplift coefficients for deep anchors. For deep vertical strip anchor in cohesionless soil:

$$Q_u/\text{unit width} = \gamma (H - \frac{h}{2}) h N_{q_u}$$

values of N_{q_u} for various internal resistance angles are shown in Figure 2.8-a.

Neely, Stuart and Graham (1973), conducted experimental and theoritical investigations to study the behaviour of shallow vertical anchor plate in sand. In this investigation the depth of embedment was examined, rigid steel plates with polished surfaces were used to give a contact friction angle $\delta = 21°$. The plate anchor was 6 mm (0.236 inch) thick and 51 mm (2 inch) high with widths ranging from 51mm (2 inch), to 255mm (10.0 inch). The tests were carried out at various width/height and embedment ratios, the results were expressed in terms of dimensionless coefficient

$M_{\gamma q} = Q_u/\gamma B h^2$ are shown in Figure (2.9-a). To examine the effect of width/height ratio on the ultimate resistance of single anchor and assuming that the effect of side shear would be negligible for plates with $B/h \geq 5$. Neely et. al. also used the term shape factor such that $S_f = M_{\gamma q}$ (single anchor)/$M_{\gamma q}$ (wide anchor of B/h = 5). Variations of

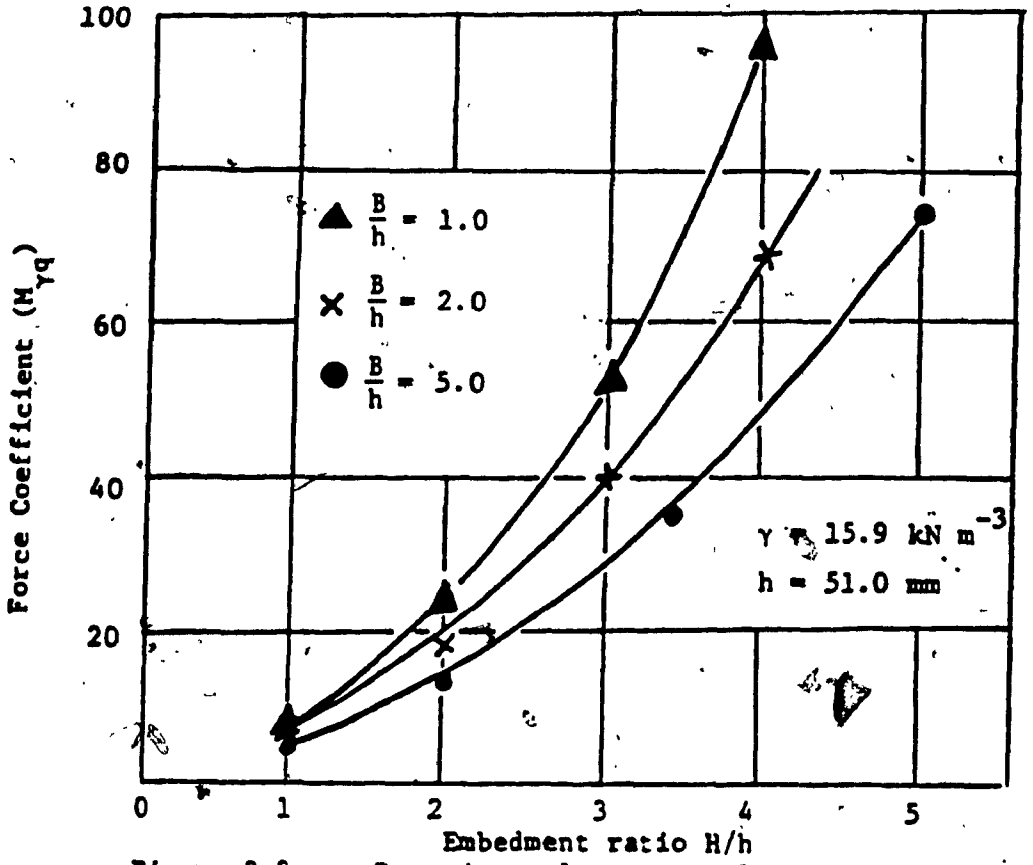

Figure 2.9-a: Experimental test results after Neely et.al. (1973)

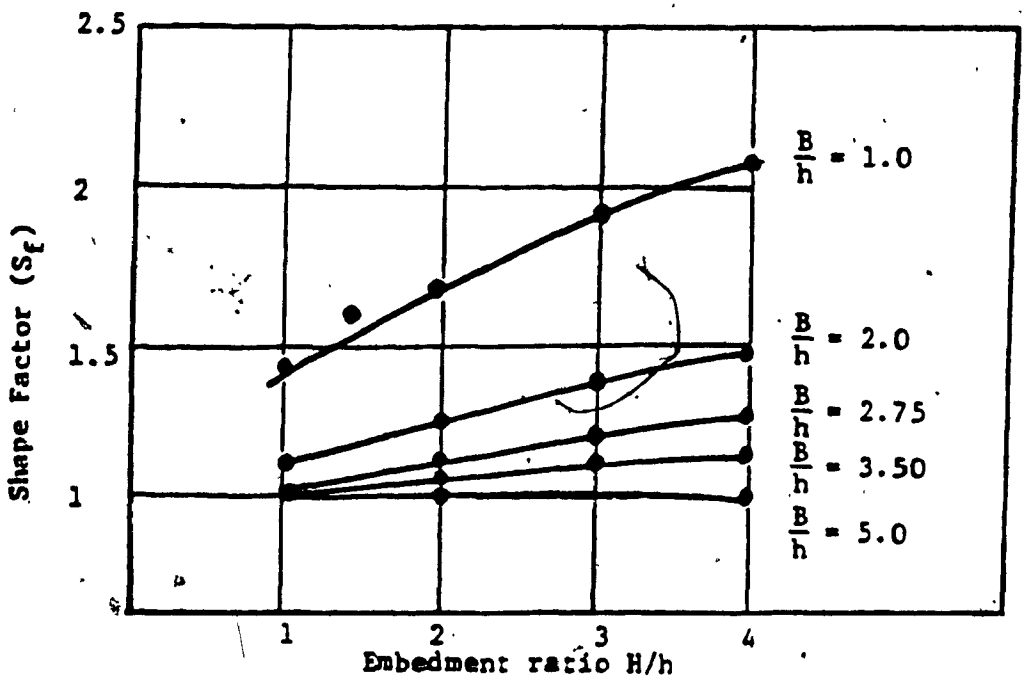

Figure 2.9-b: Variation of shape factor for 51mm rigid anchor plates (Neely et.al.1973)

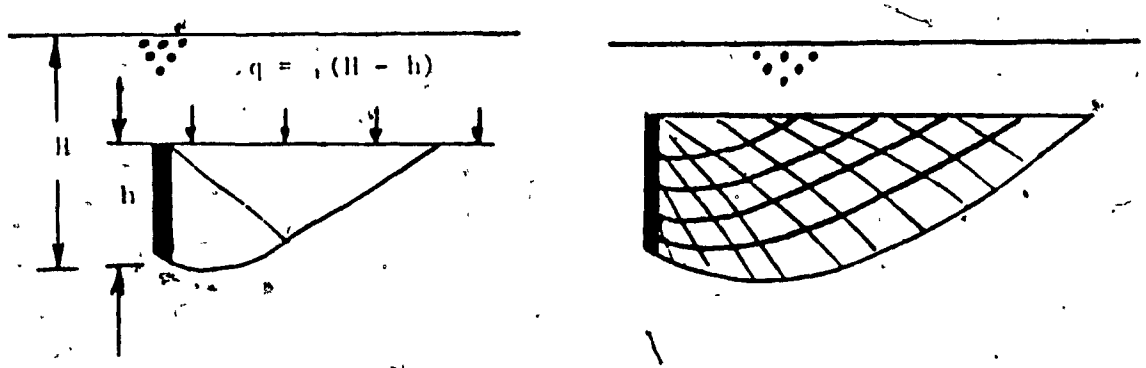

(a) Surcharge method

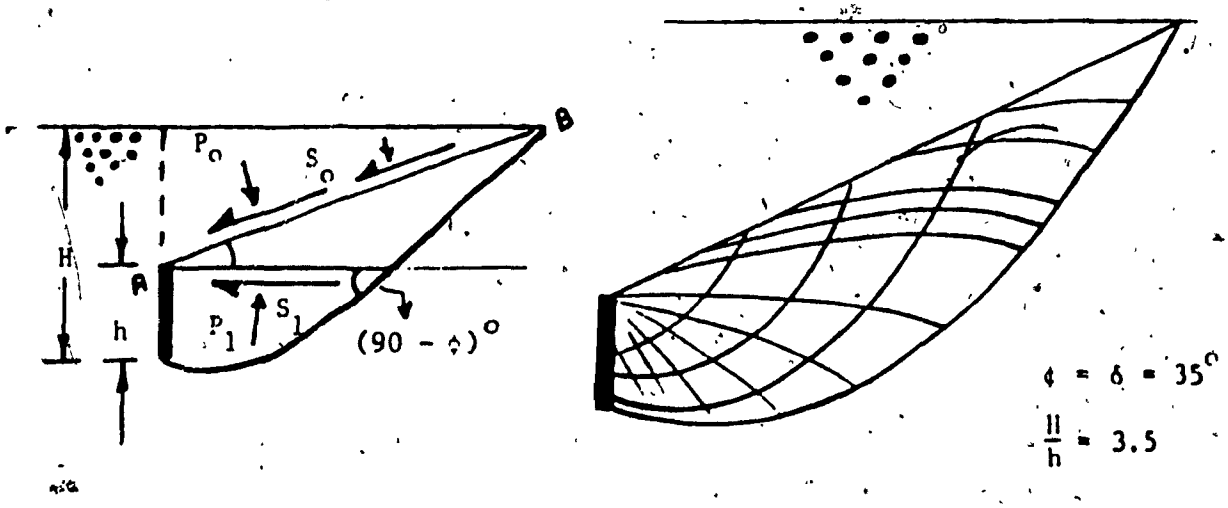

(b) Equivalent free surface method

Figure 2.10: Typical stress characteristic solution (Neely et. al. 1973)

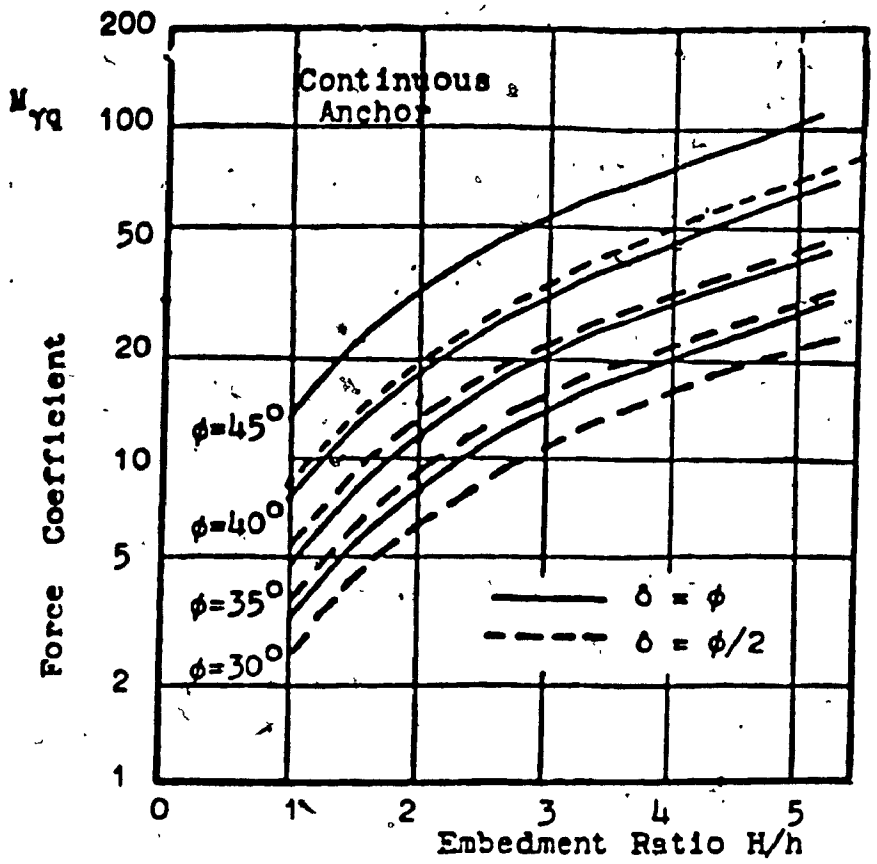

(a) Surcharge Method

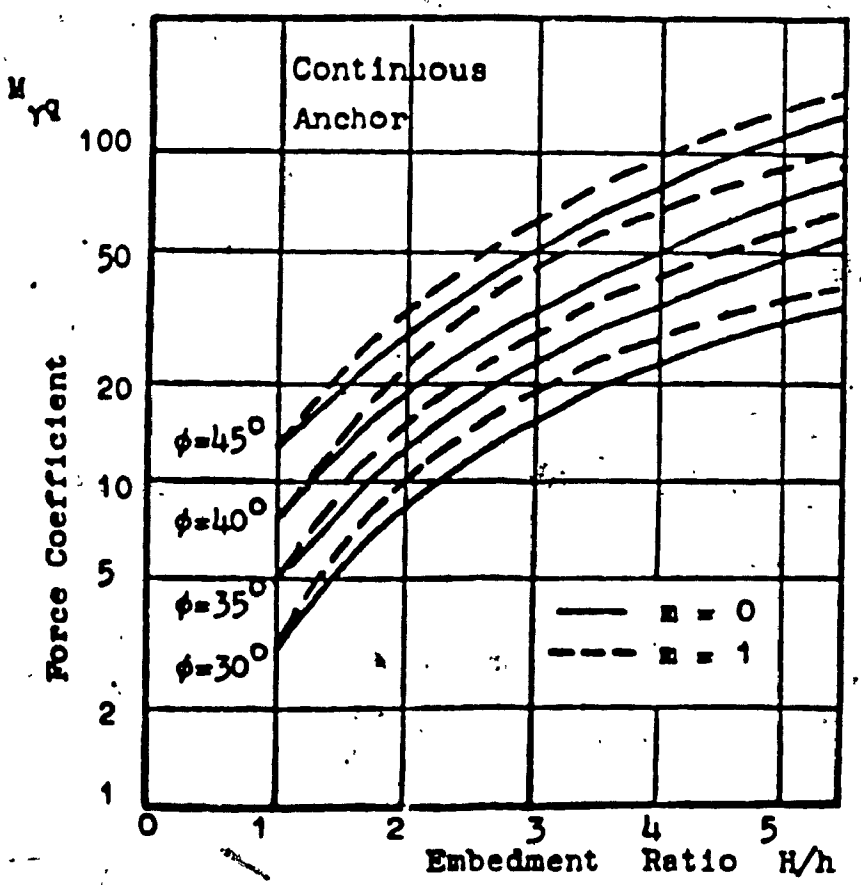

(b) Equivalent Free Surface Method

Figure 2.11: Force coefficients from stress-characteristic solution (Neely et. al. 1973)

shape factor with width/height (B/h), and embedment ratio are shown in figure 2.9-b. Neely et. al. have determined the theoretical pullout resistance of vertical anchor plates in sand using the theory of plasticity. Their trail failure surface solution was based on rupture zones bounded by combinations of logarithmac spirals and straight lines inclined at $(45 - \phi/2)^o$ to the horizontal and by assuming that the soil above the level of the top of the anchor plate act merely as a surcharge (Figure 2.10-a). This method called surcharge method, note that this method did not take account of the shearing resistance of the soil above the top of the anchor.

Neely et. al. included the effect of the shear resistance of the upper layers of soil making use "equivalant free surface concept" adapted from Meyerhof (1951) for footing problem, where it requires assumptions for (m) the degree of mobilization of shearing resistance along AB. Neely et. al. developed design charts for the two methods mentioned (see Figures 2.11-a, 2.11-b).

Das and Seely (1977), investigated the pullout resistance of vertical anchors in sand. A square model steel plate anchor was tested. The tests were carried out at three densities from loose to dense sand such that the angle of shearing resistance were 31, 34 and 40.5 degrees respectively. The ultimate pullout resistance was expressed in terms of dimensionless breakout factor ($N_{\gamma q}$) where:

$N_{\gamma q} = Q_u/\gamma BhH$, where

Q_u = the ultimate pullout capacity

γ = unit weight of soil

B = width of the anchor plate

h = height of the anchor plate

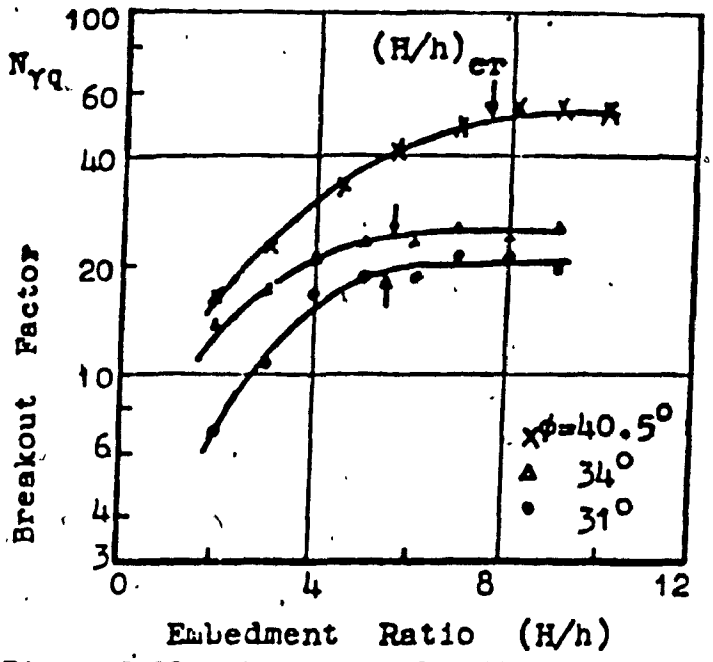

Figure 2.12: Experimental pullout capacity with embedment ratio (Das and Seely 1977)

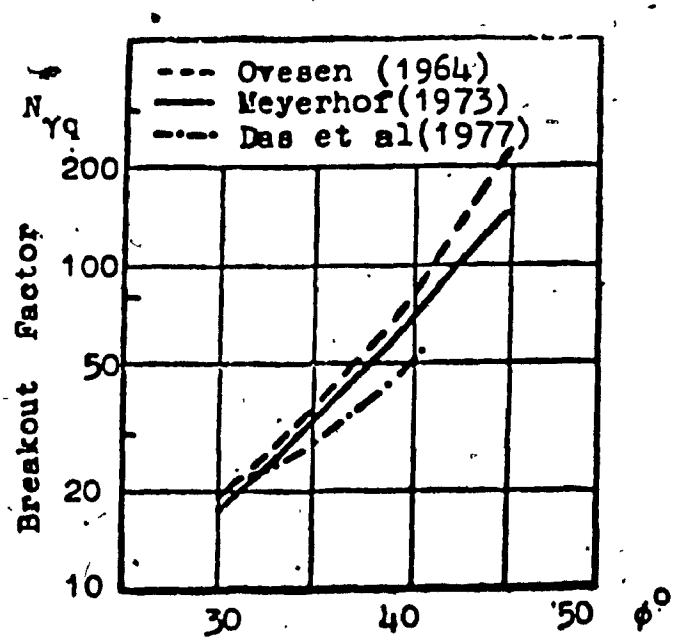

Figure 2.13: Comparison of the test results for deep anchor with the other theories (Das and Seely 1977)

H = depth of embedment

Their results are shown in Figure 2.12. Das and Seely found that the pullout capacity increased with embedment ratio (H/h) for shallow anchors, however beyond a critical depth of embedment ($N_{\gamma q}$) value appears to remain constant. In comparing their experimental results with the theories of Ovesen (1964) and Meyerhof (1973) they found that for deep anchors in loose sand both theories gave good agreement with their experimental data while theoretical values were about 60% greater for dense sand (see Figure 2.13).

Ranjan and Kaushal (1977), conducted an experimental study on continuous vertical anchor plates under horizontal pull in dry sand. Steel plates of different heights ranging from 25 mm (0.984 inch) to 100 mm (3.93 inch) were used. The steel anchor plates were tested at embedment ratios (H/h) varying from 1.5 to 14.5. The ultimate pullout capacity was expressed in terms of $M_{\gamma q} = Q_u/\gamma Bh^2$ and results are shown in Figure 2.14. The results indicated that initially the pullout capacity increased rapidly with an increase in embedment ratio, but beyond an embedment ratio of about (5) the rate of increase considerably reduced, apparently approaching a constant value at larger values of embedment ratio. The experimental results were about 2-3 times greater than the theoretical values obtained from Rankin's theory. Ranjan and Kaushal also found that the displacements at failure load increase with an increase of embedment ratio (see Figure 2.15).

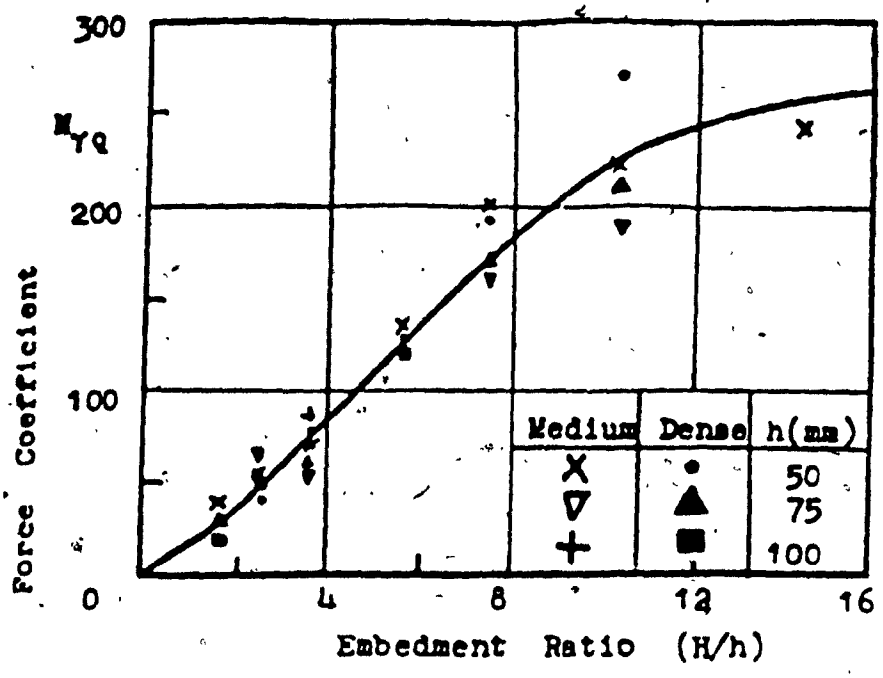

Figure 2.14: Anchor test results – Ranjan and Kaushal (1977)

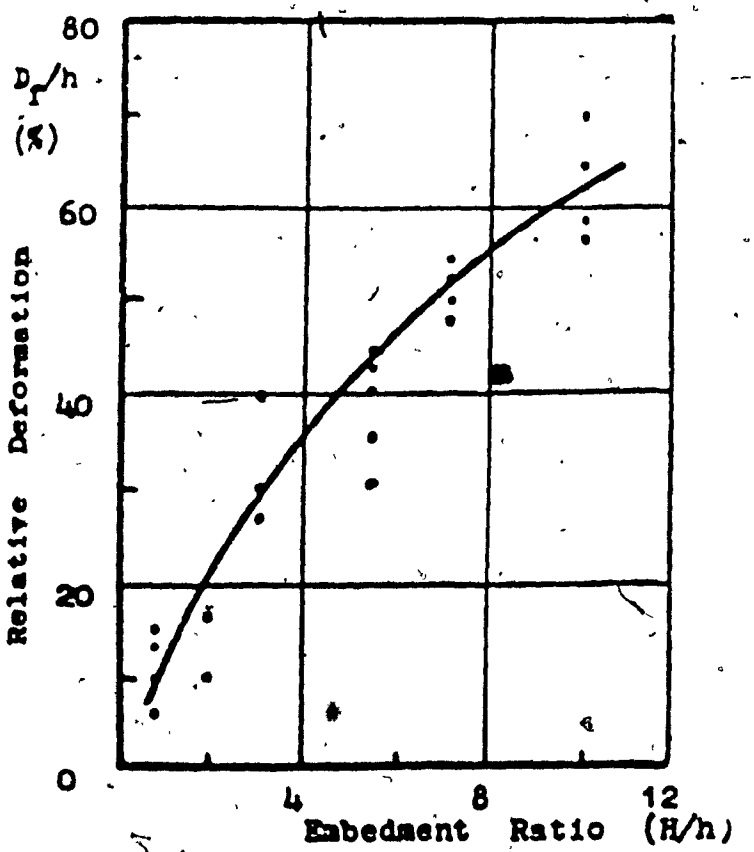

Figure 2.15: Average variation of relative deformation with embedment ratio – Ranjan and Kaushal (1977)

Wang and Wu (1981), carried out an investigation to study the anchor problem experimentally and analytically. The test soil was Ottawa sand, the sand used had two dry densities of 1780 Kg/m^3 (110 pcf) and 1618 Kg/m^3 (100 pcf).

Wang and Wu used different sizes of anchor plates of different height and constant width equal to the width of the testing box to simulate the plain strain condition. To study the effect of plate friction on anchor resistance three different materials were used, namely brass, plexiglass and brass covered with sand paper. Based on the preceding laboratory study, the slip line ABCD was approximated by two straight lines and one segment of logarithmic spiral (see Figure 2.16). Using the slip line field and velocity field given in Figure 2.16, the yielding load of the anchor was determined by equating the rate of work done by external force to the rate of internal energy dissipation. The resulting equations for computing the yielding load for shallow and deep plate anchors are given by:

$$\frac{T}{\gamma h^2} = \frac{\cos\delta}{2\cos^2\phi\,[\cos(\xi+\delta) - \sin\xi\tan\delta]}(A + B + C)$$

where

$$A = \cos\phi \sin\xi \cos(\xi - \phi) \cos(\alpha - \xi)$$

$$B = \frac{\cos^2(\xi-\phi)}{1 + 9\tan^2\phi}\{\cos(\alpha-\xi)[-3\tan\phi + (3\tan\phi\cos\theta + \sin\theta)\,e^{3\theta\tan\phi}$$

$$+ \sin(\alpha-\xi)[1 + (3\tan\phi\sin\theta - \cos\theta)\,e^{3\theta\tan\phi}]\}$$

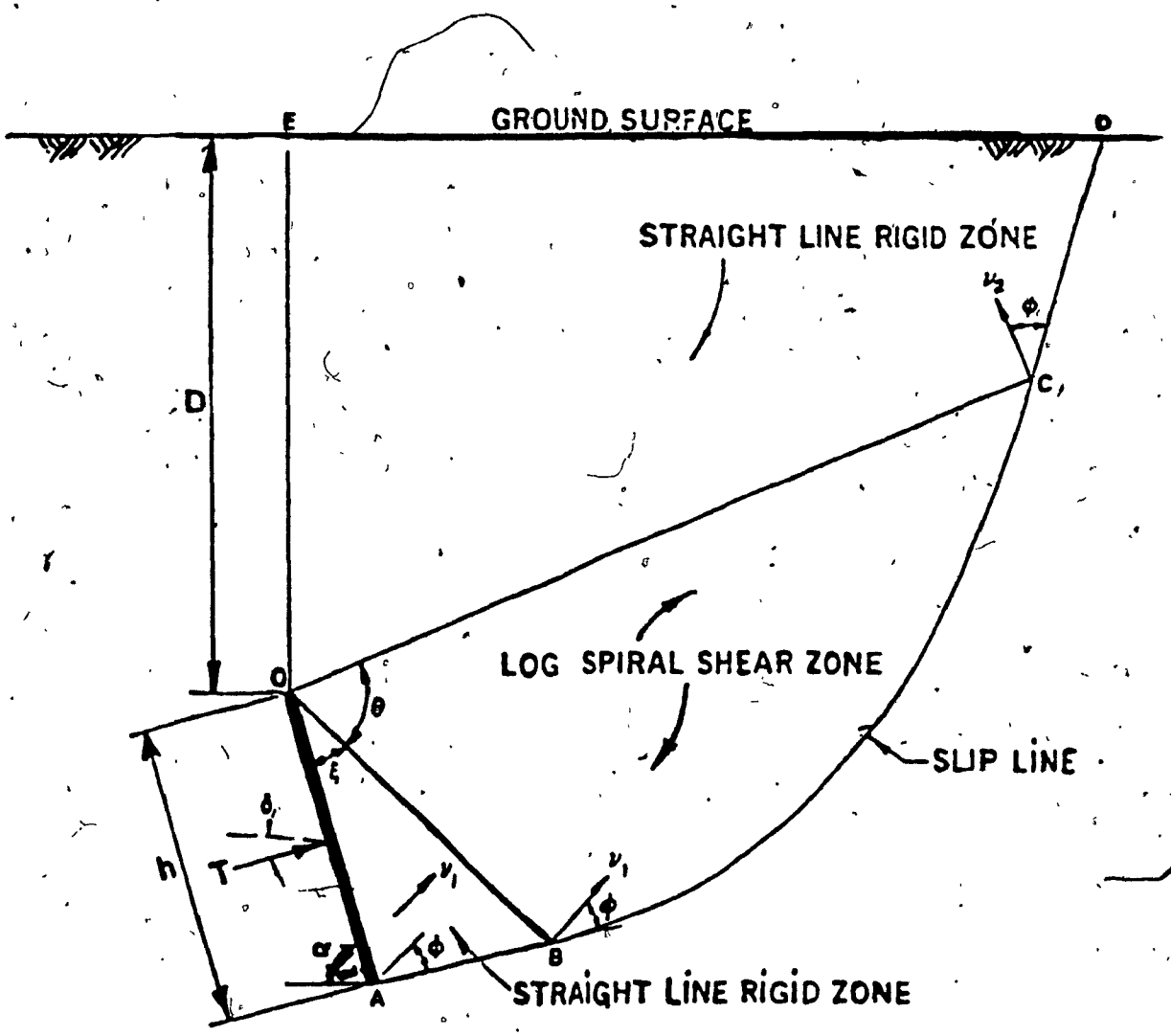

Figure 2.16: General shear failure for shallow anchor (Wang and Wu 1980)

$$C = \left(\frac{D}{h}\right)^2 e^{\theta \tan\phi} \cos(\xi - \theta - \alpha) \{\cos^2\phi \cos(\xi + \theta - \alpha) + X^2 [\tan(\phi + \alpha - \xi - \theta) - \cos(\xi + \theta - \alpha)]\}$$

and

$$X = \cos\phi - \frac{h}{D} e^{\theta \tan\phi} \sin(\xi + \theta - \alpha) \cos(\xi - \phi)$$

Foriero (1985), derived a formula for the ultimate resistance of shallow continuous anchor in sand, based on the theoretical concept of limit equalibrium, where the case of a two-dimensional failure mechanism was considered. The assumption involved in predicting the theoretical ultimate pullout capacity is that at the ultimate load, a soil mass of roughly truncated pyramidal shape is lifted up, the forces on the assumed punching failure surface (ab and cd) can be taken as the total passive earth pressure (p_1) and (p_2), inclined at an average angle (δ), and acting downwards (see Figures 2.17-a and 2.17-b). The assumed failure planes are taken parallel to the anchor rod (direction of the pullout load), for inclination angle (α_v) varying from 0 to 45 degrees (Figure 2.17-a), while they were taken at 45 degrees when (α_v) varying between 45 to 90 degrees.

Forjero represents the results of his analysis in the form of the following equations

$$Q_u = 0.5\,\gamma K_s \sin\phi\,(L_1^2 + L_2^2) + 0.5\,(L_1 + L_2)\,\gamma H \cos\alpha_v$$

For $0^\circ \le \alpha_v \le 45^\circ$

$$Q_u = \frac{0.5\,\gamma K_s \sin\phi\,(L_1^2 + L_2^2) + 0.5\,(L_1 + L_2)\,\gamma H \cos 45 \cos(45 - \alpha_v)}{\cos(45 - \alpha_v)}$$

For $45^\circ \le \alpha_v \le 90^\circ$

where K_s is the coefficient of passive pressure which is given in the form of design charts. (Figure 2.17-c.)

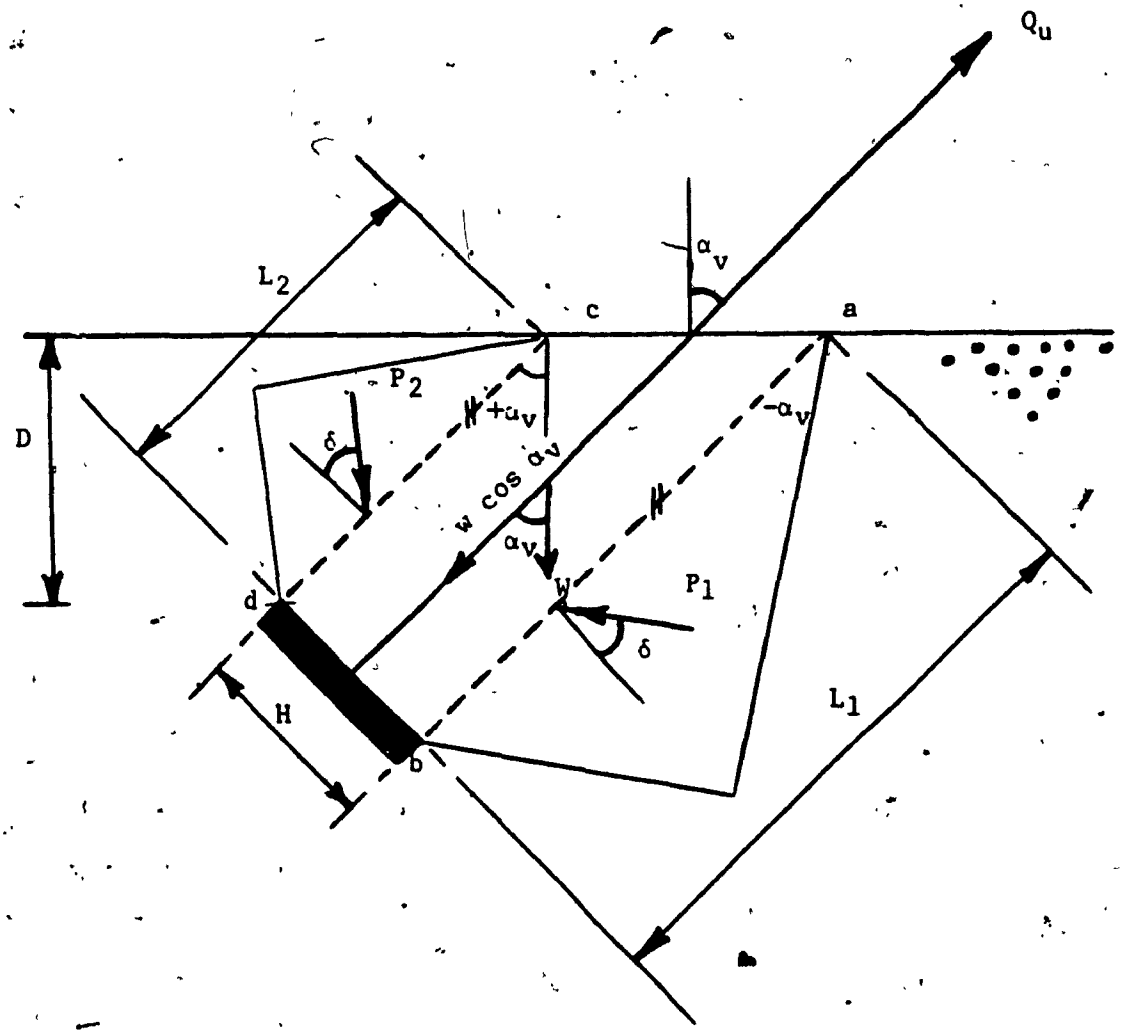

Figure 2.17-a: Stress diagram - strip anchor plate under inclined load from the vertical (Foriero 1985)

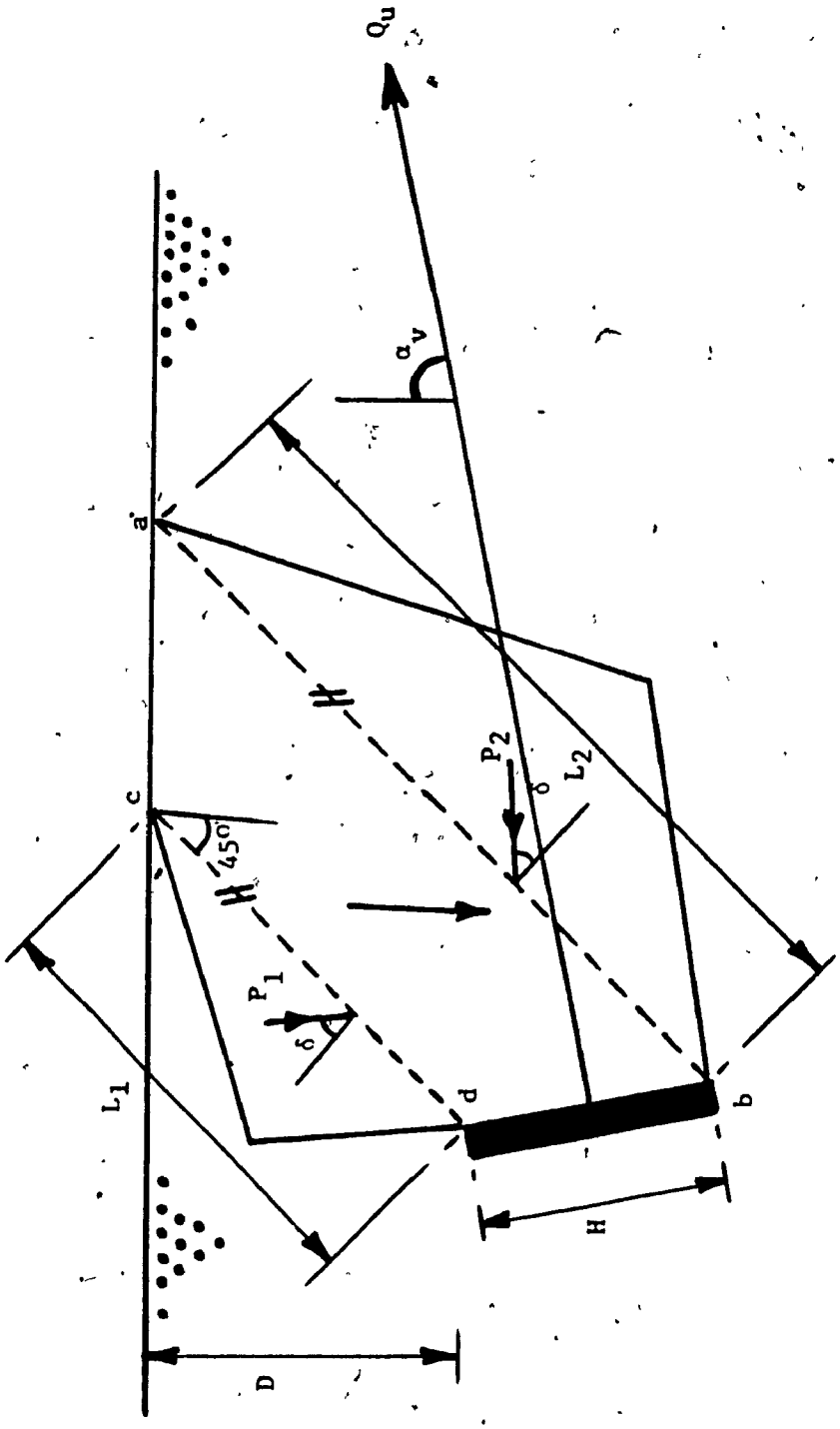

Figure 2.17-b:- Stress diagram - strip anchor plate under inclined load from horizontal (Foriero 1985)

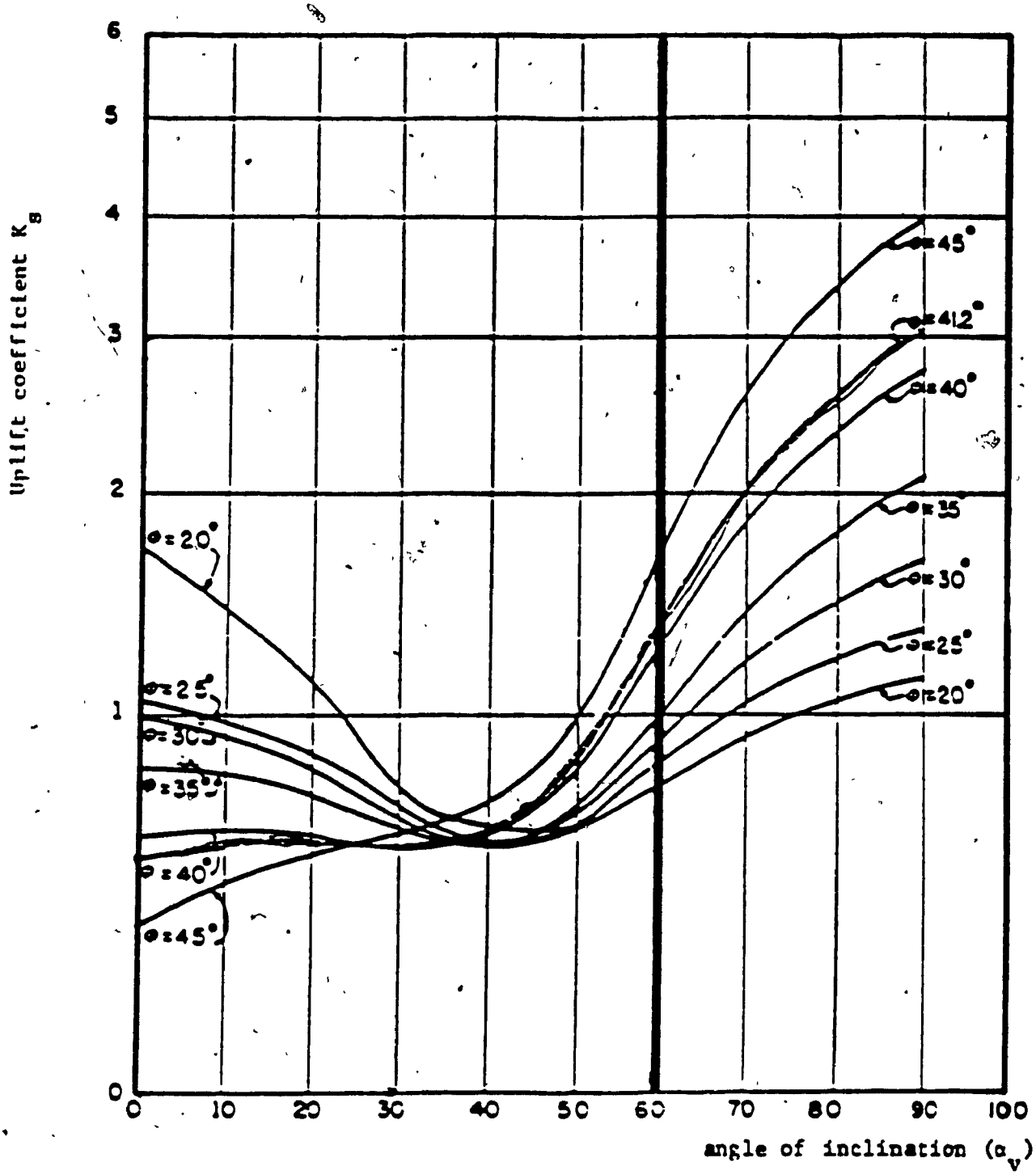

Figure 2.17-c: Design chart (Foriero 1985)

CHAPTER III

EXPERIMENTAL INVESTIGATION

3.1 General Description

The experimental set-up used in the program was designed by Foriero (1985). It comprises a narrow plexiglass sided tank, to simulate the plain-strain conditions of a strip anchor. The inside dimensions of the tank are 6"(152.4mm) x 48"(1220mm) x 40"(1016mm) (width x length x height) and loading frame as shown in Figures 3.1-a, 3.1-b, 3.1-c and 3.1-d. The loading frame and the loading equipment made up the main facility used in this experimental set-up (see figure 3-2).

The placement of sand in the test tank is carried out by rainfall method. The sand was deposited from a tank mounted upon a frame into a box lying on the loading frame at a fixed height above the test tank. Once an arborite plate was pulled through a slot at one side of the box the sand filtered through a metallic mesh.

The test anchors were placed at various depths and various angles of inclination. They were pulled by a motor at a constant displacement rate of 0.1"(2.54mm) to 1.0"(25.4mm) per minute. This rate was chosen arbitrarily within the range of strain rate normally adopted for laboratory testing. The pullout load and displacement were monitored using a load cell and a 0.025 m (0.001 inch) dial gages respectively.

3.2 Loading Equipment

The loading equipment includes a motorized screw jack with three feet maximum travel distance mounted on a steel plate which is bolted on a steel tubing of frame. The combination of a gear shift, a gear rear reducer and an electronic speed controlled device, provide the screw jack with loading and unloading speed varying from 0.01" to 1.0" per minute (see Figures 3.2-a, 3.2-b and 3.2-c).

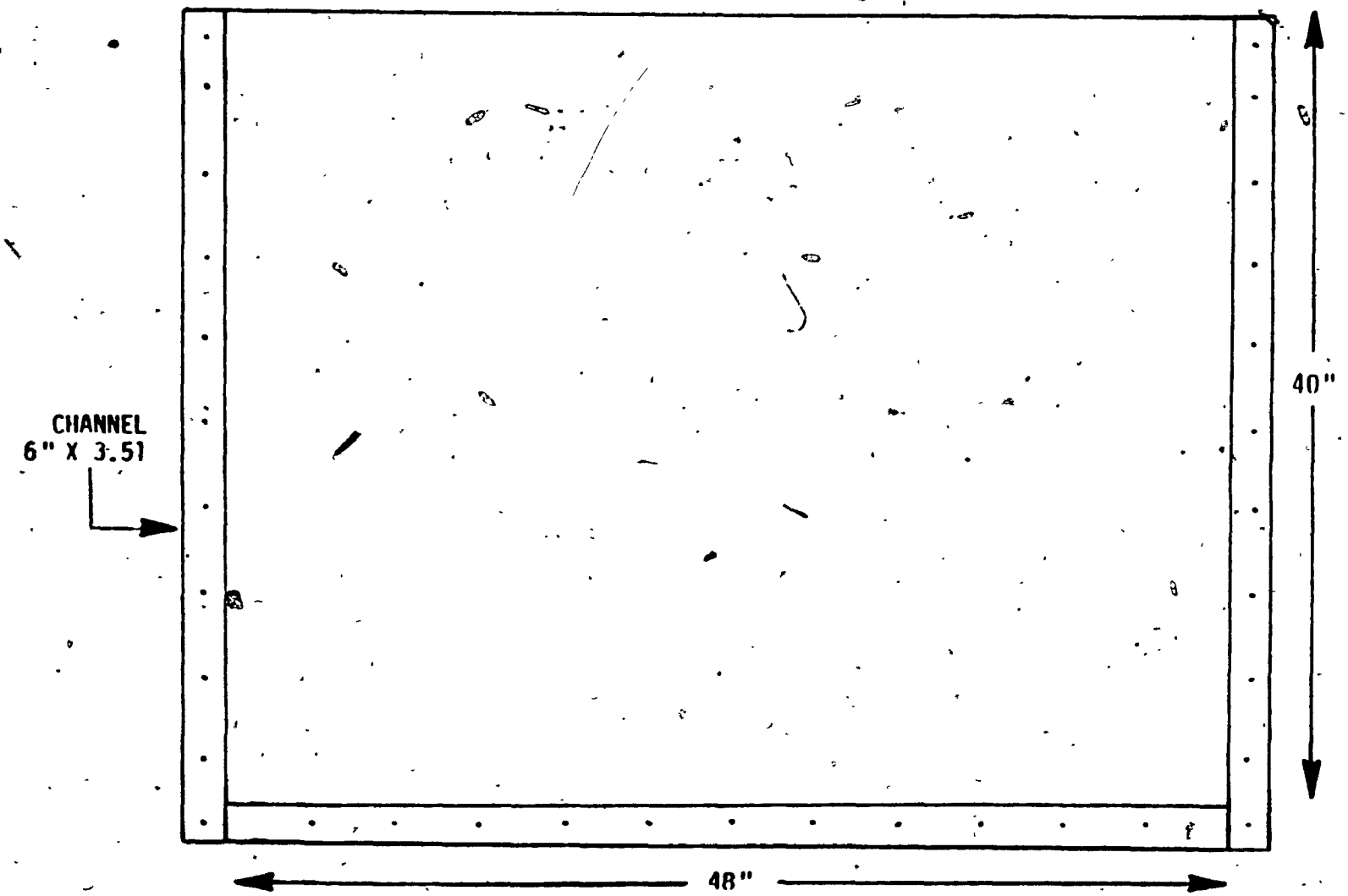

Figure 3.1-a: Plexiglass Tank (side view)

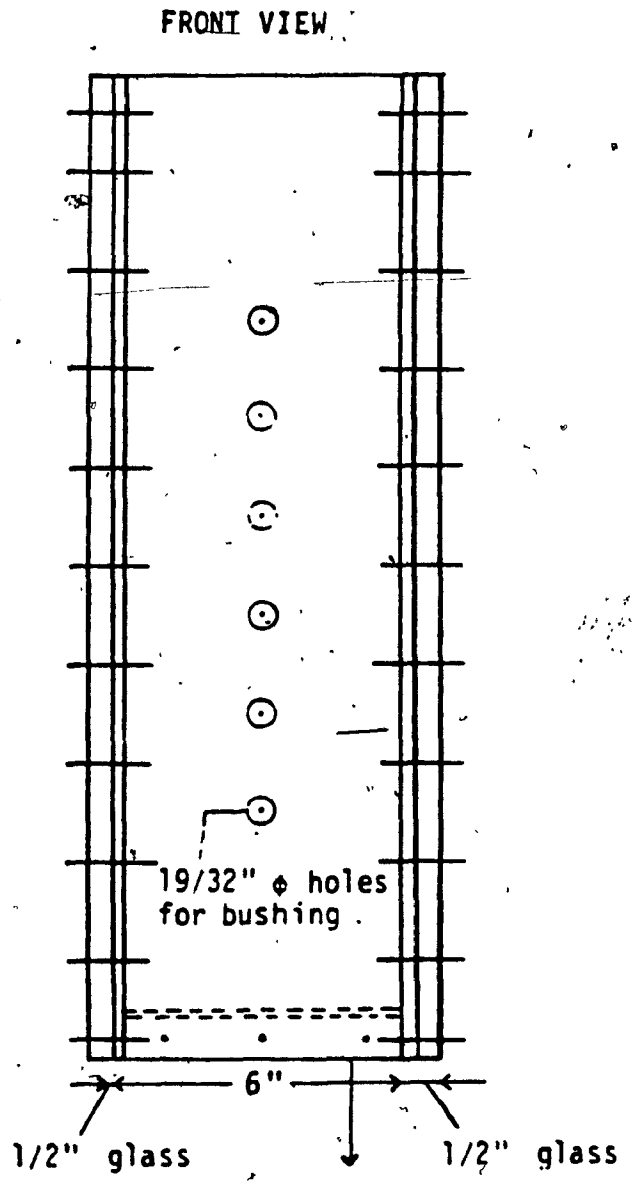

Figure 3.1-b: Plexiglass Tank

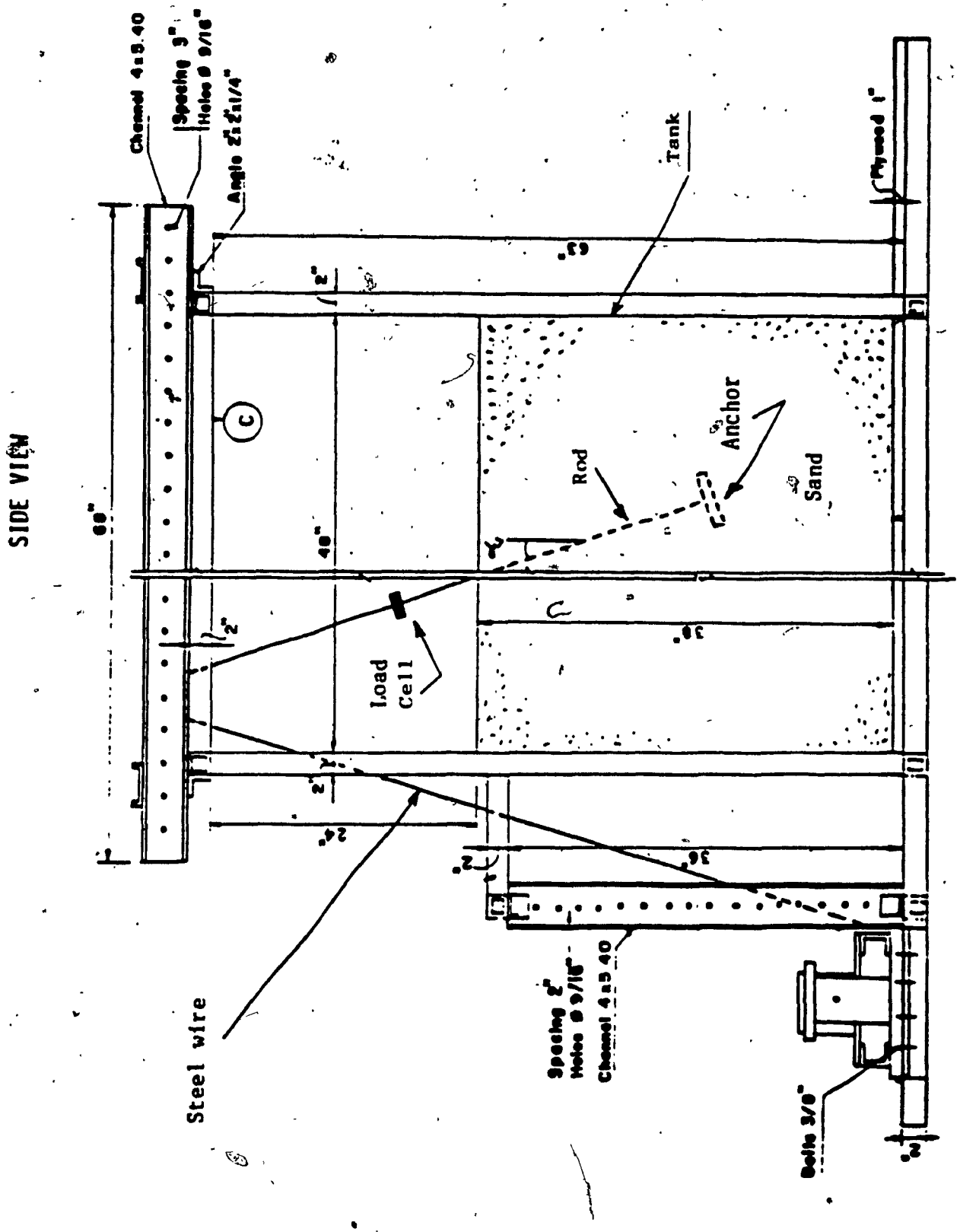

Figure 3.1-c: Experimental Loading Frame

FRONT VIEW

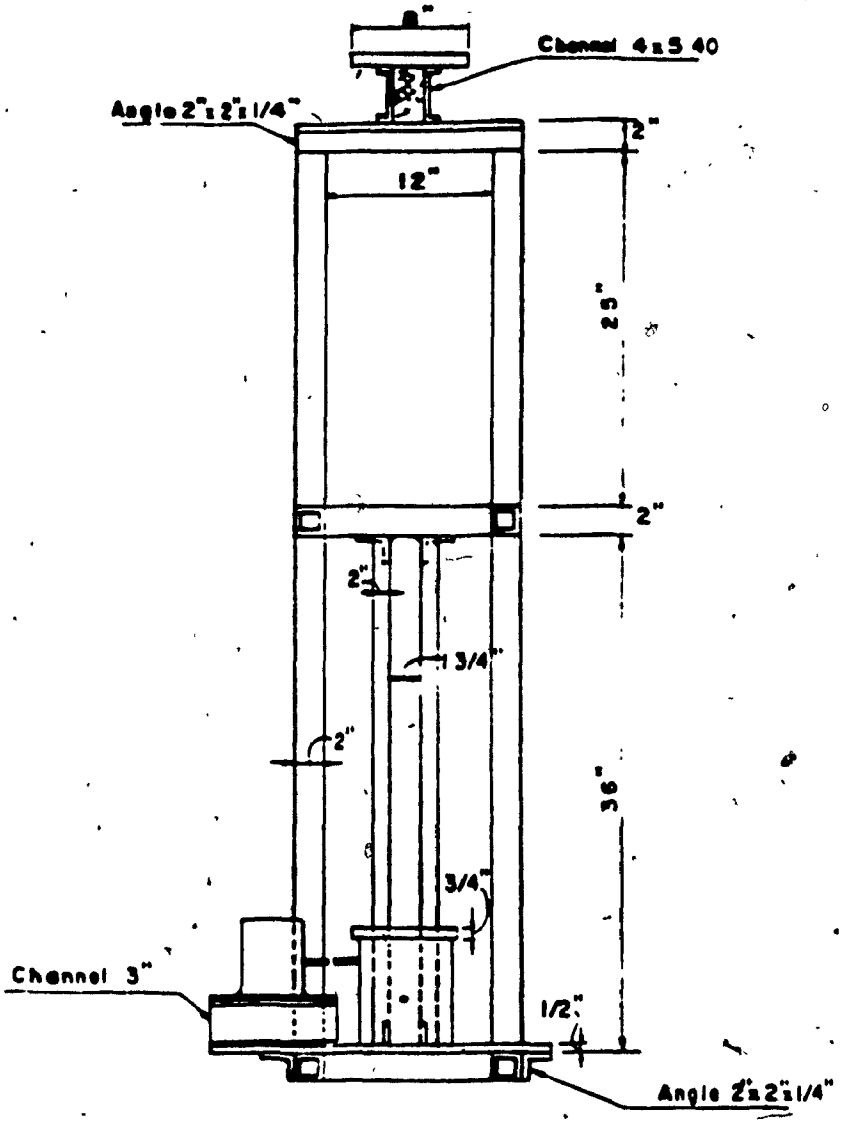

Figure 3.1-d: Experimental Loading Frame

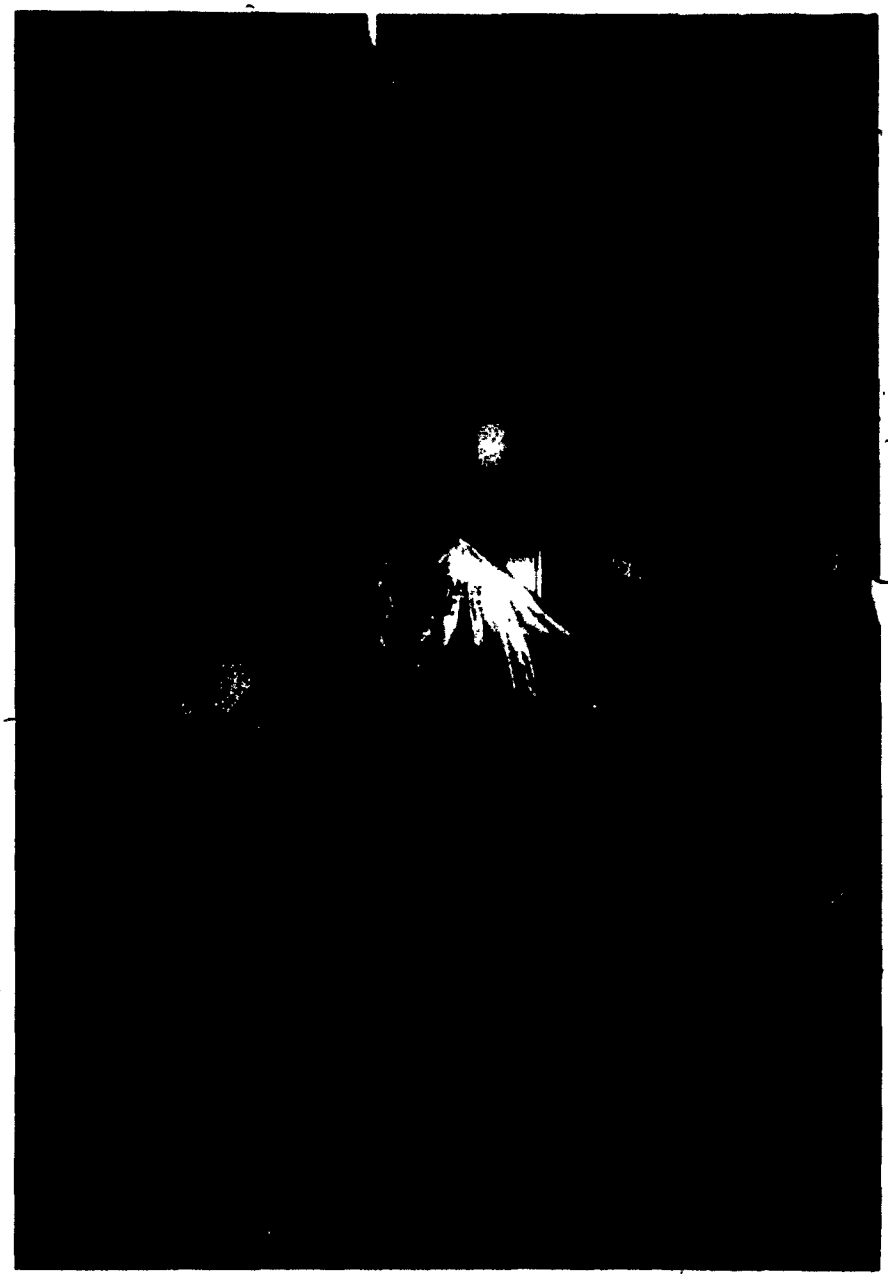

Figure 3.2: Experimental setup

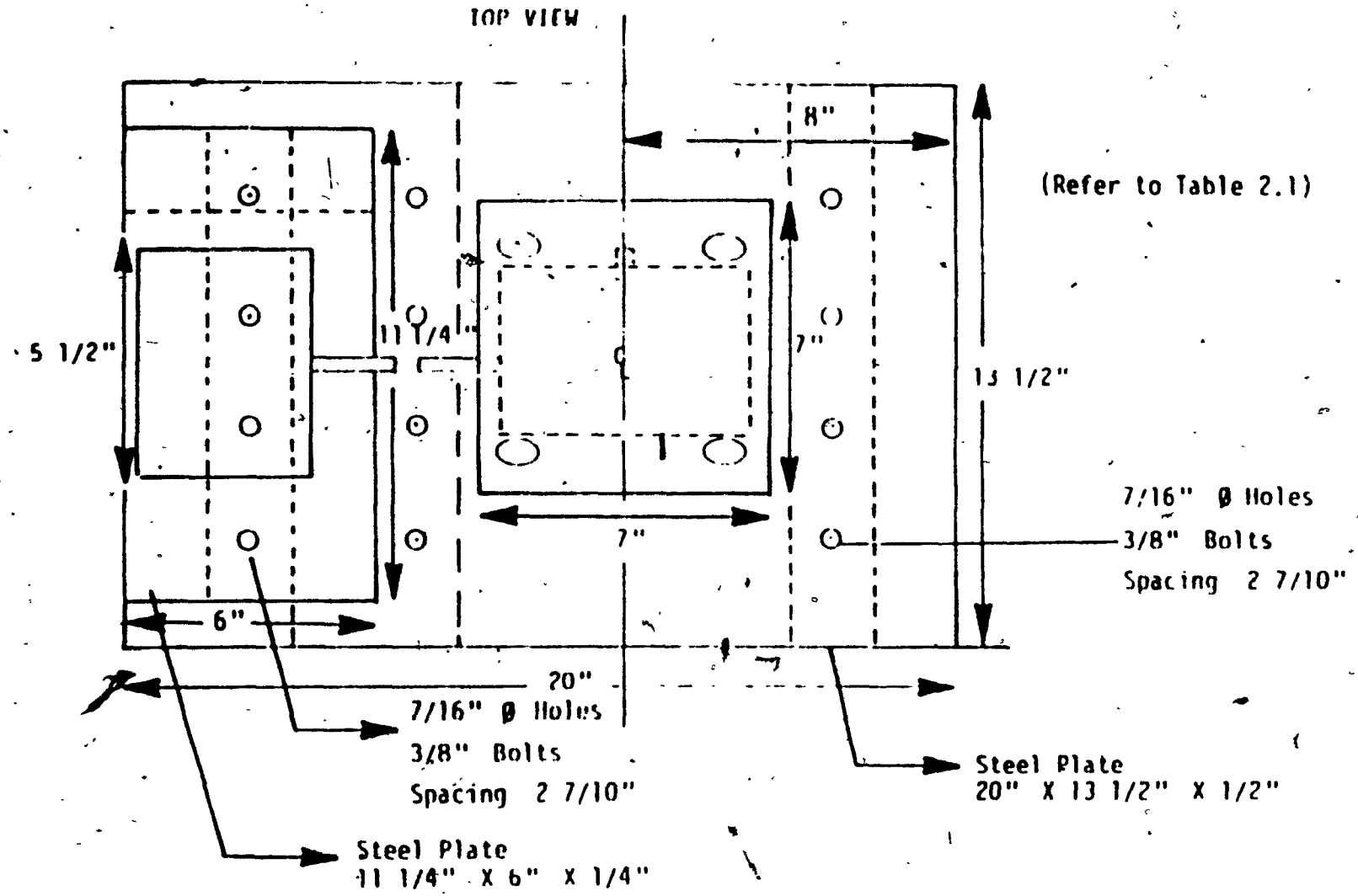

Figure 3.2-a: Loading equipment

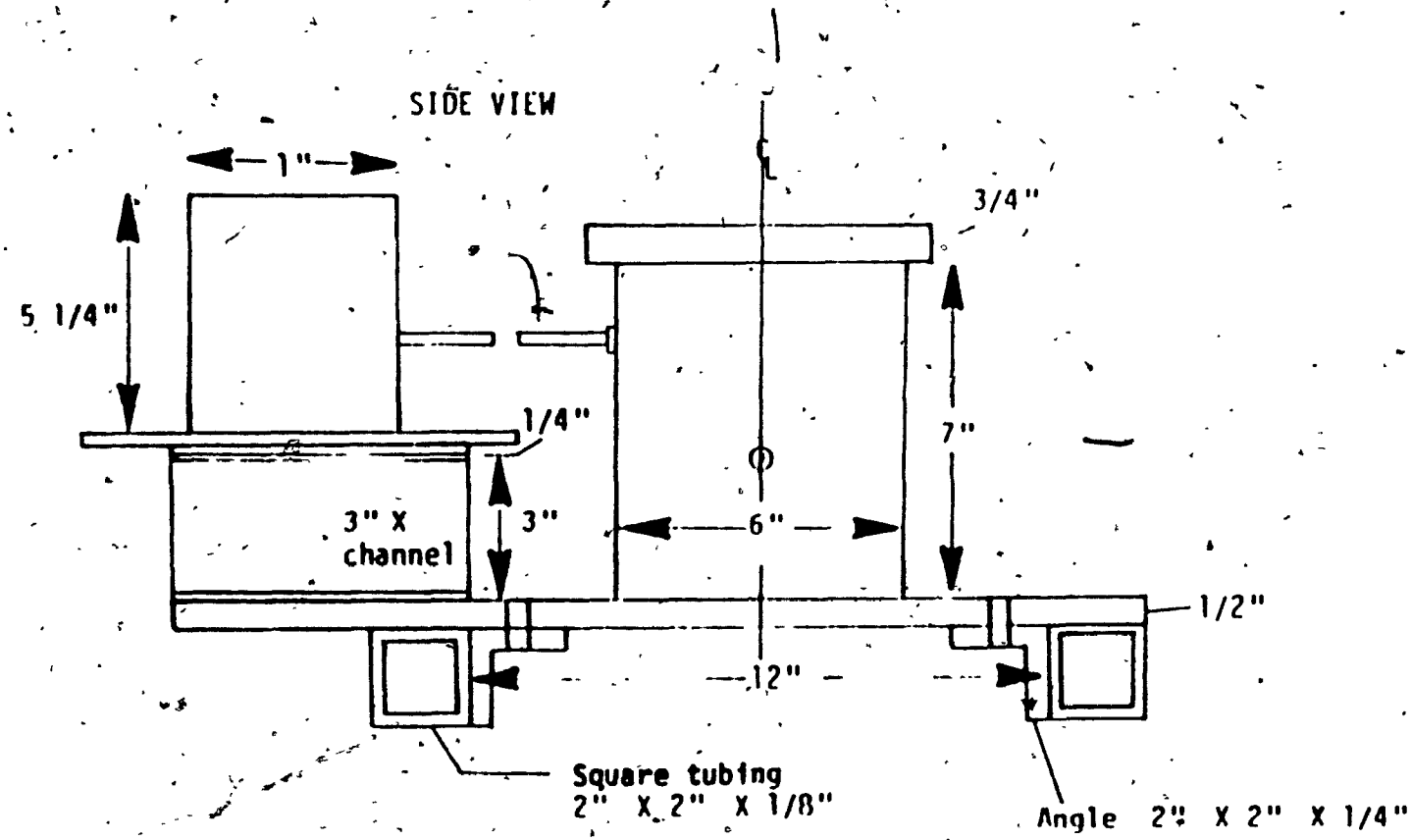

Figure 3.2-b: Loading equipment

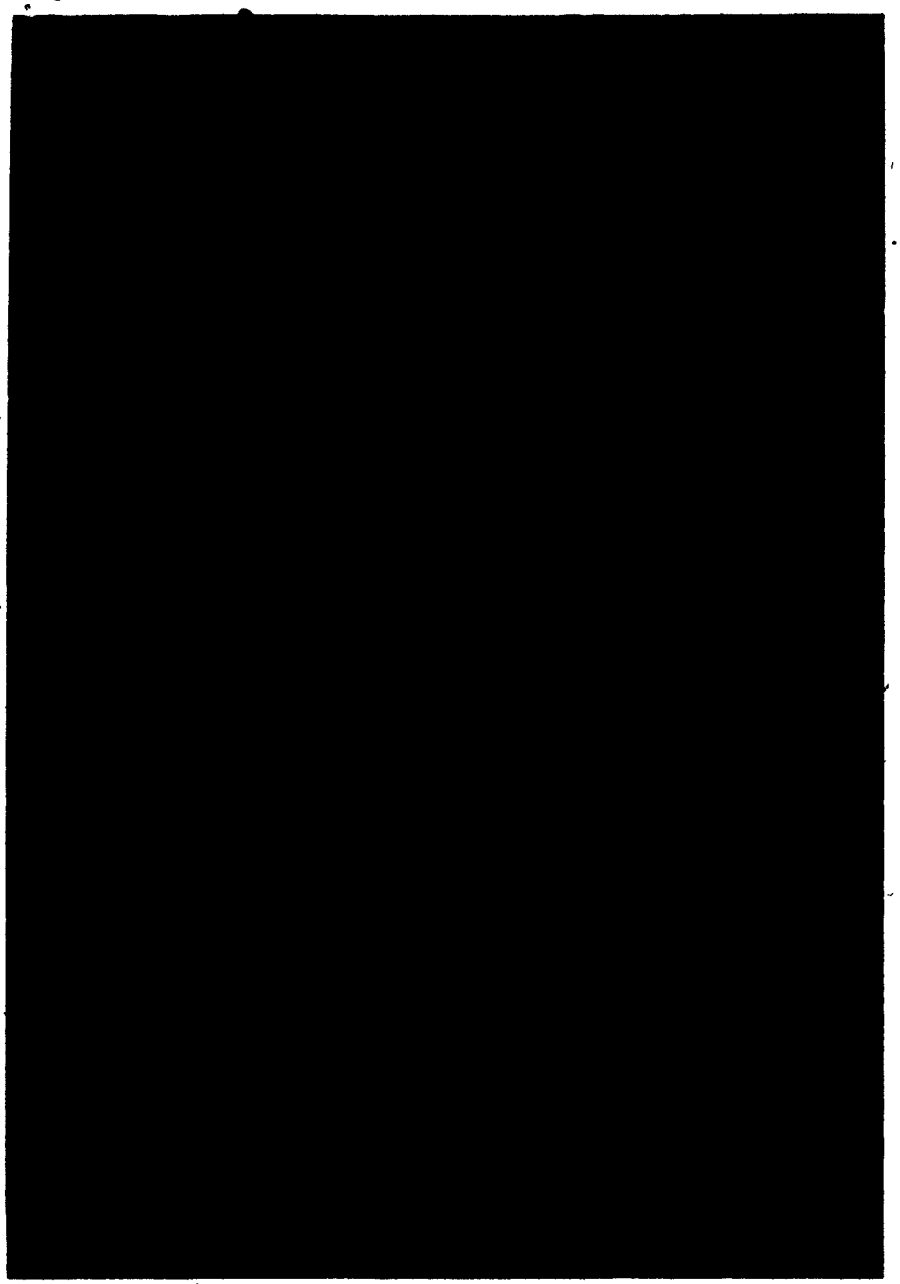

Figure 3.2-c: Loading equipment

3.3 Model Anchor

The model anchors used in the investigation were made of aluminum plate 0.5 inches thick. In order to simulate plane-strain condition, the model anchor width had to be the same as the testing tank width (6 inches). The height of the model anchors were 2 inches, 4 inches and 6 inches. Pressure transducers were placed in circular openings cut out of the plate. The plates were covered with sand paper to ensure that the surface characteristics of the plate remained constant between tests. A one inch outer diameter, steel, hollow rod was rigidly fastened to the center of the plate. The rod served two functions: mainly to pull of the anchor plate, and as enclosure of wiring. (See Figures 3.3-a to 3.3-d.)

3.4 Soil Properties

The sand used in this investigation is called Morie sand which is imported from the U.S.A. A detailed study of the physical properties of this sand used in this experimental work was given by A. Afram (1984). A brief description of some aspects of these properties will be given here.

The grain size distribution indicated a medium uniform sand with a uniformity coefficient of 1.45. The effect of this uniformity is reflected in the measured minimum and maximum densities of 91.5 per cent and 104.5 per cent respectively. Test results showing the variation of the angle of friction with relative density are shown in Fig. 3.4-a.

3.4.1 Relative density calculation:

$$e = \frac{G\gamma_w \cdot 1}{\gamma} \qquad \text{and} \qquad R.D. = \frac{e_{max} - e}{e_{max} - e_{min}}$$

Knowing that the average value of sp.gr. $G_s = 2.662$, $e_{max} = 0.815$, $e_{min} = 0.590$. The relative density in those tests was 63.33%. From Figure 3.4-a this corresponds to an angle of friction of 41.2% (Direct shear test).

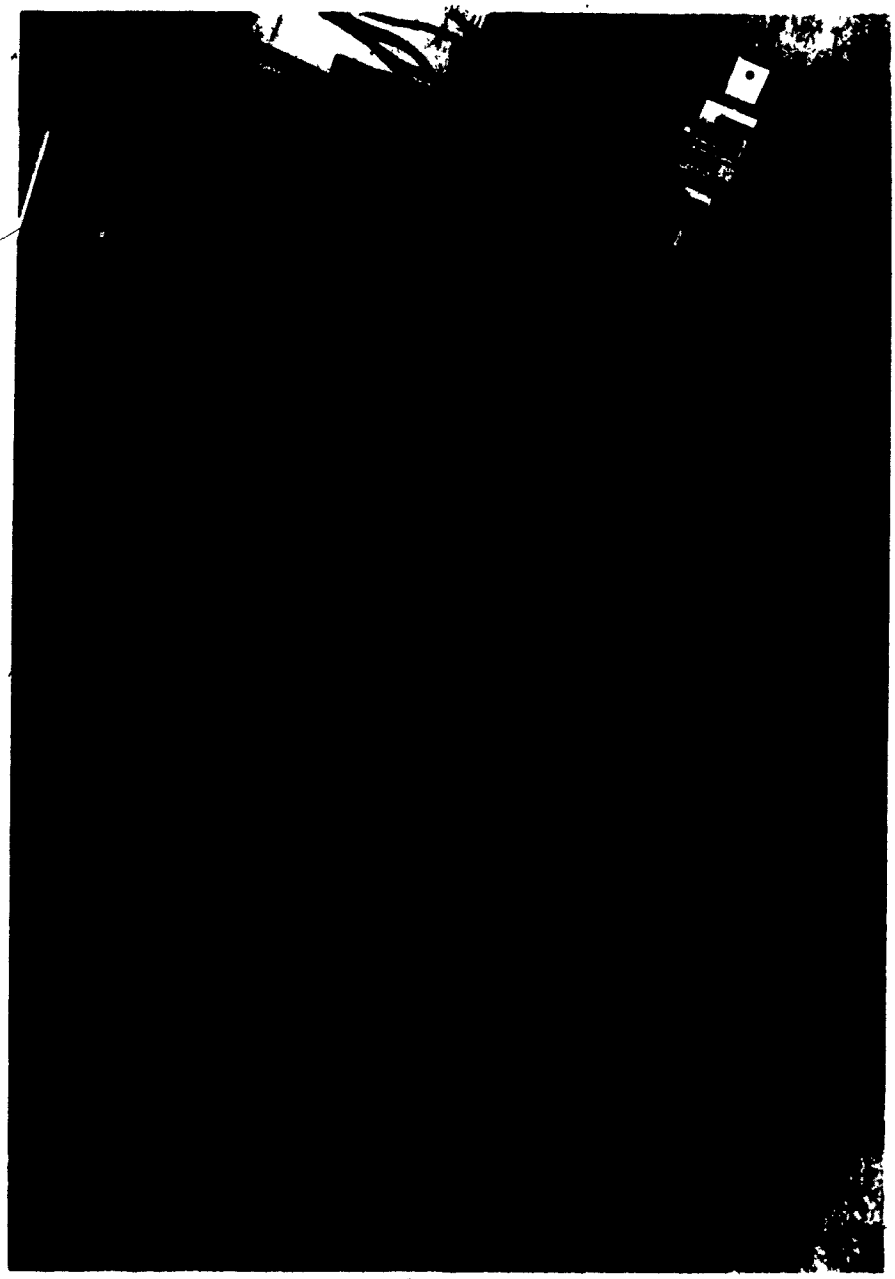

Figure 3.3-a: The model anchors

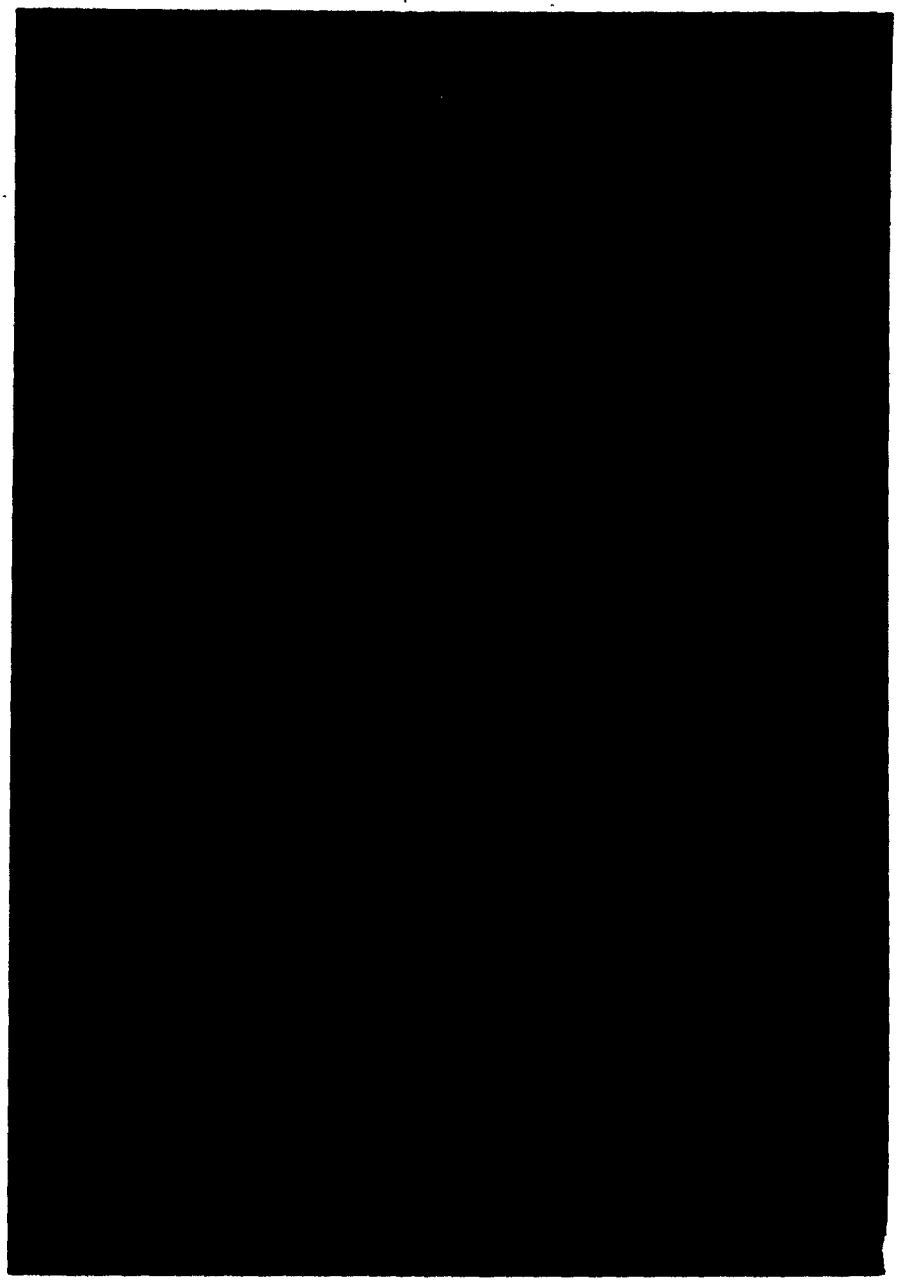

Figure 3.3-b: Model anchor

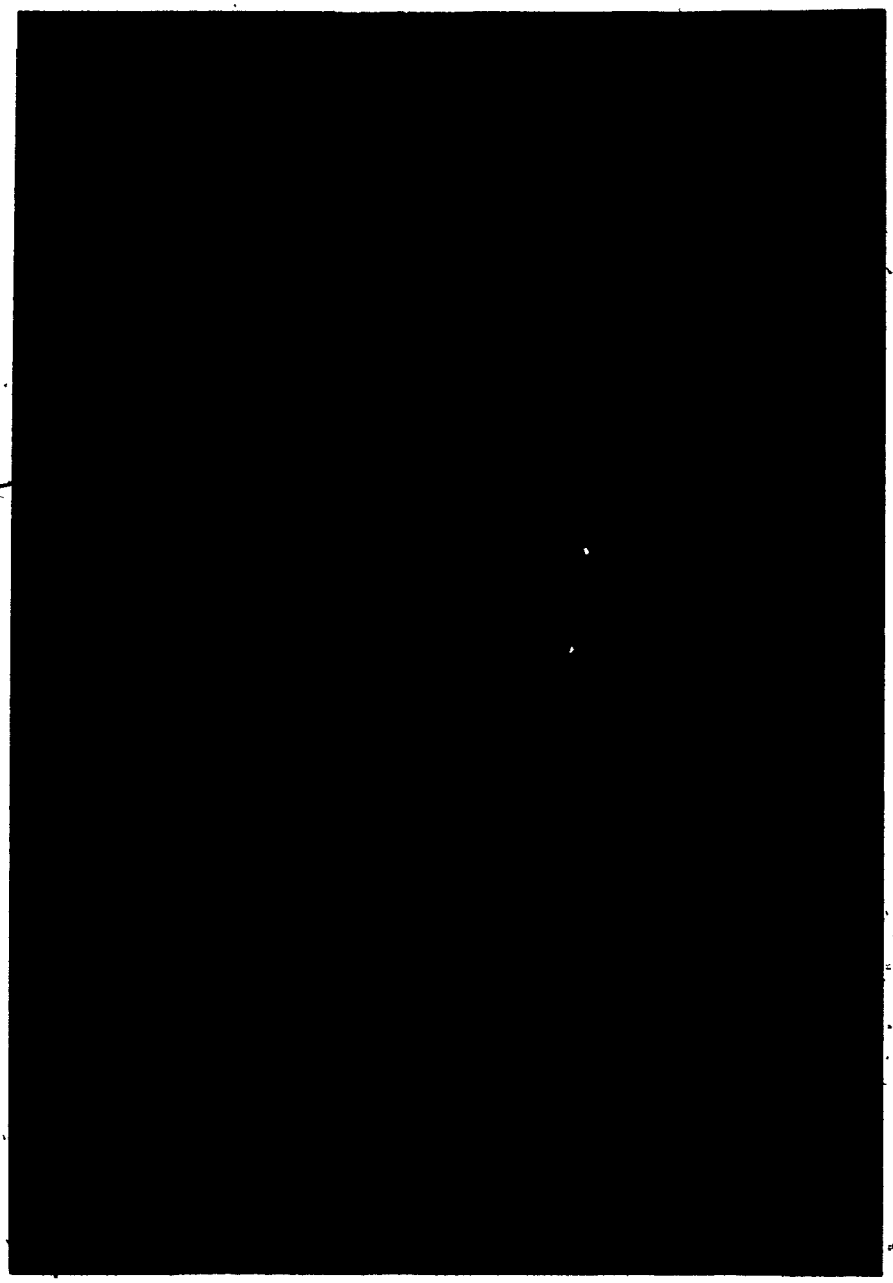

Figure 3.3-c: Model anchor plates

Figure 3.3-d: Model anchor plate
Inside view

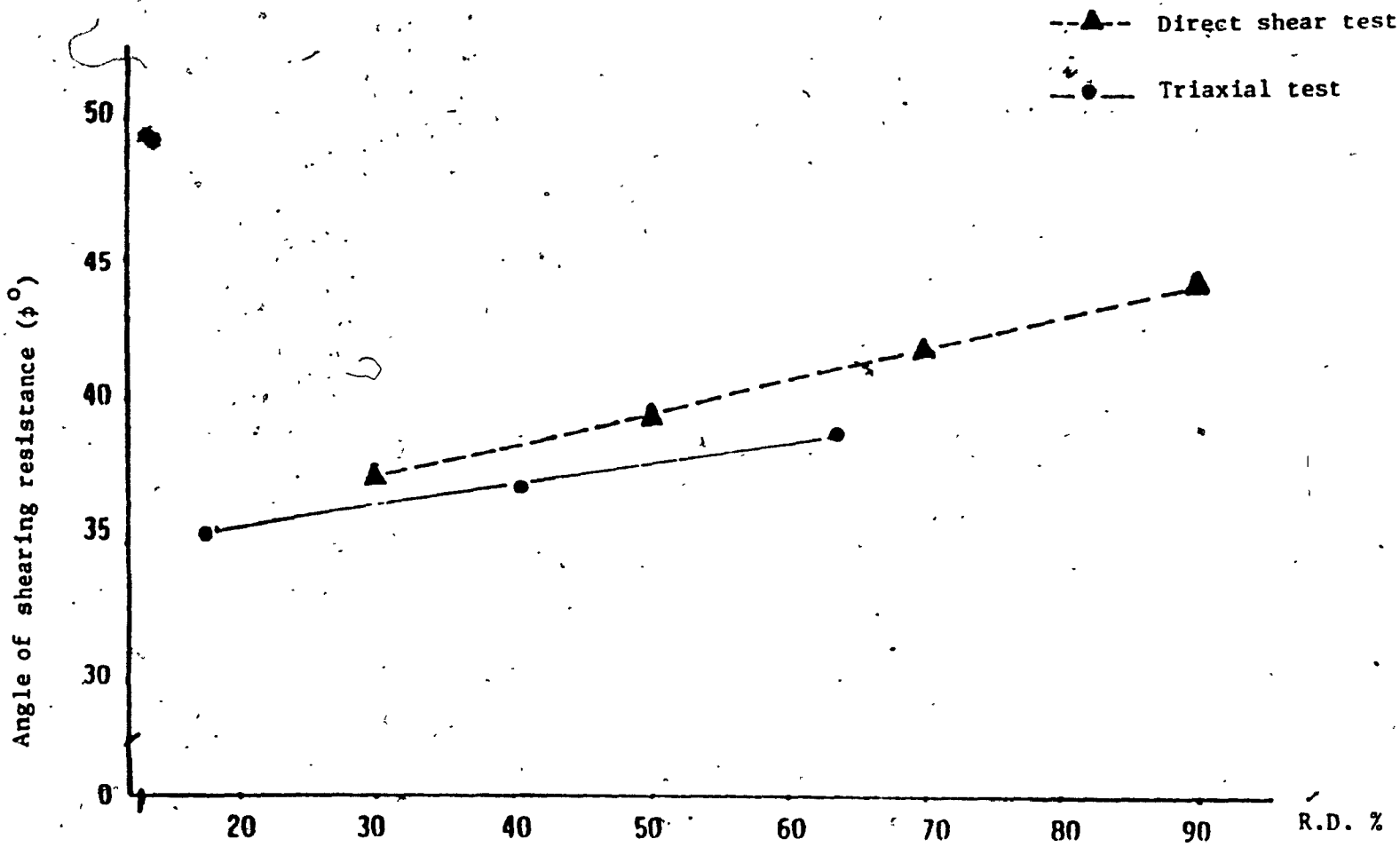

Figure 3.4-a: Angle of shearing resistance vs. relative density of sand (after Afram 1984)

3.4.2 Determination of unit weight

The density pot provided an excellent way of obtaining the density at any location in the test pit. Twelve pots of known weights and volumes are placed on a leveled surface of sand (see Fig. 3.4.2). After each test the pots were carefully removed and the excess sand was scraped off. Each pot was then weighed. The density calculations are shown in Tables 3.4.2a through 3.4.2e.

3.5 Calibration of Pressure Transducers

Pressure transducers were indispensable for the measurement of the normal pressure acting on the face of the plate, in particular the integration of these pressures yielded the total passive earth pressure and consequently the ultimate load. Calibration of the pressure transducers was achieved inside a special pressure chamber, the transducers were independently subjected to air pressure on their frontal surfaces, calibration curves were then obtained for excitation versus pressure (see Figure 3.5-a)

3.6 Calibration of Load Cell

The load cell in the present investigation primarily served the two following purposes: First, as monitoring device for possible malfunction of the pressure transducers and second, to determine frictional resistance produced in every test (Figures 3.6-a, 3.6-b) by means of stress control procedure, the calibration of the load cell was carried out. Incremental loads were added up to a total of about 600 pounds, and the calibration curve was then obtained (see Figure 3.6-c).

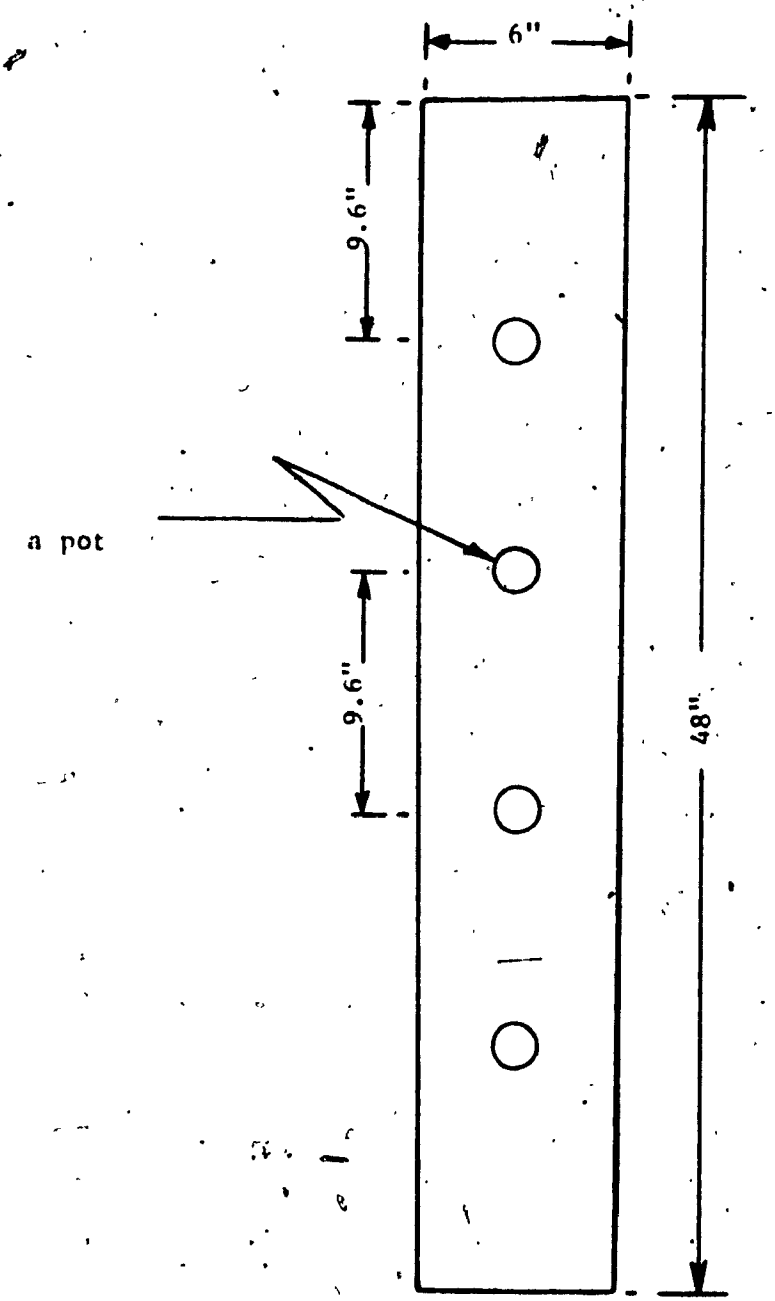

Figure 3.4-2 Density pot placement

Level No.	Pot No.	Vol. of Can in^3	Weight of Can lbs.	Weight of Can and Soil lbs.	Weight of Soil lbs.	Unit Weight lb/ft^3
	1	8.16	0.0436	0.51	0.47	99.53
I	2	9.03	0.0698	0.59	0.52	99.59
	3	7.98	0.0436	0.50	0.46	99.60
	4	8.16	0.0458	0.51	0.47	99.55
	1	8.50	0.0698	0.56	0.49	99.59
II	2	7.98	0.0436	0.50	0.46	99.58
	3	8.51	0.0698	0.56	0.47	99.59
	4	8.67	0.676	0.56	0.50	99.60
	1	8.33	0.0697	0.54	0.47	99.58
III	2	7.98	0.0435	0.50	0.46	99.60
	3	7.47	0.0436	0.47	0.43	99.58
	4	8.16	0.0698	0.54	0.47	99.55

Table 3.4-2a Unit weight calculation (Test No. 1)

Level No.	Pot No.	Vol. of Can in^3	Weight of Can lbs.	Weight of Can and Soil lbs.	Weight of Soil lbs.	Unit Weight lb/ft^3
	1	8.85	0.0677	0.58	0.51	99.59
I	2	8.85	0.0678	0.51	0.51	99.58
	3	8.51	0.0437	0.49	0.49	99.59
	4	8.16	0.0677	0.47	0.47	99.59
	1	8.51	0.0459	0.53	0.49	99.58
II	2	8.16	0.0677	0.54	0.47	99.58
	3	8.85	0.0677	0.51	0.51	99.59
	4	8.85	0.0677	0.57	0.51	99.59
	1	9.02	0.0698	0.59	0.52	99.62
III	2	8.50	0.0458	0.54	0.49	99.59
	3	9.01	0.0698	0.59	0.52	99.60
	4	7.98	0.0436	0.50	0.46	99.59

Table 3.4-2b Unit weight calculation (Test No. 2)

Level No.	Pot No.	Vol. of Can in^3	Weight of Can lbs.	Weight of Can and Soil lbs.	Weight of Soil lbs.	Unit Weight lb/ft^3
	1	7.98	0.0435	0.50	0.46	99.60
I	2	8.50	0.0676	0.56	0.49	99.58
	3	8.50	0.0676	0.56	0.49	99.59
	4	8.16	0.0436	0.51	0.47	99.59
	1	8.84	0.0698	-	-	-
II	2	9.02	0.0698	0.59	0.52	99.58
	3	9.02	0.0698	0.59	0.52	99.59
	4	7.98	0.0436	0.50	0.46	99.59
	1	8.84	0.0697	0.58	0.51	99.59
III	2	9.02	0.0698	0.51	0.47	99.57
	3	8.16	0.0436	0.51	0.47	99.58
	4	8.33	0.0436	0.52	0.48	99.59

Table 3.4-2c Unit weight calculation (Test No. 3)

Level No.	Pot No.	Vol. of Can in^3	Weight of Can lbs.	Weight of Can and Soil lbs.	Weight of Soil lbs.	Unit Weight lb/ft^3
I	1	8.16	0.0436	0.51	0.47	99.60
	2	8.50	0.0458	0.54	0.49	99.58
	3	9.02	0.0698	0.59	0.52	99.58
	4	8.50	0.0671	0.55	0.49	99.54
II	1	9.02	0.0698	0.59	0.52	99.55
	2	8.16	0.0436	0.51	0.47	99.62
	3	7.98	0.0436	0.50	0.46	99.57
	4	8.67	0.0698	0.57	0.50	99.59
III	1	7.98	0.0436	0.50	0.46	99.58
	2	8.51	0.0698	0.56	0.49	99.59
	3	8.67	0.0698	0.57	0.50	99.59
	4	9.02	0.0698	0.59	0.52	99.57

Table 3.4-2d Unit weight calculation (Test No. 4)

Level No.	Pot No.	Vol. of Can in^3	Weight of Can lbs.	Weight of Can and Soil lbs.	Weight of Soil lbs.	Unit Weight lb/ft^3
	1	9.19	0.0698	0.60	0.53	99.60
I	2	9.19	0.0698	0.60	0.53	99.59
	3	8.85	0.0698	0.58	0.51	99.58
	4	8.16	0.0437	0.51	0.47	99.59
	1	8.85	0.0698	0.58	0.51	99.59
II	2	8.51	0.0437	0.53	0.49	99.57
	3	8.51	0.0437	-	-	-
	4	8.16	0.0437	0.51	0.47	99.60
	1	7.98	0.0436	0.50	0.46	99.58
III	2	9.02	0.0698	0.59	0.52	99.61
	3	7.98	0.0436	0.50	0.46	99.57
	4	8.33	0.0436	0.52	0.48	99.59

Table 3.4-2e Unit weight calculation (Test No. 5)

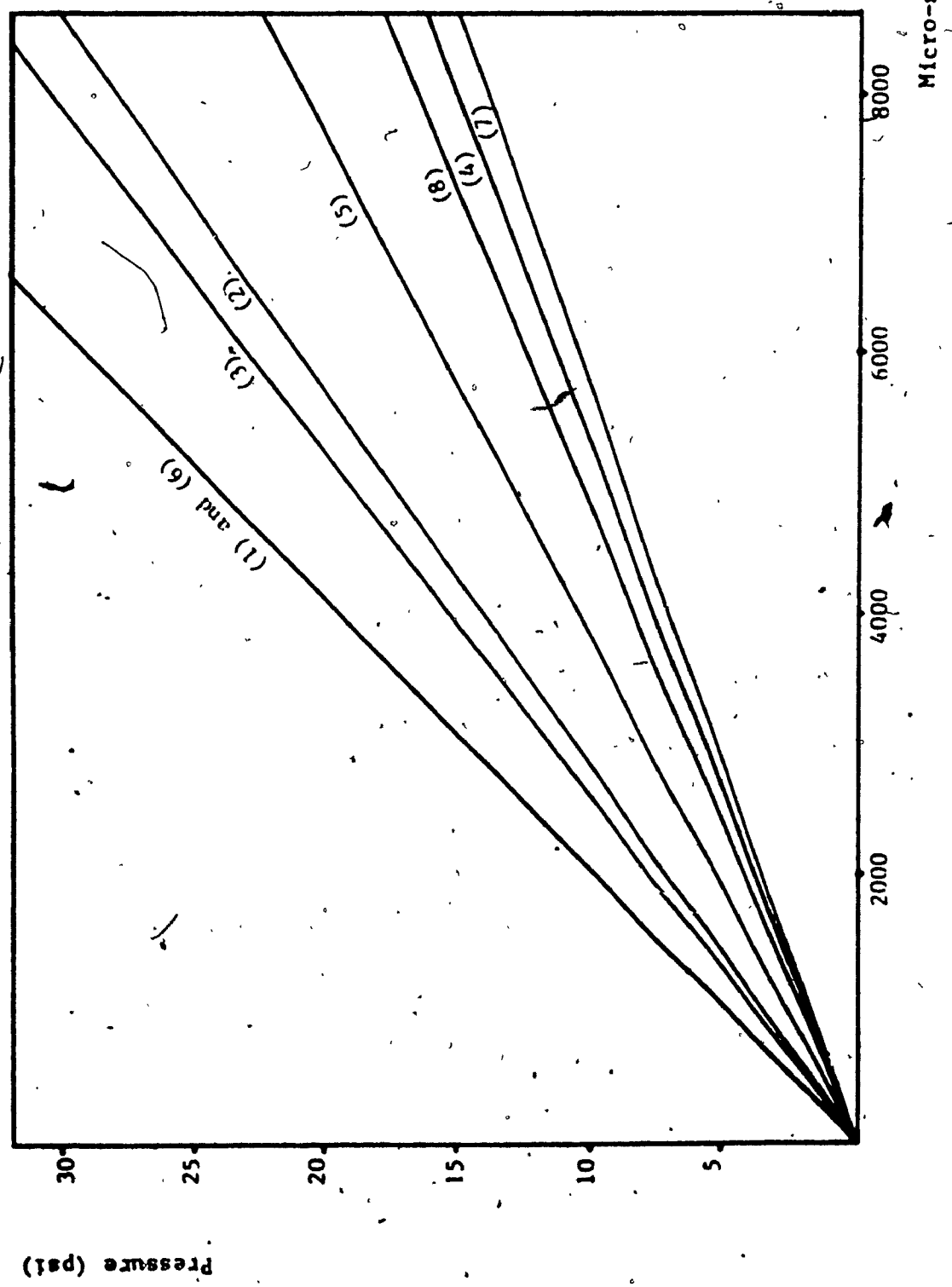

Figure 3.5-a: Calibration curves of tranducers number 1 to 8

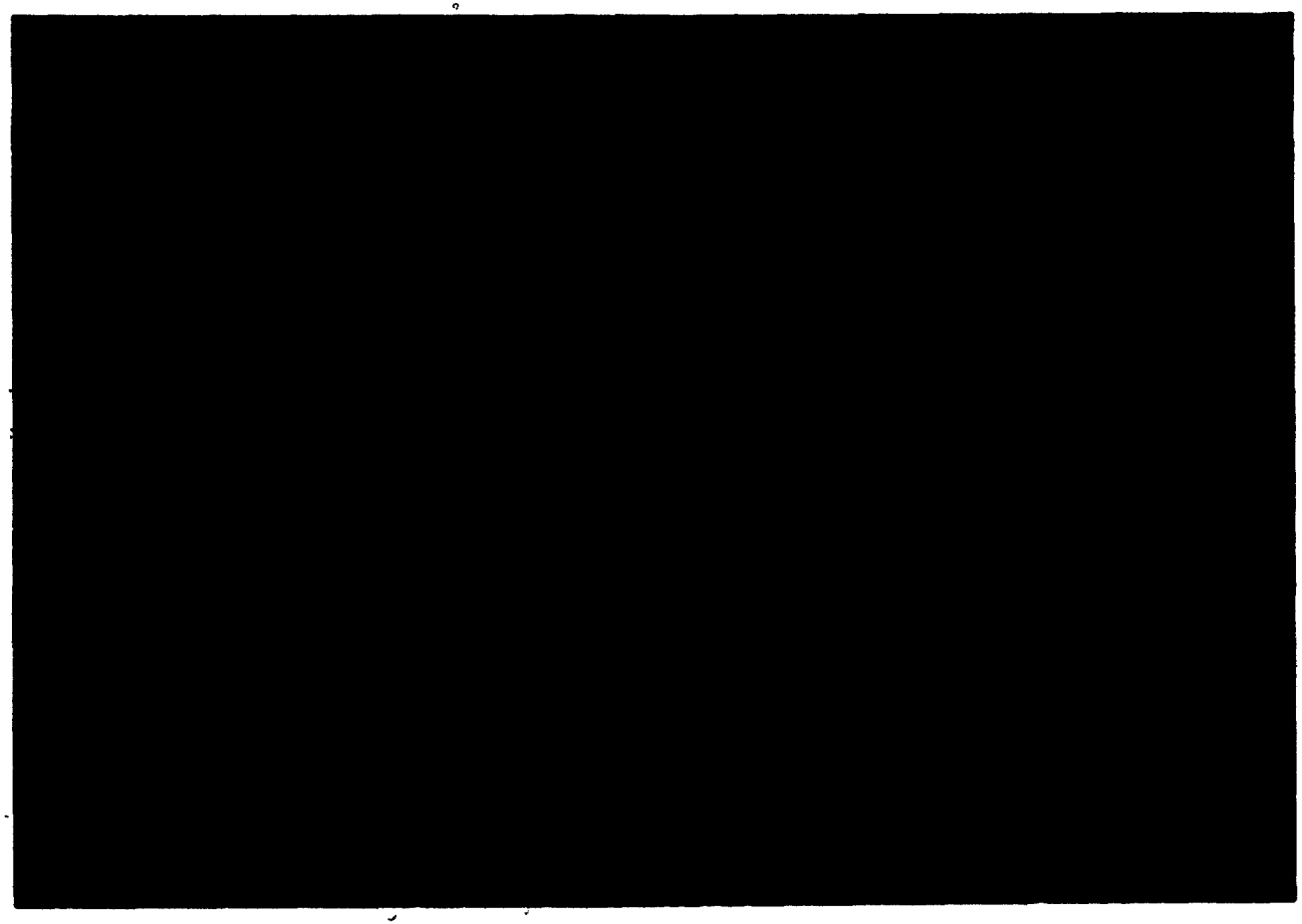

Figure 3.6-a: Load cell used in the measuring of frictional resistance

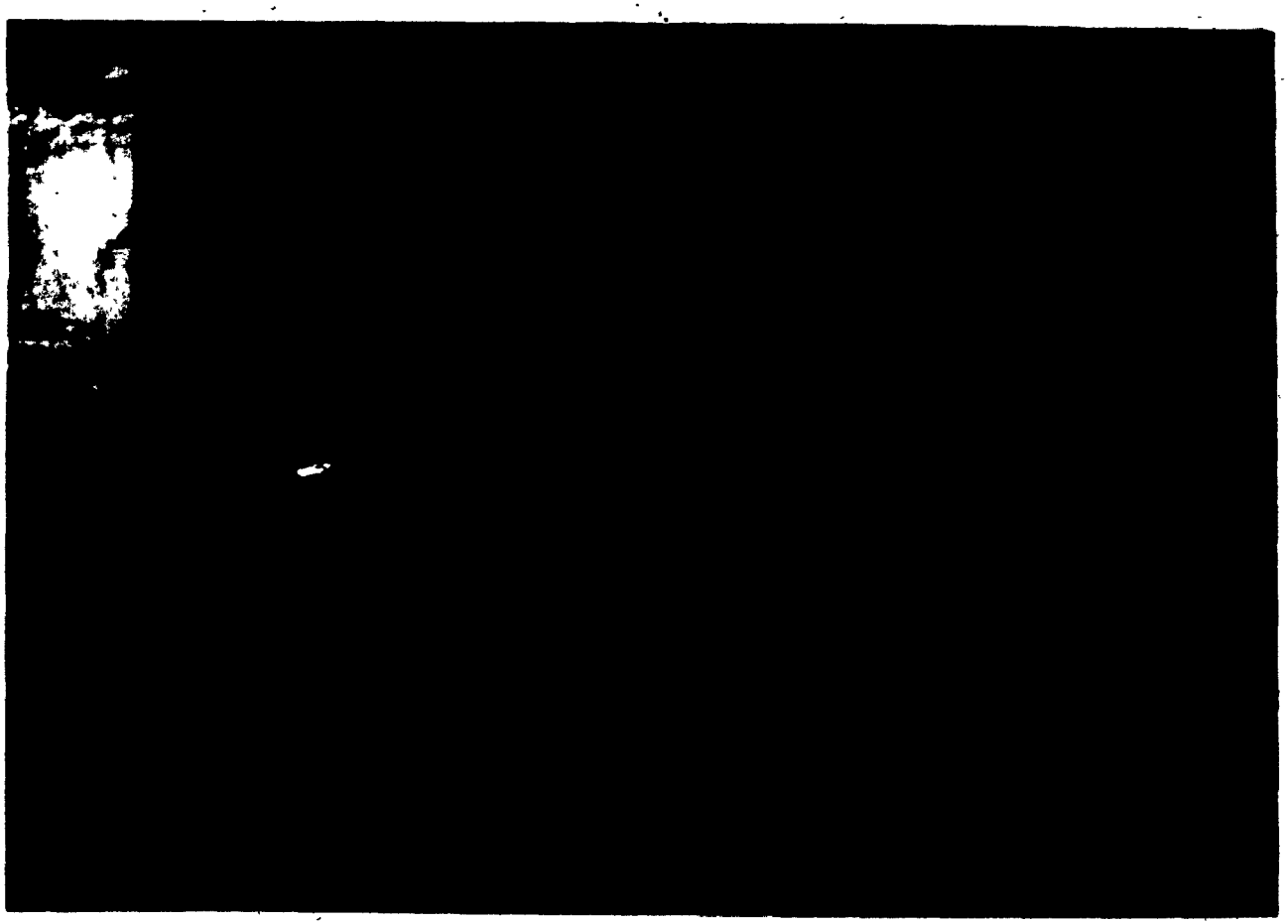

Figure 3.6-b: Top view of anchor subject to horizontal pull

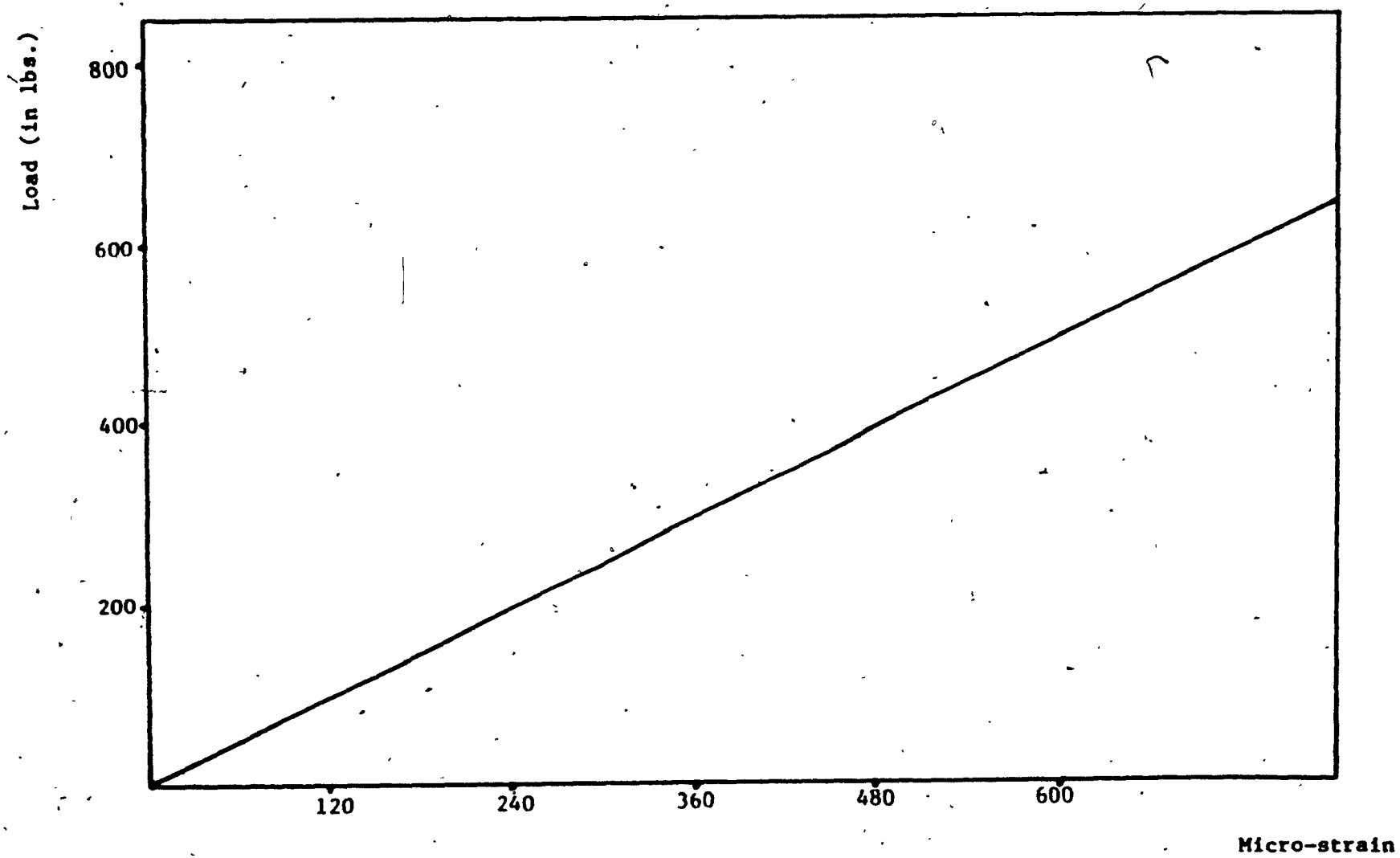

Figure 3.6-c: Load cell calibration

3.7 Testing Procedures

The main objective of this testing program was to study the effect of anchor embedment depth, anchor inclination (α_v) and anchor size on its anchor pullout capacity. In order to study the effect of the anchor embedment depth, at the beginning of each test the required height of sand was deposited by rain fall method in the box, the anchor plate with the tie rod was placed on top of the sand at the required fixed inclination (α_v), then sand placement was continued until the plate was buried at the required depth (D).

The pullout load on the anchor plate was applied by a motor (see section 3.2) at a constant displacement rate of (0.50 inch per minute). This displacement rate was chosen arbitrarily within the range of strain rate normally adopted for laboratory testing. Total pullout load, the passive earth pressure on the front side of the anchor and the displacement were monitored using a load cell, pressure Tranducers and dial gages respectively. Load cell details are shown in Figures 3.7-a to 3.7-c and Table 3.7-a.

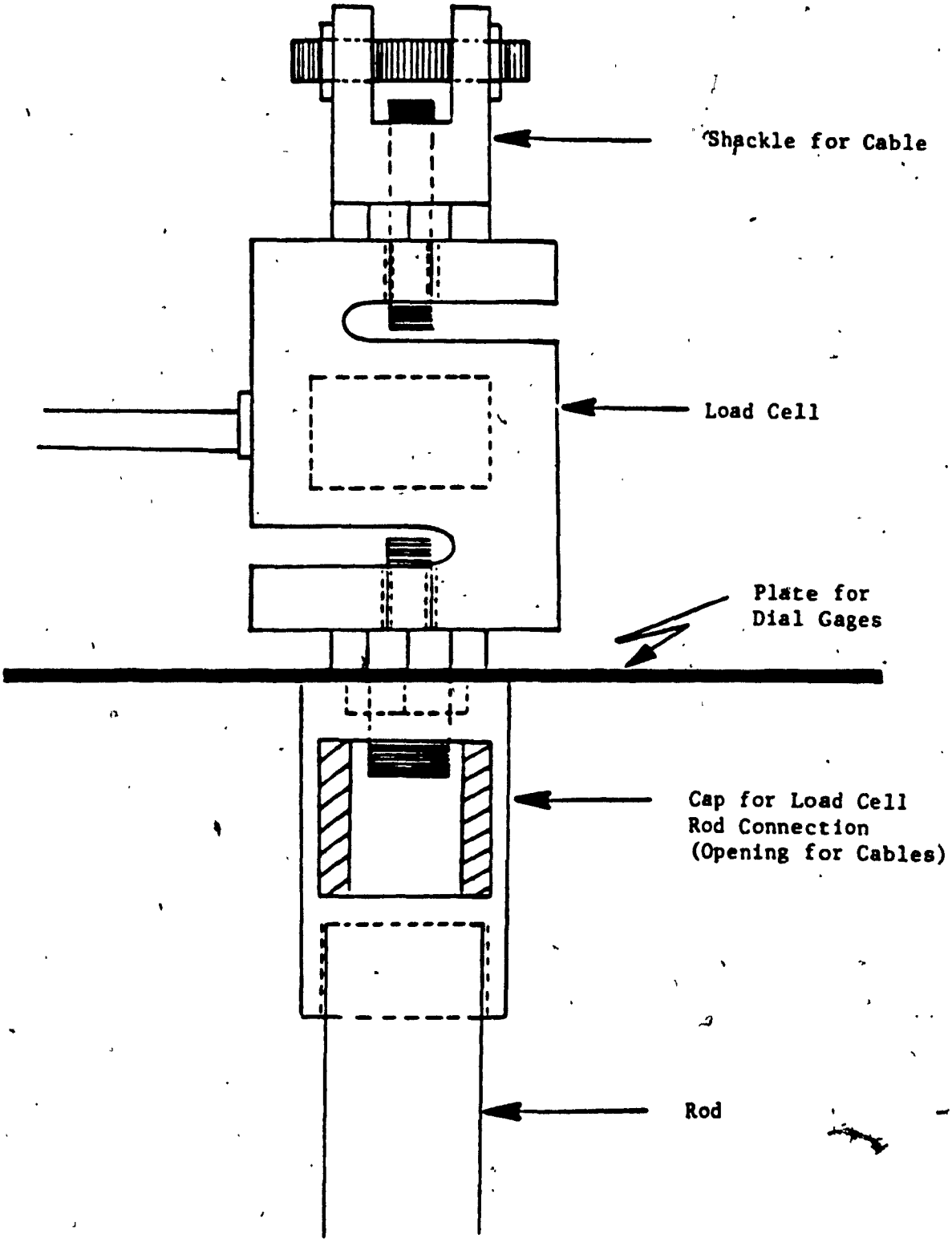

Figure 3.7-a: Cable Load Cell Connection

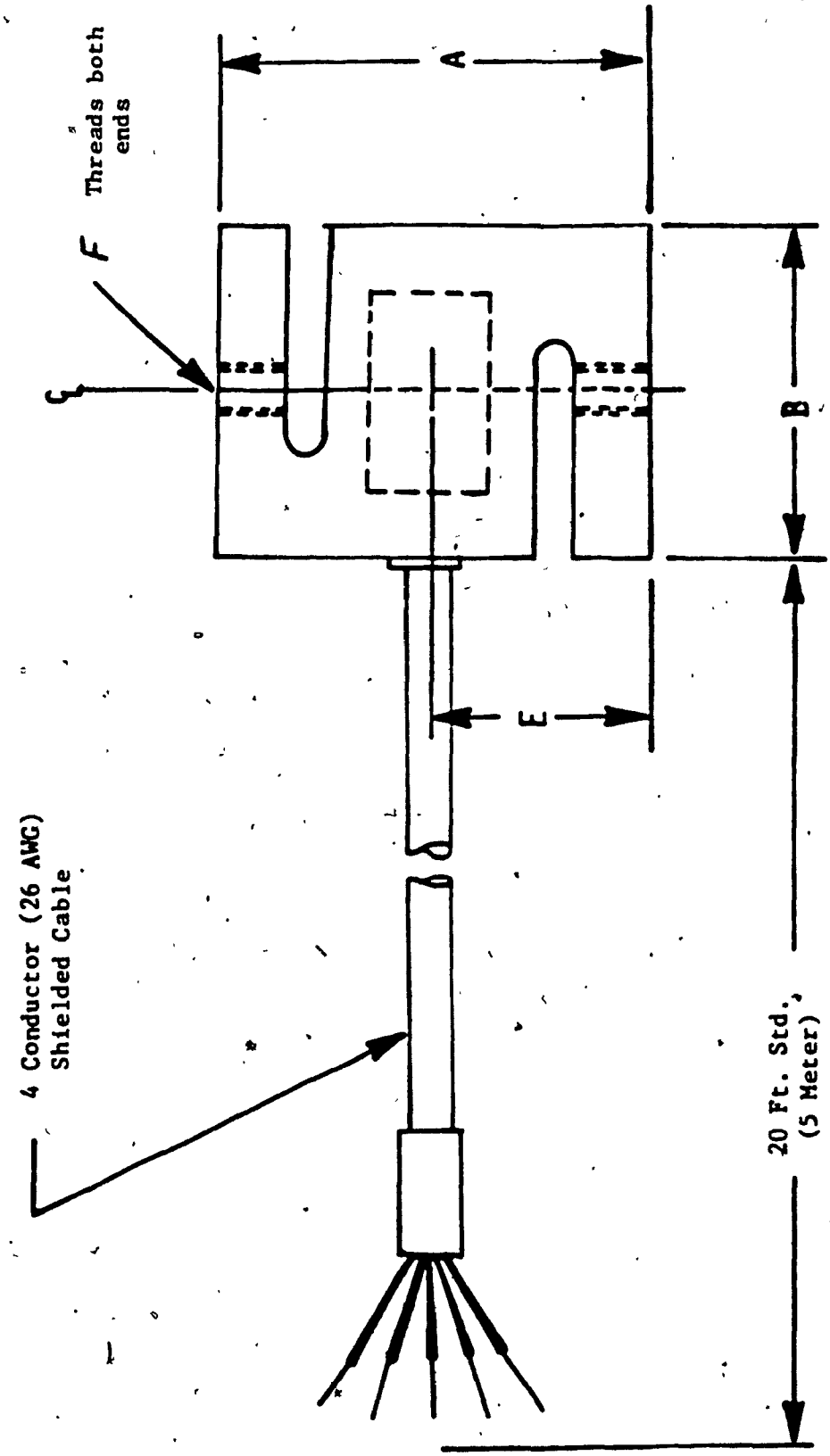

Figure 3.7-b: Load cell (side view)

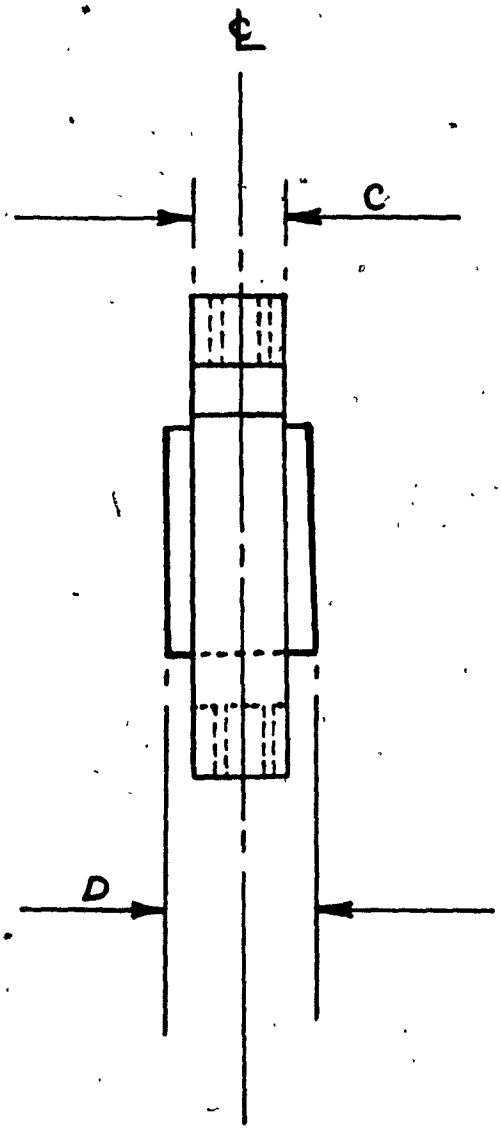

Figure 3.7-c: Load Cell (Front View)

PKG. SIZE	CAP. LBS. (kg or TON)	A	B	C	D max	E	F TH'D
2	600	2.50	2.00	0.75	1.00	1.25	
	(272.16)	(63.50)	(50.80)	(19.05)	(25.40)	(31.75)	1/2-20 UNF-2B

MECHANICAL RATINGS		
STD. CAP. LBS. (Kg or TON)	DEFLECTION (In. or MM)	WT. LBS. (kg)
600	.015	1
(272.16)	(.38)	(.5)

Table 3.7-a: Load Cell Details

CHAPTER IV

EXPERIMENTAL RESULTS

4.1 General

Structures such as: bulkheads, suspension bridges, antenna towers, mobile homes and pipeline bends, their foundation stabilities are commonly designed using classical theories which based on simplified assumptions which are now considered to be inadequate, and may lead to incorrect predictions in design. Thus full scale field tests are the ideal method for obtaining data. However, cost, the time consumed, and the difficulty in controlling the test conditions greatly reduce the viability of such field tests. Although there are no fully adequate substitutes for full-scale field tests, tests at Laboratory scale could provide very useful data, and close control of the most important variables encountered in practice.

Numerous attempts have been made in the past to develop analytical solutions to the problem under investigation, nevertheless most of the previous experimental work done showed some limitations such as:

a. Most of the experiments were conducted on vertical anchors and some on horizontal, whereas very few on inclined anchors.

b. Very small model anchor plates were used. For example the height of the plate is 25.0 mm (0.985 inch) Ranjan & Kaushal (1973), 25.4 mm (1.0 inch) Meyerhof (1973) and 38.05 mm (1.5 inch) Wang and Wu (1980).

c. The pullout load in most of the previous experimental work was applied by adding weights on a hanger attached to one end of a wire which hooked to the tie rod of the anchor from the other end where that could cause fictitious results.

d. In most of the previous work done the side friction in plane strain tests has been ignored, where that could affect the values of pullout resistance.

In order to avoid these limitations, and to develop a better understanding of anchor behaviour in sand, the present experimental study on model plate anchors in sand was carried out with care and a great deal of reliability.

4.2 Results of Plate Anchor A (6 inch)

The experimental results of this anchor plate are summarized in Tables 4.2-a, 4.2-b and 4.2-c, also the curves of ultimate load per anchor for all tests of this plate anchor are shown in Figures 4.2-1 through 4.2-5.

4.3 Test Results of Plate Anchor B (4 inch)

The experimental test results of plate anchor B (4 inch x 6 inch) are summarized in Tables 4.3-a, 4.3-b and 4.3-c. Curves of ultimate load per anchor versus displacement are shown in Figures 4.3-1, 4.3-2 and 4.3-3.

4.4 Test Results of Plate Anchor C (2 inch)

The experimental test results of plate anchor C (2 inch x 6 inch) are summarized in Table 4.4-a, also curves of ultimate load per anchor versus displacement are shown in Figures 4.4-1 through 4.4-5.

Series	Test No.	α_v Degrees	Depth D Inch	Plate Height H Inch	$\frac{D}{H}$	Loadcell Readings Q_{tot} lb(kg)	Integration of pressure Transducers Q_{net} lb(kg)	Friction Resistance $Q_{tot} - Q_{net}$ lb(kg)	Failure Displacement inch
A	1	0	12	6.0	2.0	57.420 (26.045)	43.570 (19.763)	13.850 (6.282)	0.450
	2	30	"	"	"	65.060 (29.511)	49.850 (22.611)	15.210 (6.899)	0.750
	3	45	"	"	"	108.570 (49.247)	89.650 (40.665)	18.920 (8.582)	0.800
	4	60	"	"	"	188.760 (85.621)	168.430 (76.399)	20.330 (9.221)	0.950
	5	90	"	"	"	340.200 (154.314)	317.250 (143.904)	22.950 (10.410)	0.970

Table 4.2-a: Summary of test results for plate A (6 inch x 6 inch)

Series	Test No.	α_v Degrees	Depth D inch	Plate Height H inch	$\frac{D}{H}$	Loadcell Readings Q_{tot} lb(kg)	Integration of pressure Transducers Q_{net} lb(kg)	Friction Resistance $Q_{tot} - Q_{net}$ lb(kg)	Failure Displacement inch
A	6	0	18.00	6.0	3.00	90.680 (41.132)	74.700 (33.884)	15.980 (7.248)	0.700
	7	30	"	"	"	102.490 (46.489)	85.800 (38.918)	16.690 (7.570)	0.900
	8	45	"	"	"	173.340 (78.629)	153.150 (69.468)	20.190 (9.158)	1.100
	9	60	"	"	"	264.286 (119.880)	242.736 (110.105)	21.550 (9.775)	1.250
	10	90	"	"	"	538.830 (244.413)	514.80 (233.513)	24.030 (10.900)	1.400

Table 4.2-b: Summary of test results for plate A (6 inch x 6 inch)

Series	Test No.	α_v Degrees	Depth D Inch	Plate Height H Inch	$\frac{D}{H}$	Loadcell Readings Q_{tot} lb(kg)	Integration of pressure Transducers Q_{net} lb(kg)	Friction Resistance $Q_{tot} - Q_{net}$ lb(kg)	Failure Displacement inch
A	11	0	24.00	6.0	4.00	141.610 (64.234)	124.500 (56.473)	17.110 (7.761)	0.900
	12	30	"	"	"	176.610 (80.228)	158.950 (72.099)	17.920 (8.128)	1.150
	13	45	"	"	"	283.320 (128.514)	261.450 (118.593)	21.870 (9.920)	1.350
	14	60	"	"	"	502.030 (227.720)	478.890 (217.224)	23.140 (10.496)	1.450
		90	"	"	"				

Table 4.2-c: Summary of test results for plate A (6 inch x 6 inch)

Series	Test No.	α_v Degrees	Depth D Inch	Plate Height H Inch	$\frac{D}{H}$	Loadcell Readings Q_{tot} lb(kg)	Integration of pressure Transducers Q_{net} lb(kg)	Friction Resistance $Q_{tot} - Q_{net}$ lb(kg)	Failure Displacement inch.
B	15	0	13.00	4.0	3.25	52.935 (24.011)	40.195 (18.232)	12.740 (5.778)	0.350
	16	30	"	"	"	58.678 (26.616)	45.038 (20.429)	13.640 (6.1871)	0.500
	17	45	"	"	"	99.936 (45.331)	83.015 (37.655)	16.921 (7.675)	0.550
	18	60	"	"	"	176.178 (79.914)	157.208 (71.309)	18.970 (8.604)	0.800
	19	90	"	"	"	344.942 (156.465)	324.060 (146.993)	20.882 (9.472)	0.850

Table 4.3-a: Summary of test results for plate B (4 inch x 6 inch)

Series	Test No.	α_v Degrees	Depth D Inch	Plate Height H Inch	$\frac{D}{H}$	Loadcell Readings Q_{tot} lb(kg)	Integration of pressure Transducers Q_{net} lb(kg)	Friction Resistance $Q_{tot} - Q_{net}$ lb(kg)	Failure Displacement inch
B	20	0	19.00	4.0	4.75	88.199 (30.970)	73.098 (33.157)	15.021 (6.813)	0.600
	21	30	"	"	"	103.809 (47.087)	87.702 (39.781)	16.107 (7.306)	0.800
	22	45	"	"	"	170.991 (77.561)	151.093 (68.535)	19.898 (9.025)	0.85
	23	60	"	"	"	322.480 (146.277)	299.830 (136.002)	22.650 (10.274)	1.150
	-	90	"	"	"	-	-	-	-

Table 4.3-b: Summary of test results for plate B (4 inch x 6 inch)

Series	Test No.	α_v Degrees	Depth D Inch	Plate Height H Inch	$\frac{D}{H}$	Loadcell Readings Q_{tot} lb(kg)	Integration of pressure Transducers Q_{net} lb(kg)	Friction Resistance $Q_{tot} - Q_{net}$ lb(kg)	Failure Displacement inch
B	24	0	25.00	4.0	6.75	128.228 (58.164)	12.190 (50.934)	15.938 (7.229)	0.900
	25	30	"	"	"	154.588 (70.121)	138.795 (62.957)	15.793 (7.163)	1.100
	26	45	"	"	"	264.728 (120.080)	247.369 (112.206)	17.359 (7.874)	1.150
	27	60	"	"	"	512.088 (232.283)	489.907 (222.221)	22.181 (10.061)	1.250
	-	90	"	"	"	-	-	-	-

Table 4.3-c: Summary of test results for plate B (4 inch x 6 inch)

Series	Test No.	α_v Degrees	Depth D Inch	Plate Height H Inch	$\frac{D}{H}$	Loadcell Readings Q_{tot} lb(kg)	Integration of pressure Transducers Q_{net} lb(kg)	Friction Resistance $Q_{tot} - Q_{net}$ lb(kg)	Failure Displacement inch
C	28	0	14.00	2.0	7.0	46.714 (21.189)	35.729 (16.206)	10.985 (4.982)	0.400
	29	30	"	"	"	56.341 (25.562	44.112 (20.009)	12.229 (5.547)	0.450
	30	45	"	"	"	83.983 (38.094)	68.949 (31.275)	15.034 (6.819)	0.700
	31	60	"	"	"	166.818 (72.668)	149.824 (67.960)	16.994 (7.708)	0.800
	32	90	"	"	"	280.861 (127.398)	261.915 (118.804)	18.946 (8.594)	0.950

Table 4.4-a: Summary of test results for plate C (2 inch x 6 inch)

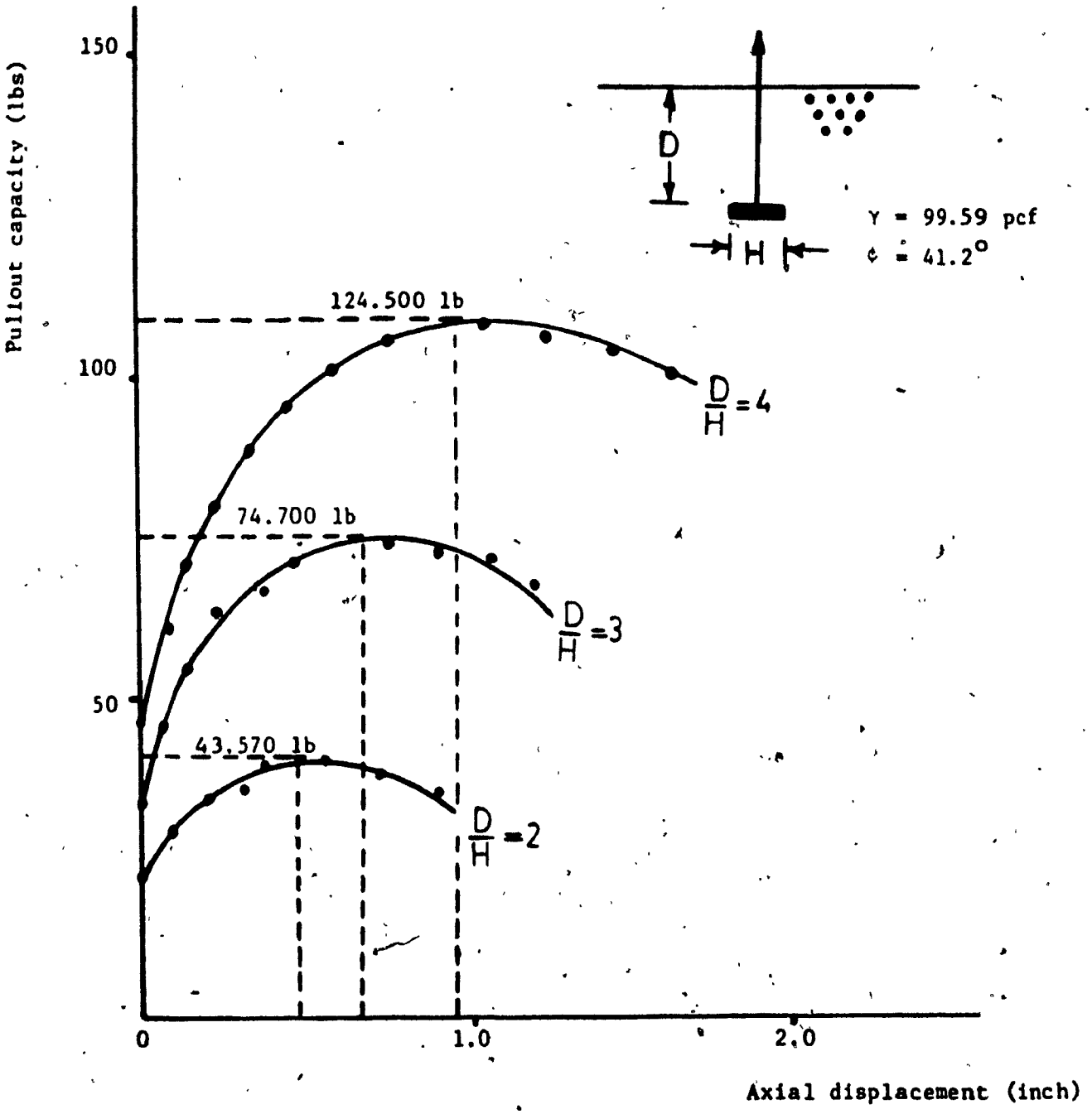

Figure 4.2-1: Axial displacement vs. pullout capacity for plate A (6" x 6"), $\alpha_v = 0$

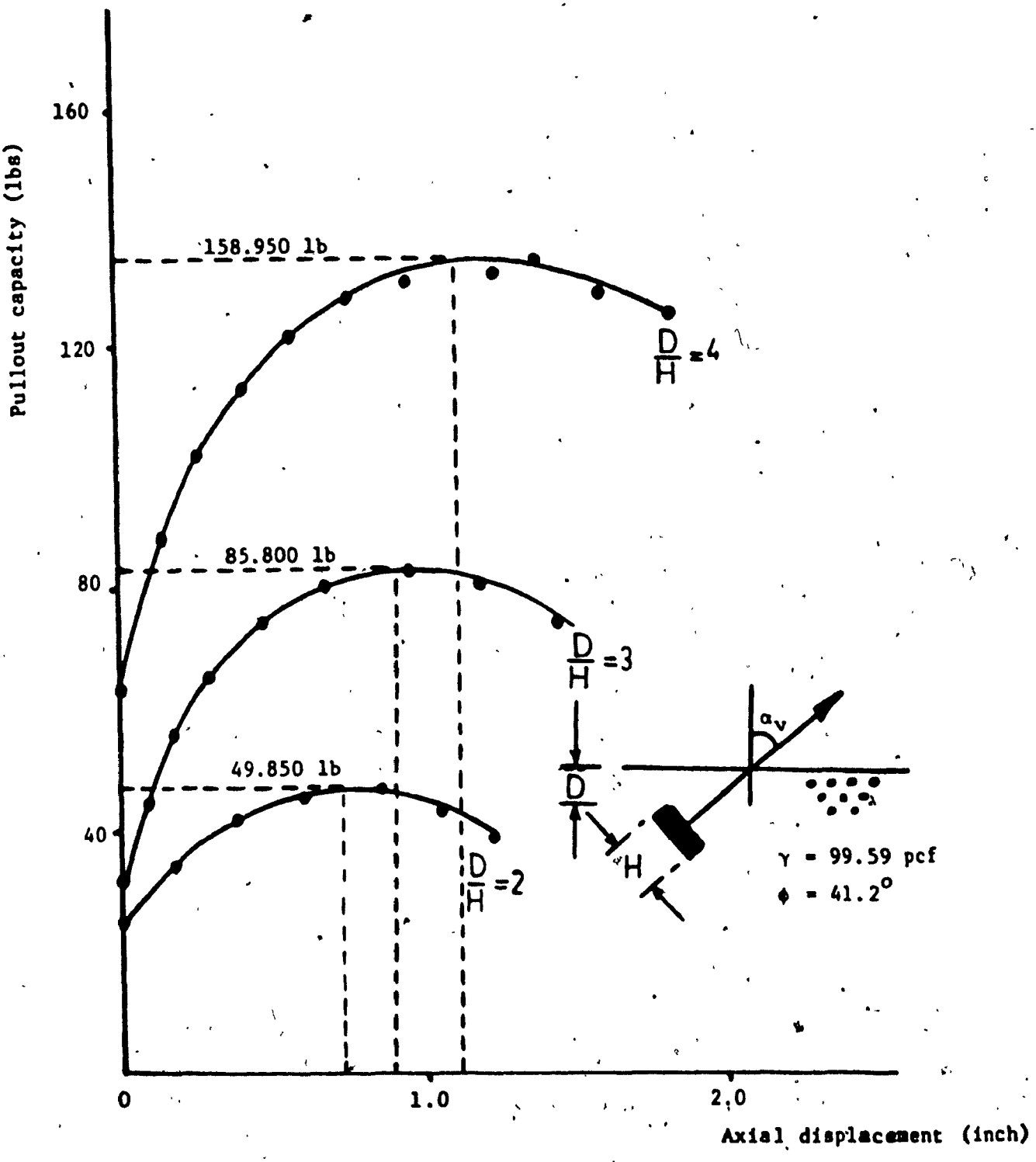

Figure 4.2-2: Axial displacement vs. pullout capacity for plate A(6" x 6"), $\alpha_v = 30^0$

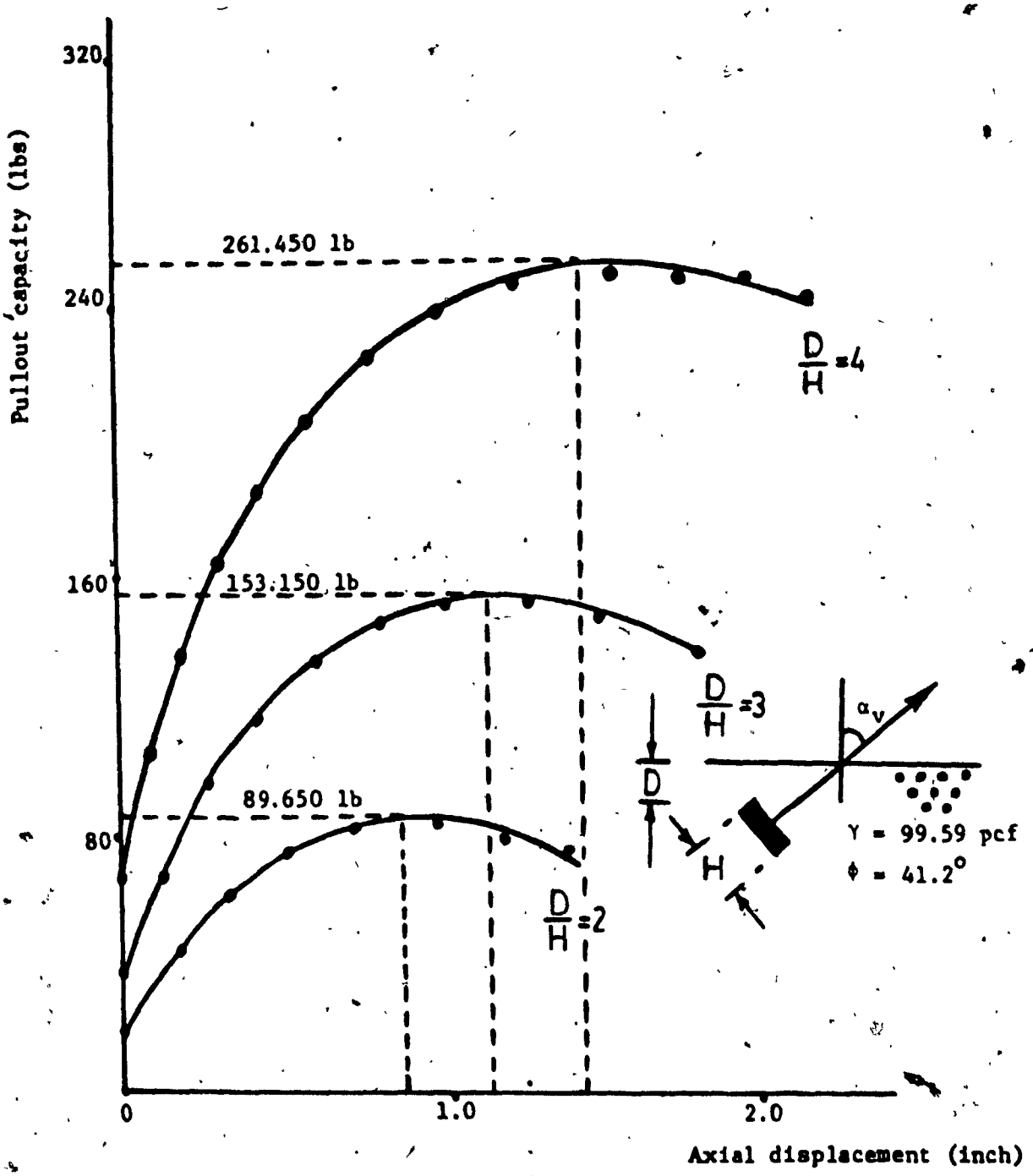

Figure 4.2-3: Axial displacement vs. pullout capacity for plate A (6" x 6"), $\alpha_v = 45^o$

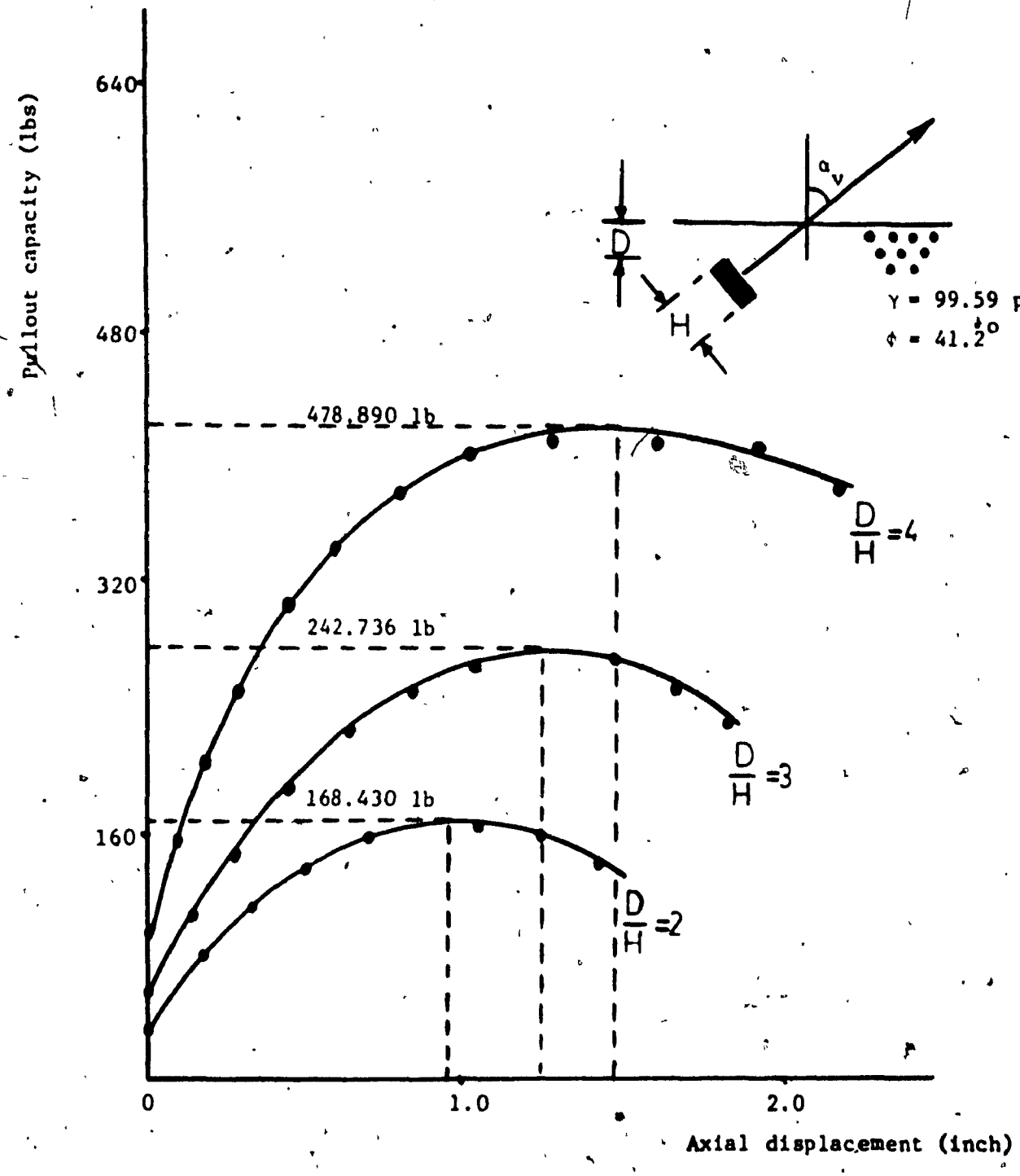

Figure 4.2-4: Axial displacement vs. pullout capacity for plate A (6" x 6"), $\alpha_v = 60^o$

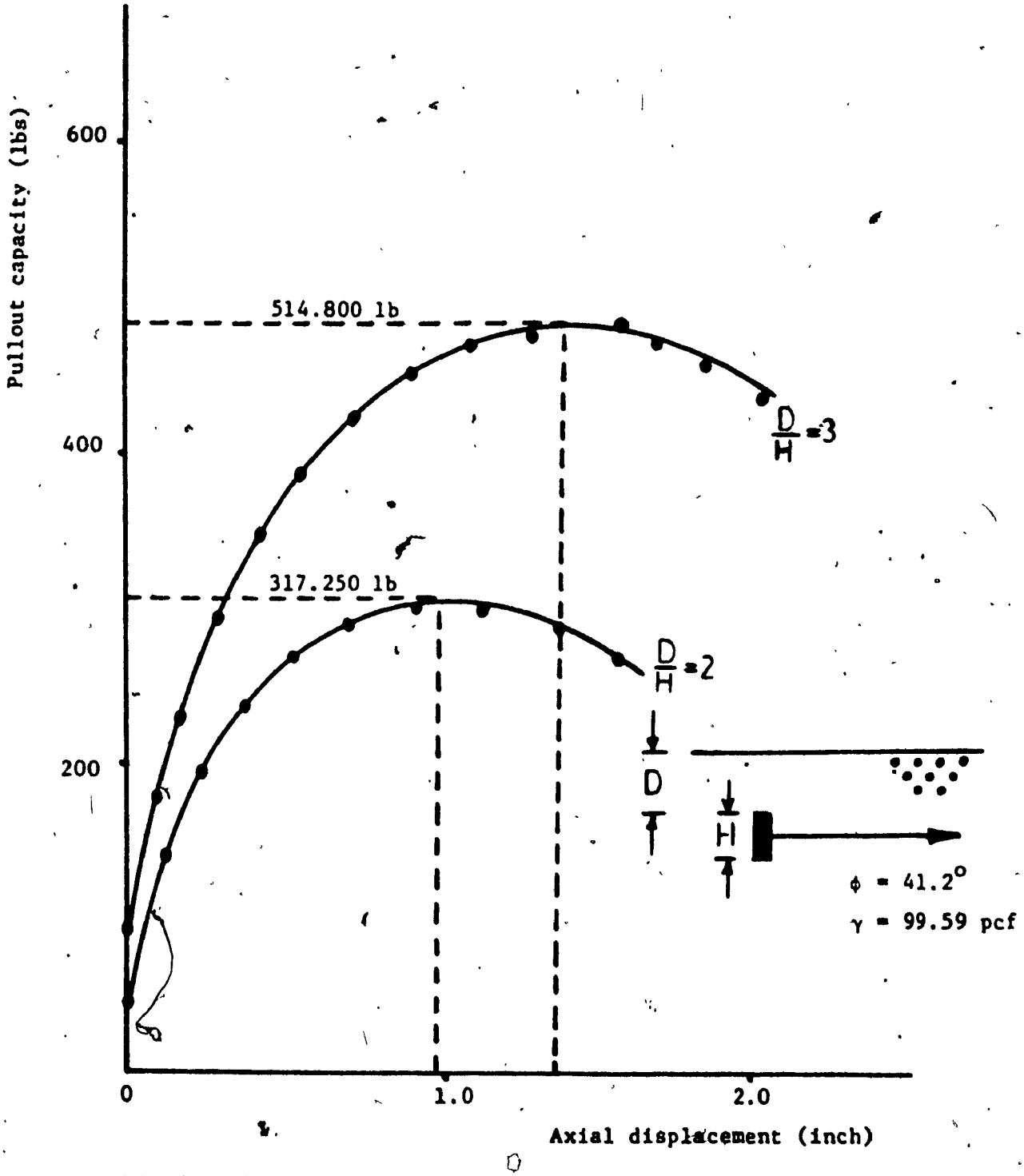

Figure 4.2-5: Axial displacement vs. pullout capacity for plate anchor A (6" x 6"), $\alpha_v = 90^o$

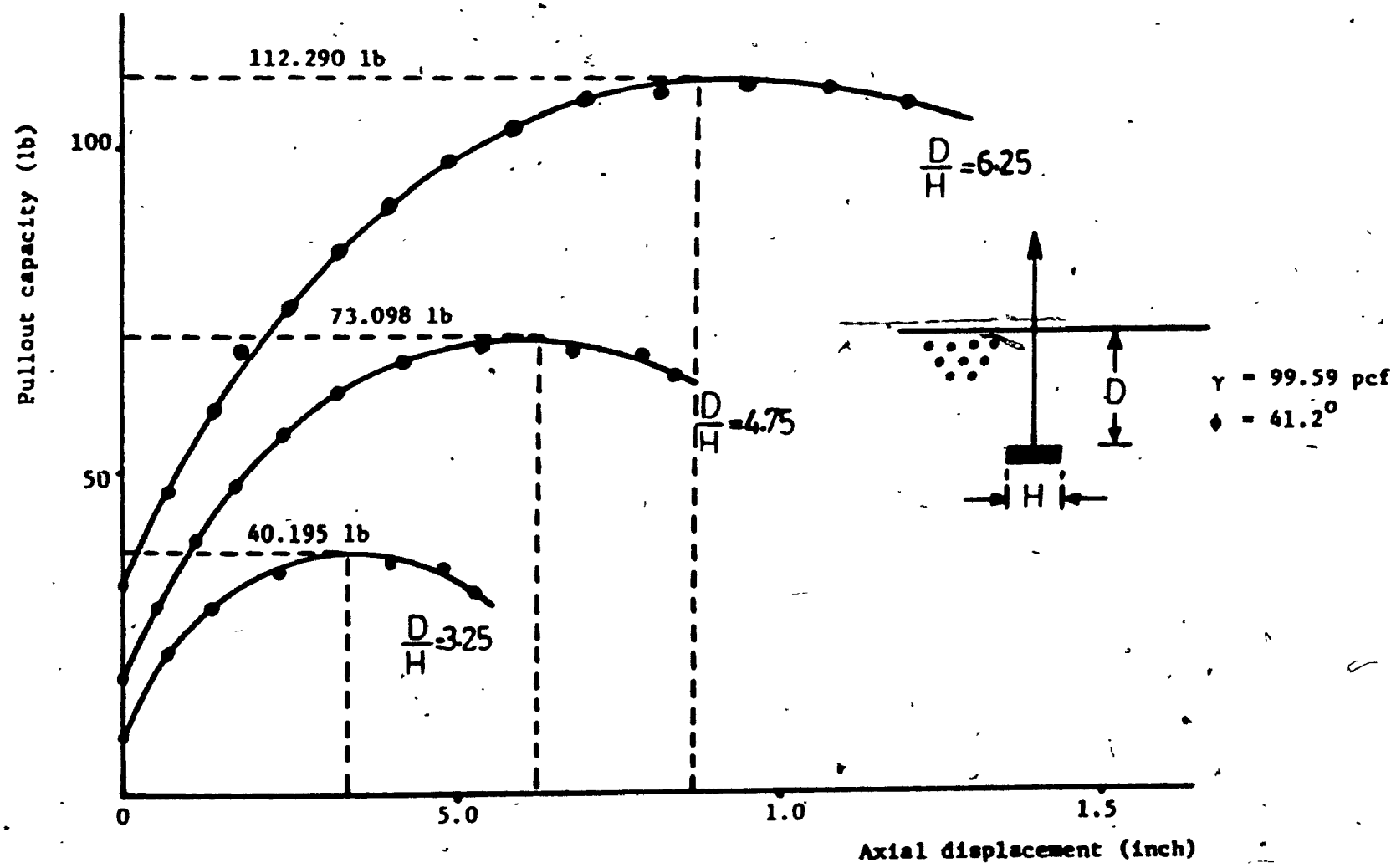

Figure 4.3-1: Axial displacement vs. pullout capacity for plate B (4" x 6"), $\alpha_v = 0$

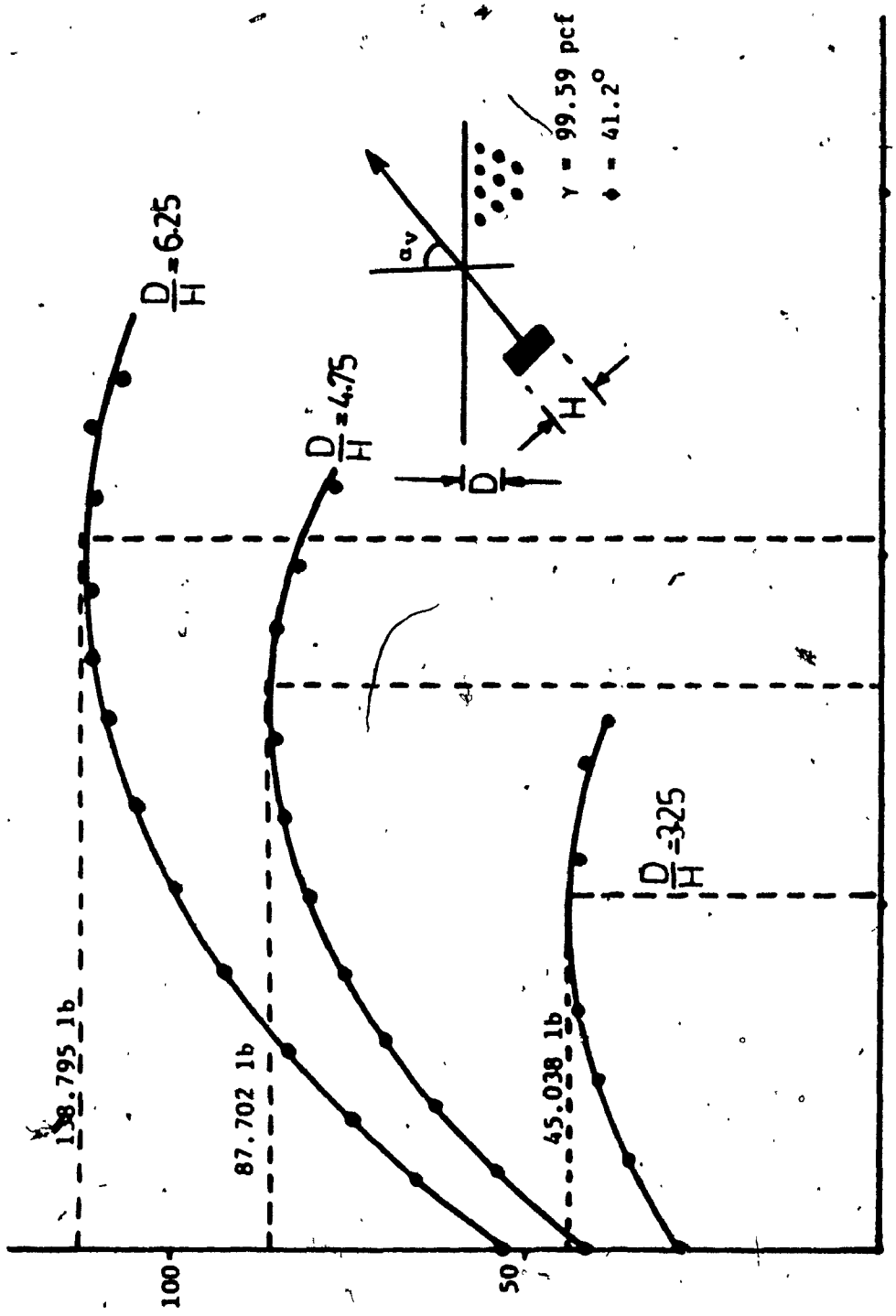

Figure 4.3-2: Axial displacement vs. pullout capacity for plate B(4" x 6"), $\alpha'_v = 30^\circ$

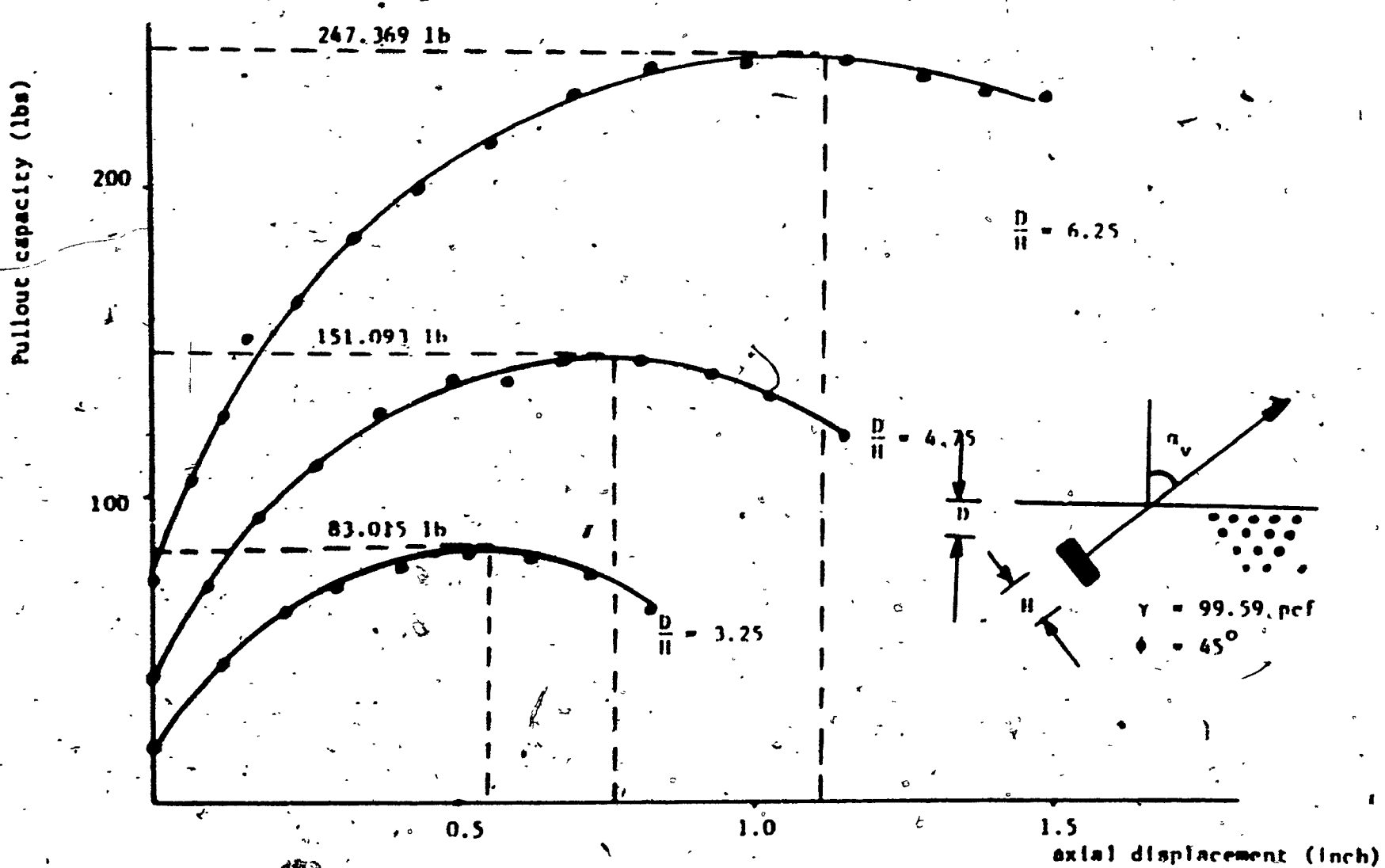

Figure 4.3-3 Axial displacement vs pullout capacity for plate B(4" x 6"), α_v = 45°

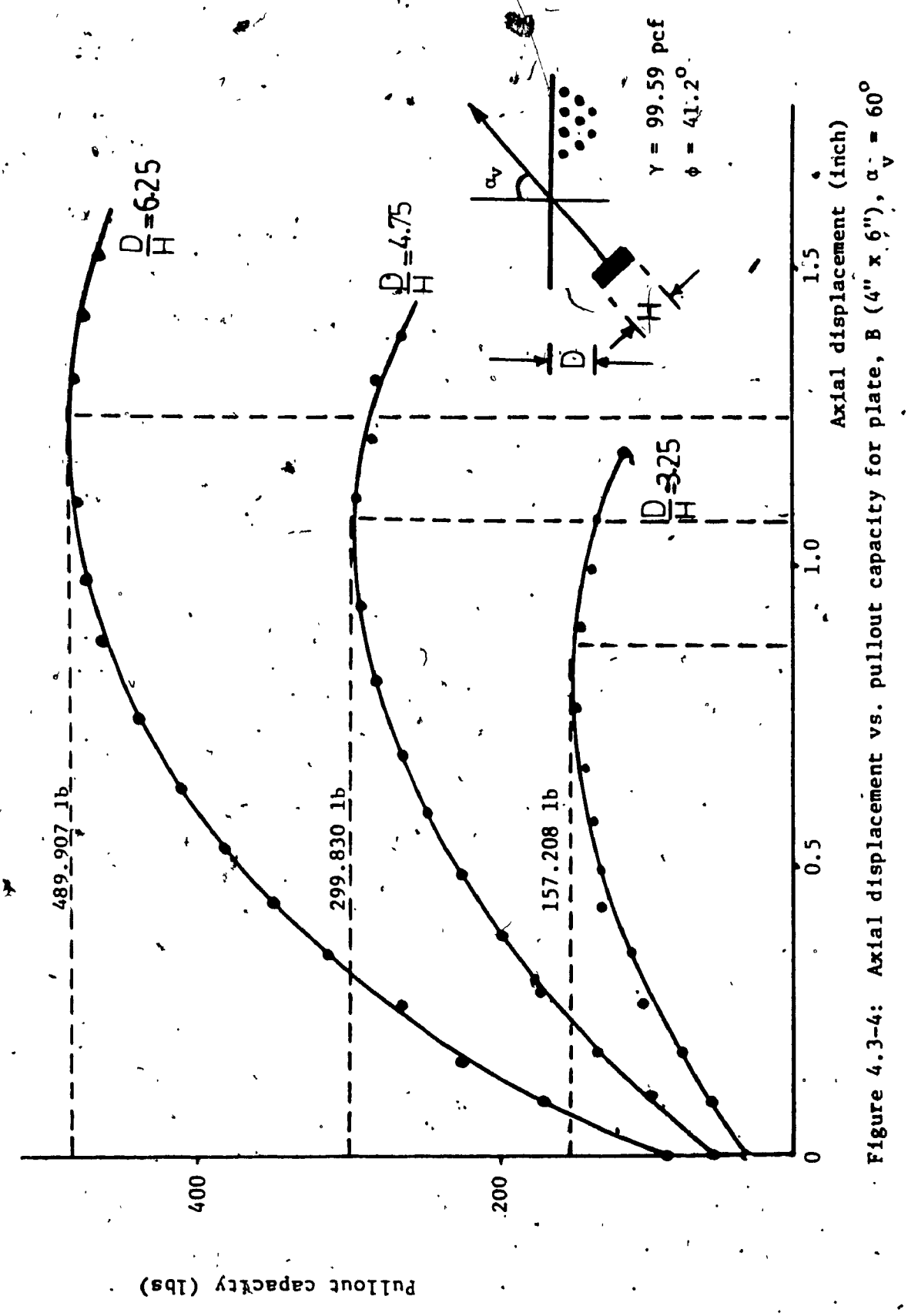

Figure 4.3-4: Axial displacement vs. pullout capacity for plate, B (4" x 6"), α_v = 60°

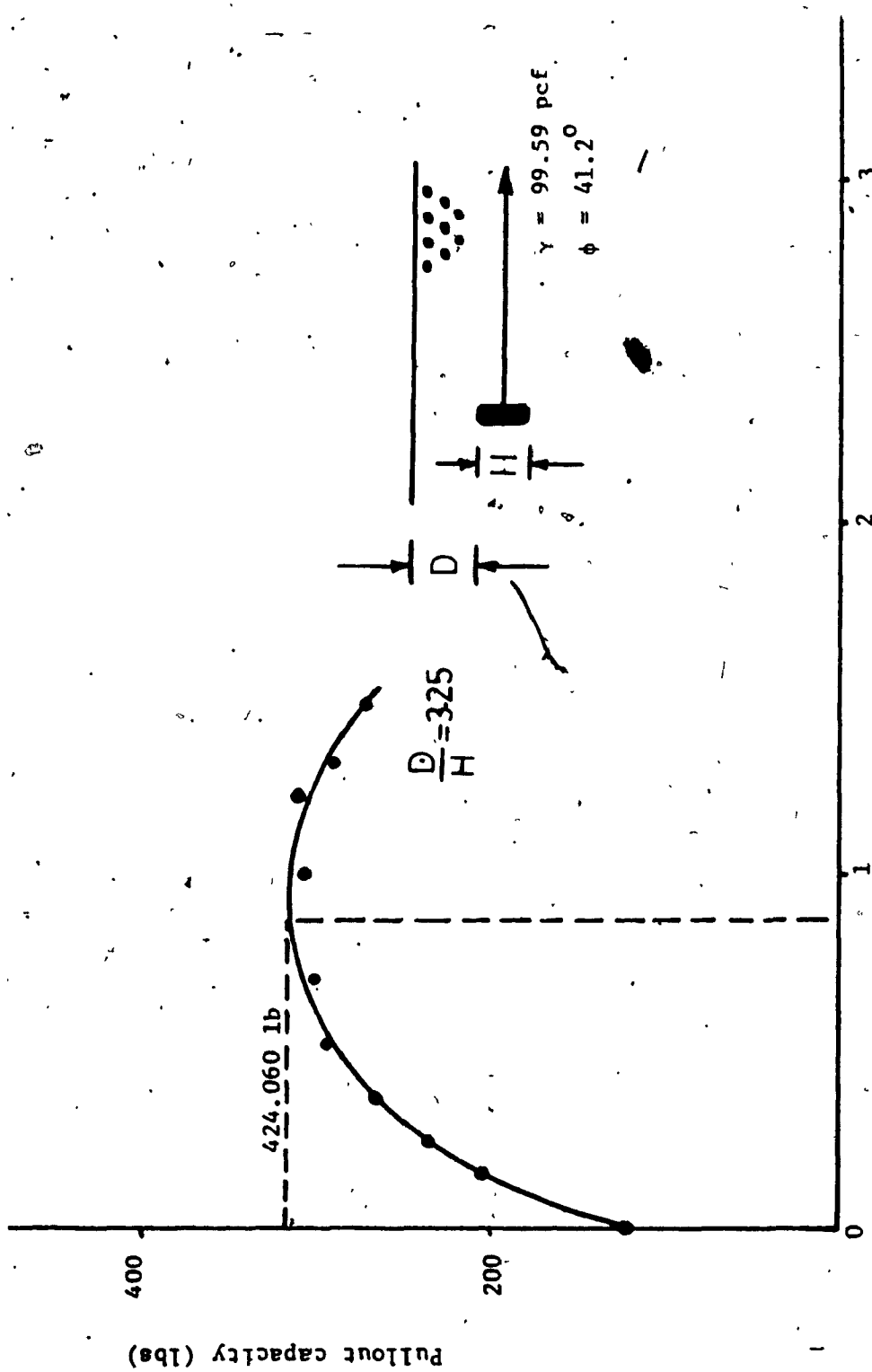

Figure 4.3-5: Axial displacement vs. pullout capacity for plate B (4" x 6"), $\alpha_v = 90^\circ$

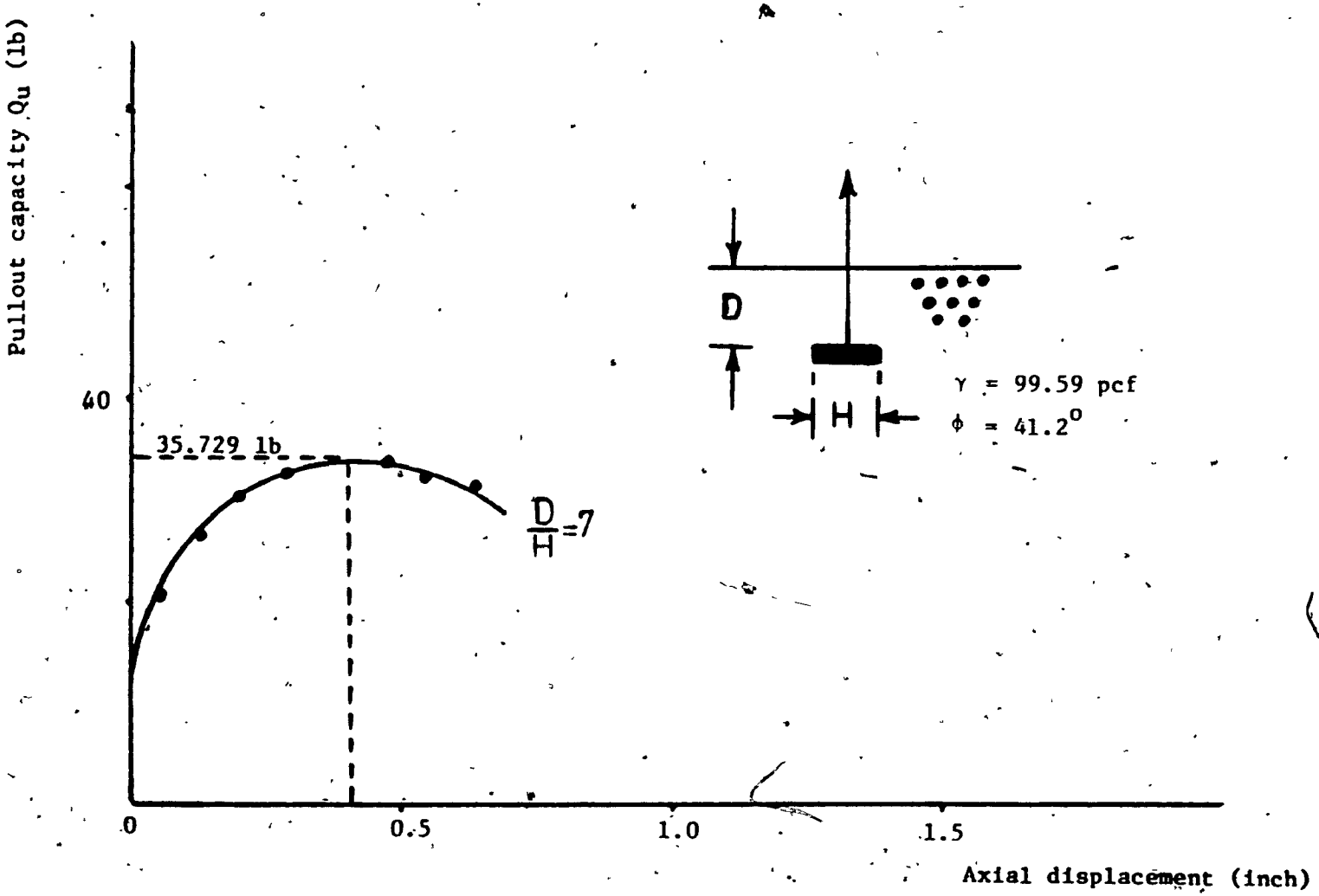

Figure 4.4-1: Axial displacement vs. pullout capacity for plate C (2" x 6"), $\alpha_v = 0$

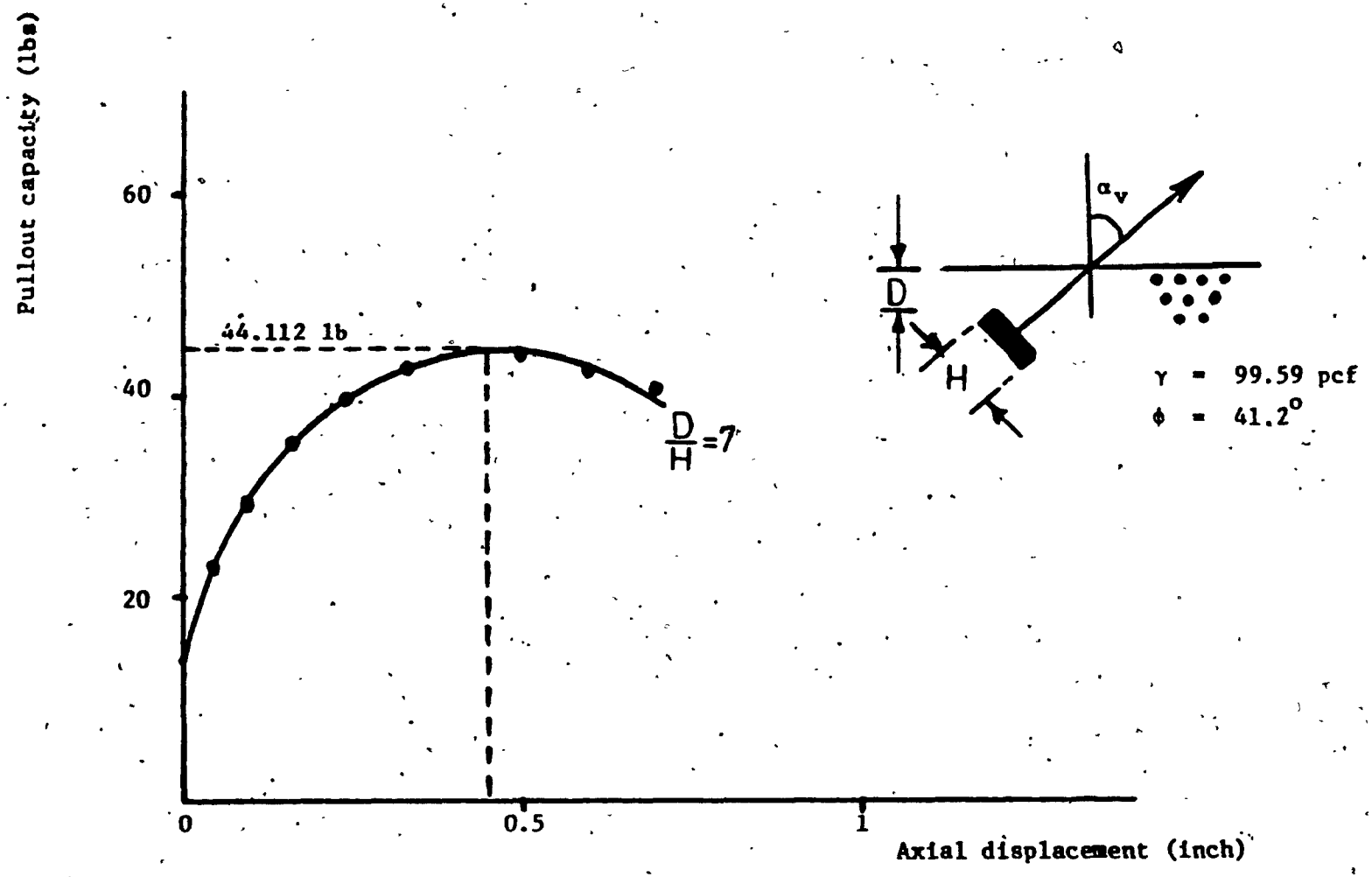

Figure 4.4-2: Axial displacement vs. pullout capacity for plate C (2" x 6"), $\alpha_v = 30^\circ$

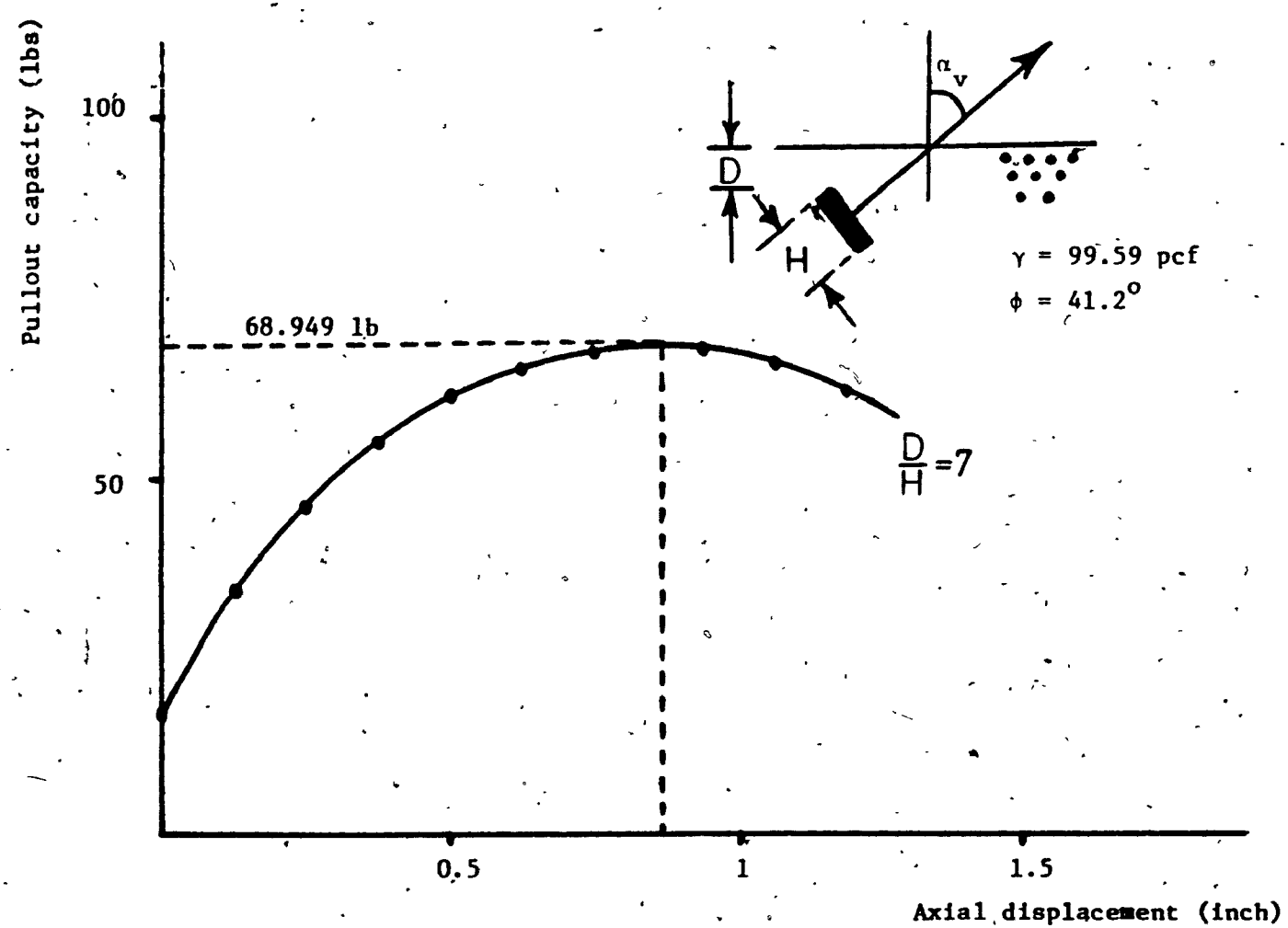

Figure 4.4-3: Axial displacement vs. pullout capacity for plate C (2" x 6"), $\alpha_v = 45^o$

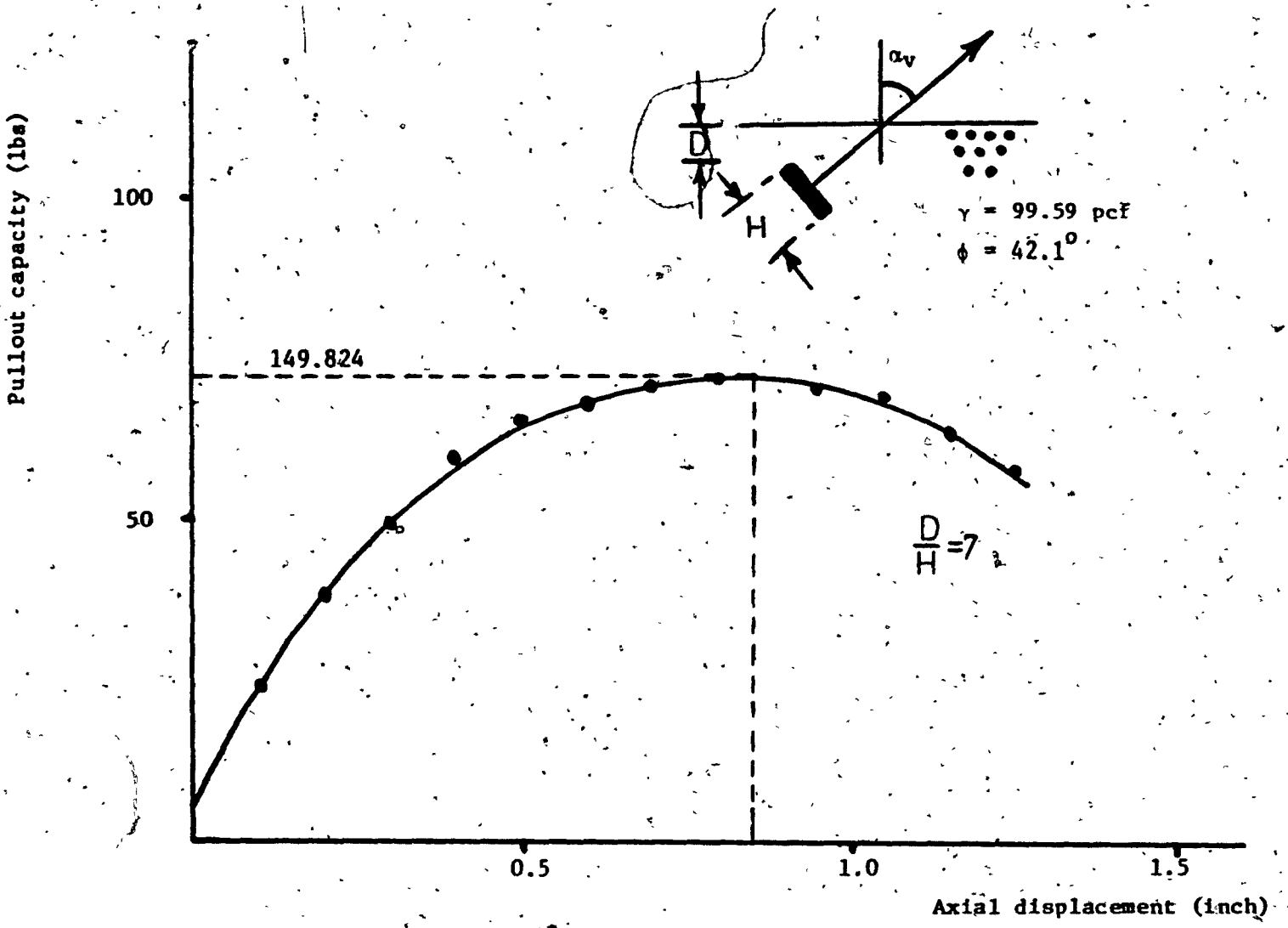

Figure 4.4-4: Axial displacement vs. pullout capacity for plate C (2" x 6"), $\alpha_v = 60^\circ$

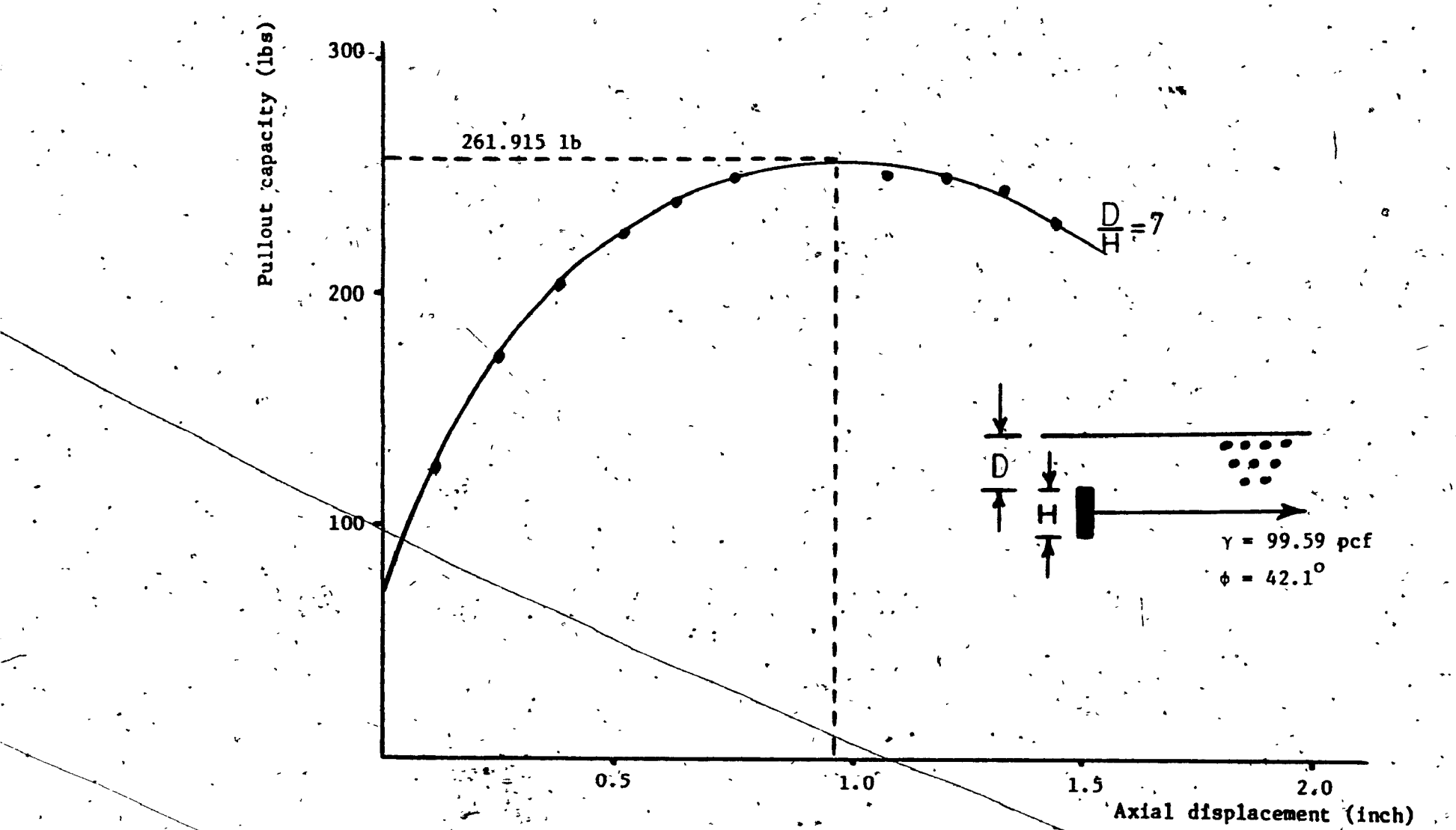

Figure 4.4-5: Axial displacement vs. pullout capacity for plate C (2" x 6") $\alpha_v = 90^o$

4.5 Anchor Failure Mechanism

During the stages of anchor plate loading, the development of failure surfaces were carefully examined through the plexiglass-sided test tank. It has been observed that for anchor inclination angle $30 < \alpha_v \leq 90$ degrees, there is a cavity initiated behind the anchor plate, when it had only slightly moved due to a small magnitude of pullout force. As the pullout force increases the cavity behind the anchor plate enlarges, and soil from the top starts to fill in the cavity. The active zone extends progressively, and the surfaces bcd and ag develop, as shown in the schematic figure 4.5-a. Up to this early stage of loading there is practically no effect on the passive zone except that the soil in front of the plate probably compresses. With further travel of the anchor plate, the passive planes of rupture begin to develop progressively towards the surface. Numerous minor planes could be found within the pattern. Any further movement of the anchor plate did not result in significant changes in the pattern, but the planes of rupture became more prominent. For anchor inclination angle $0 \leq \alpha_v \leq 30$ degrees, the failure surfaces are initiated at the bottom and the top of the plate at smaller deformations. Once the pattern started to develop, the whole plane of rupture formed almost instantaneously particularly at very shallow depths. (Figure 4.5-b.) Almost in all tests, the edge of the passive plane of the pattern on the sand surface curved inwards. This was certainly attributable to the friction between sand and glass at the sides of the tank.

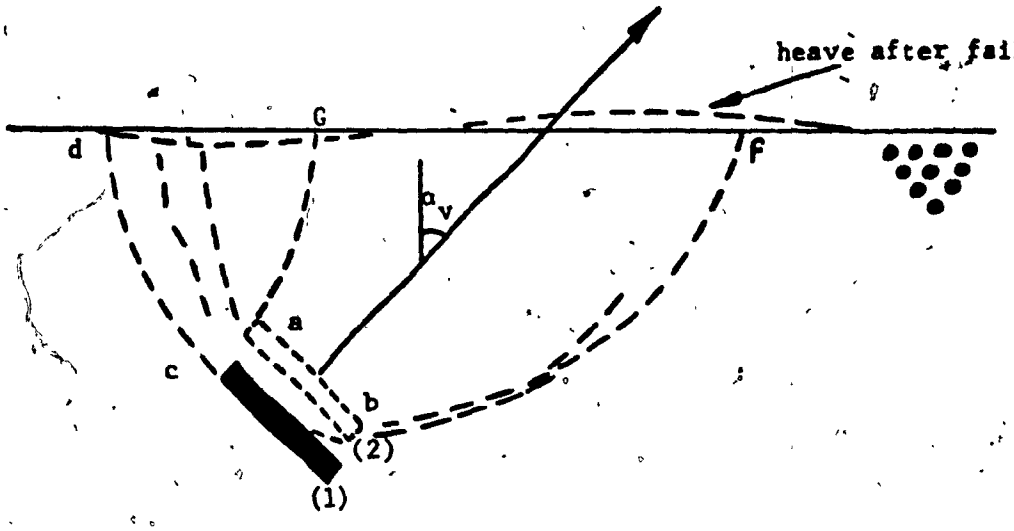

- a - $30 < \alpha_v \leq 90$ degrees

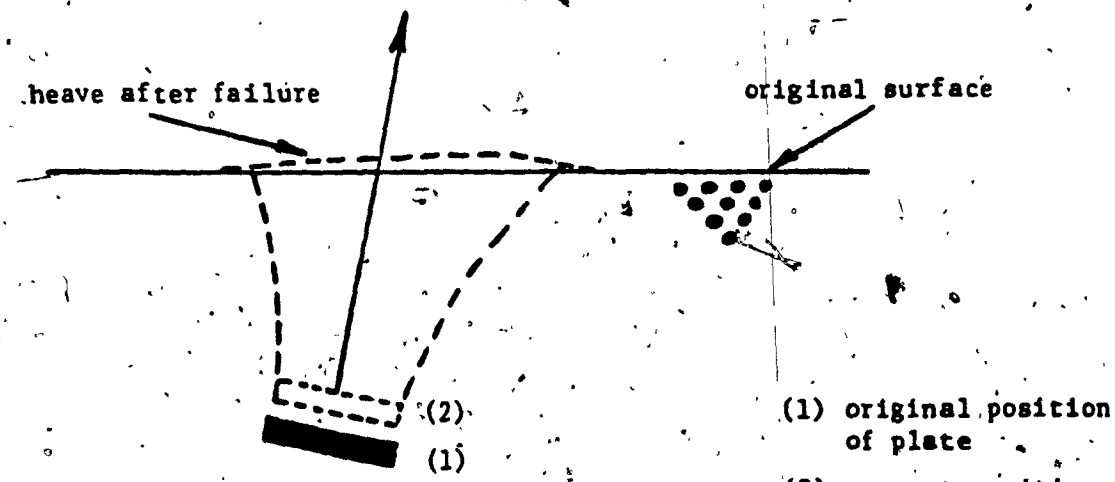

- b - $0 \leq \alpha_v < 30$ degrees

Figure 4.5: Shallow anchor plate failure mechanism

CHAPTER V

ANALYSIS OF TEST RESULTS

Test results are given in terms of a dimensionless ratio ($Q_u/\gamma BH^2$), where,

Q_u = the ultimate pullout capacity

γ = unit weight of soil

B = anchor plate width

H = anchor plate height

5.1 Effect of Anchor Embedment

Figures 5.1-a shows the anchor pullout capacity versus embedment ratio (D/H) for the three anchor plates A, B, C repsectively where (A) is a notation for anchor size 6 inch x 6 inch (width x height), (B) is a notation for anchor size 6 inch x 4 inch (width x height) and (C) is a notation for anchor size 6 inch x 2 inch (width x height). The results indicate that for a given anchor plate size at any angle of inclination from the vertical (α_v), the anchor pullout capacity increases with an increase in embedment ratio. This is possibly due to the fact that as the embedment ratio increases a larger mass of soil is involved which offers greater resistance.

5.2 Effect of Anchor Inclination

Figure 5.1-a, also shows the effect of anchor inclination with respect to the vertical (α_v) on the anchor pullout capacity, where for any constant embedment ratio

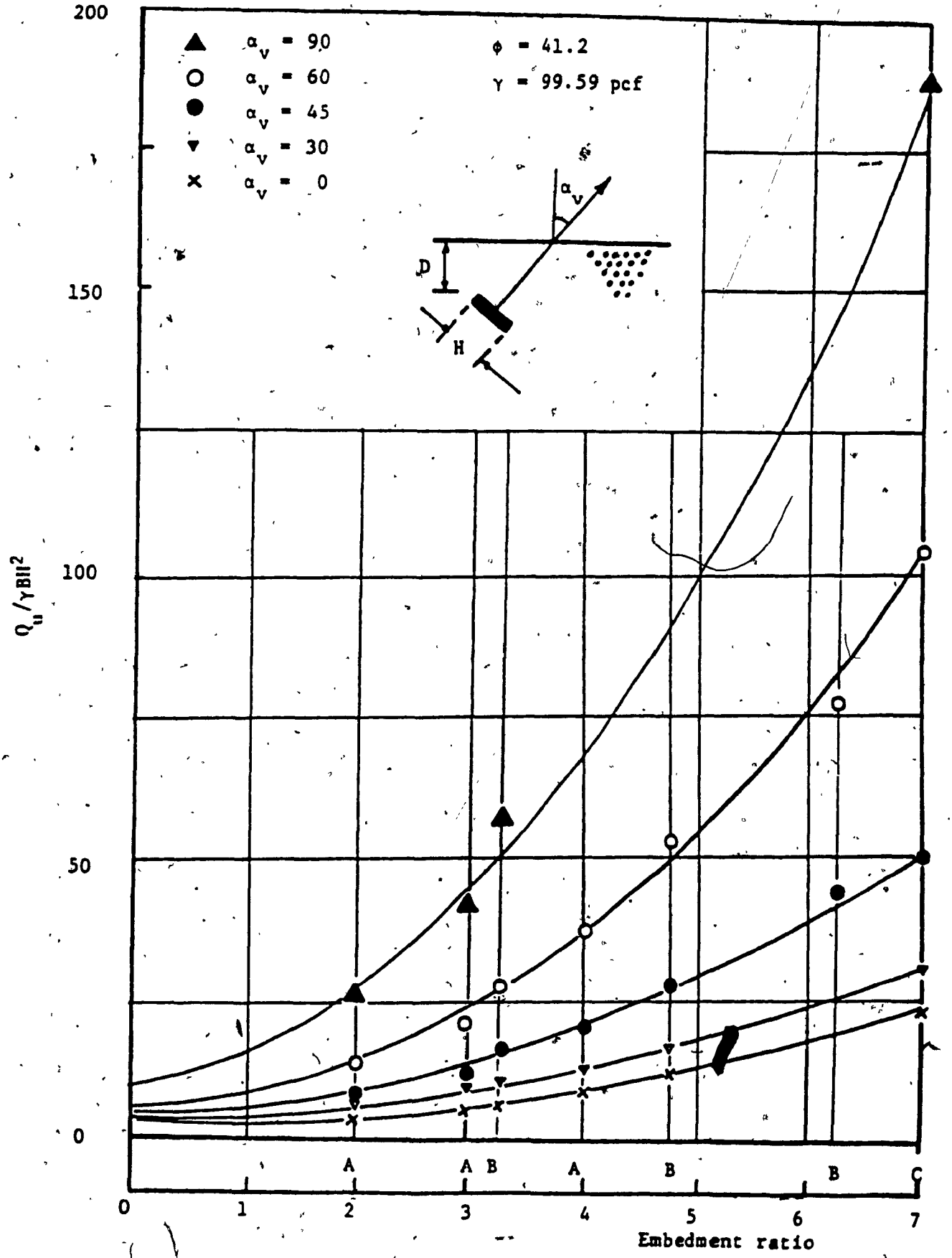

Figure 5.1-a: Summary of test results

$(D/H)_f$ the anchor pullout capacity increases with an increase in the angle of anchor inclination (α_v). The rate of increase is greater as the inclination angle becomes larger. The minimum pullout capacity is when $\alpha_v = 0$ degrees (horizontal anchor with vertical pull) and the maximum pullout capacity is when $\alpha_v = 90$ degrees (vertical anchor with horizontal pull). However, the increase in the pullout capacity is less significant when $\alpha_v \leq 30$ degrees, while it is rapid when $\alpha_v > 30$ degrees.

5.3 Effect of Anchor Size

At any constant embedment ratio, and constant angle of inclination (α_v), the ultimate pullout capacity increases with the increase in size of anchor plate, where that is obviously due to the increase of the bearing area exposed to passive pressure in front of anchor plate (see Figures 5.3-a through 5.3-c).

5.4 Failure Displacement

Figures 5.4-a through 5.4-c show a plot between displacement at failure load and the embedment ratio. It was observed that:

a. At any particular embedment ratio (D/H) and constant angle of inclination to the vertical (α_v) the failure displacement increases with the increase in the size of the anchor plate.

b. At any particular embedment ratio and particular size of anchor plate, the displacement of failure increases with the increase of

inclination (α_v).

c. For any size of plate anchor, the failure displacement increases with the increase of the embedment ratio.

d. If the failure displacement versus the embedment ratio curves are represented on a a non-dimensional basis (S_f against D/H) where (S_f) is the relative displacement expressed as a percentage of displacement at failure per height of anchor plate. For all model anchors A, B and C as shown in Figure 5.4-f , it is indicated that with the increase of the embedment ratio, the relative displacement for any plate size increases in the neighbourhood of straight line fashion, at any angle of inclination (α_v). Principally the slope of these approximate linear relationship increases as the (α_v) increase, however for $\alpha_v \leq 30$ degres the slope is more or less the same.

It has been noticed that in some tests there is a sudden and temporary sharp rise in displacement and a slight reduction in plate resistance to the pullout loading. Although the detailed cause of this phenomena is still unknown, it is assumed that this would not affect the ultimate resistance of the shallow anchors but would give relatively an artificially high failure displacement. Hence all those readings of displacements were disregarded.

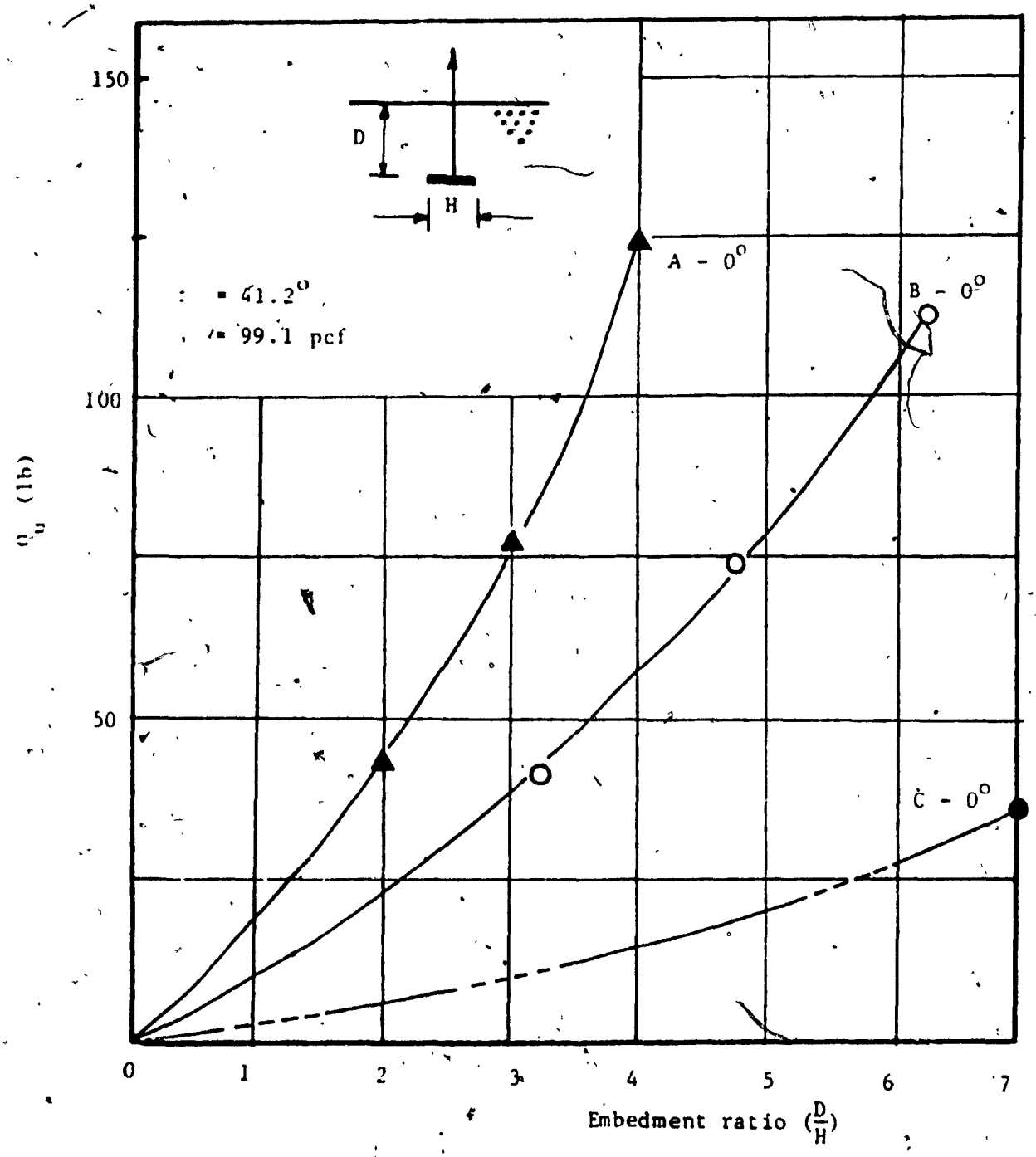

Figure 5.3-a: Anchors capacity versus embedment ratio for inclination α_v = 0 degrees

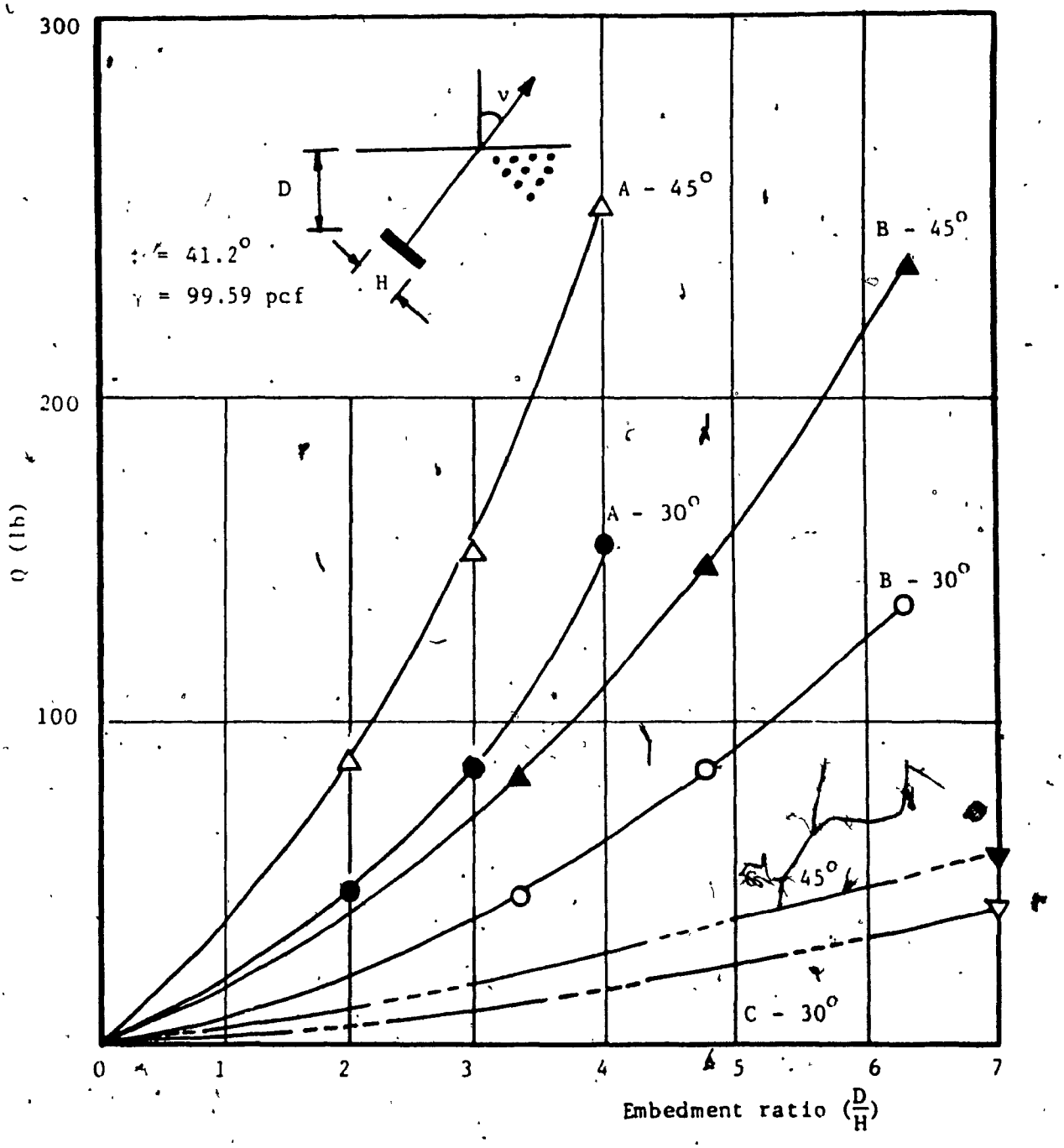

Figure 3.5-b: Anchors capacity versus embedment ratio for inclination α_v = 30, 45 degrees

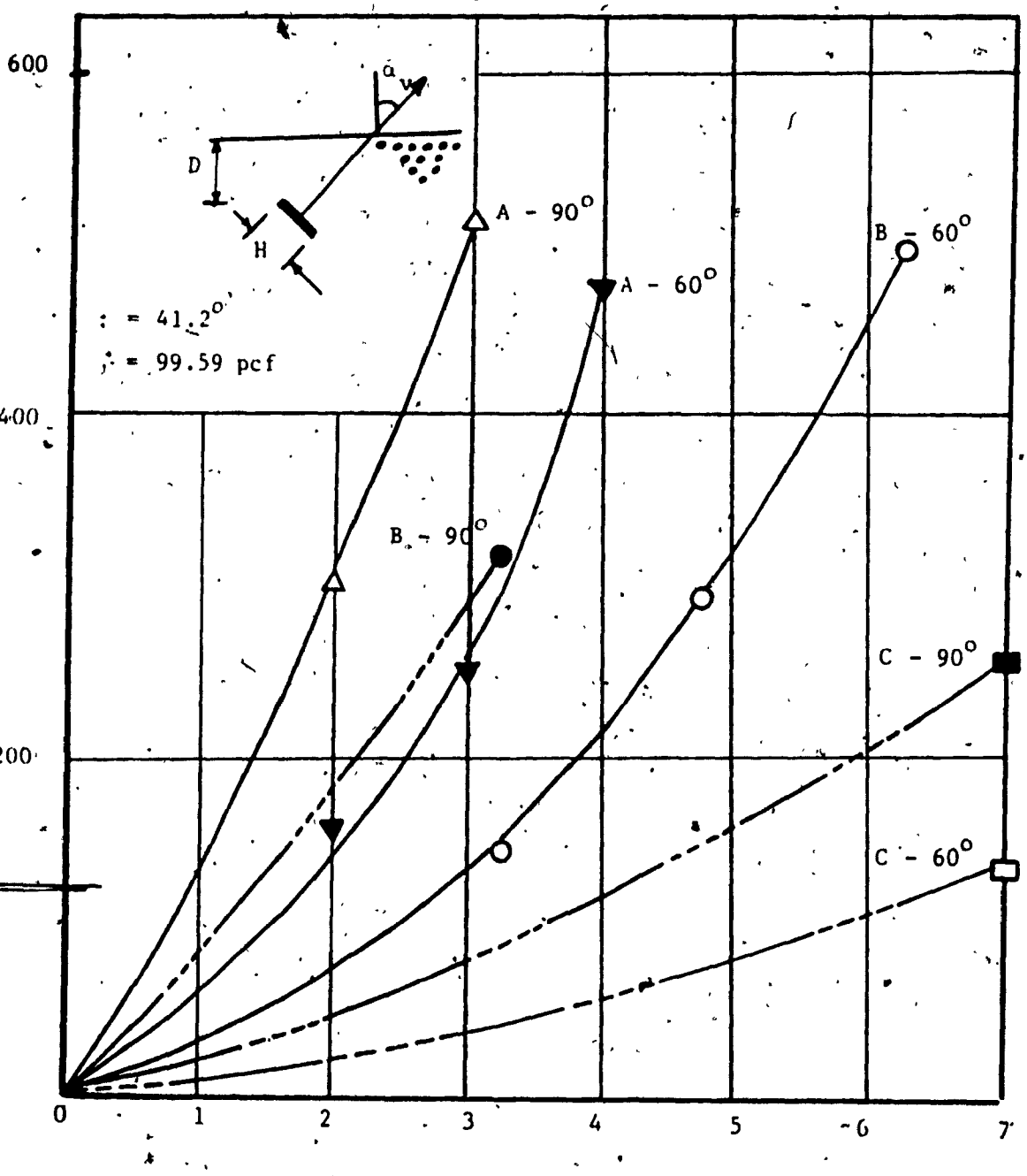

Figure 5.3-c: Anchors capacity versus embedment ratio for inclination α_v = 60, 90 degrees

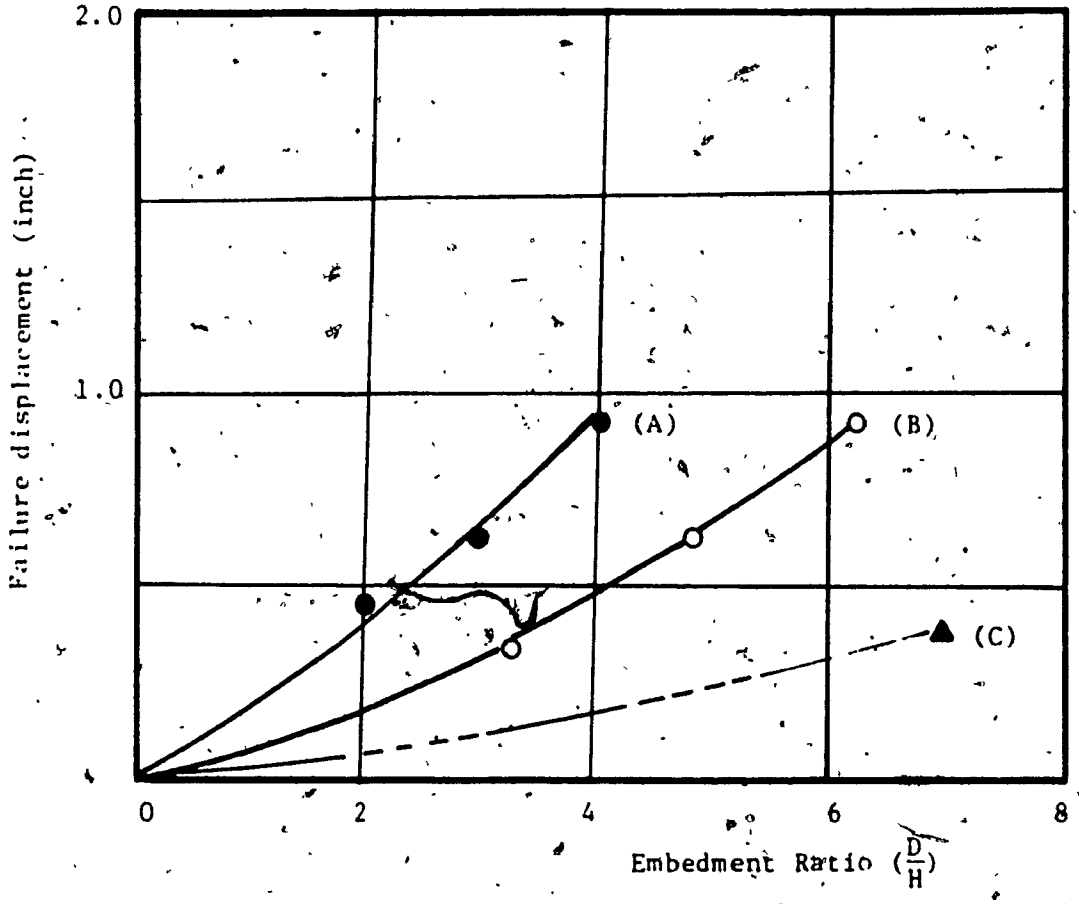

Figure 5.4-a: Failure displacement versus embedment ratio for α_v = 0 degrees

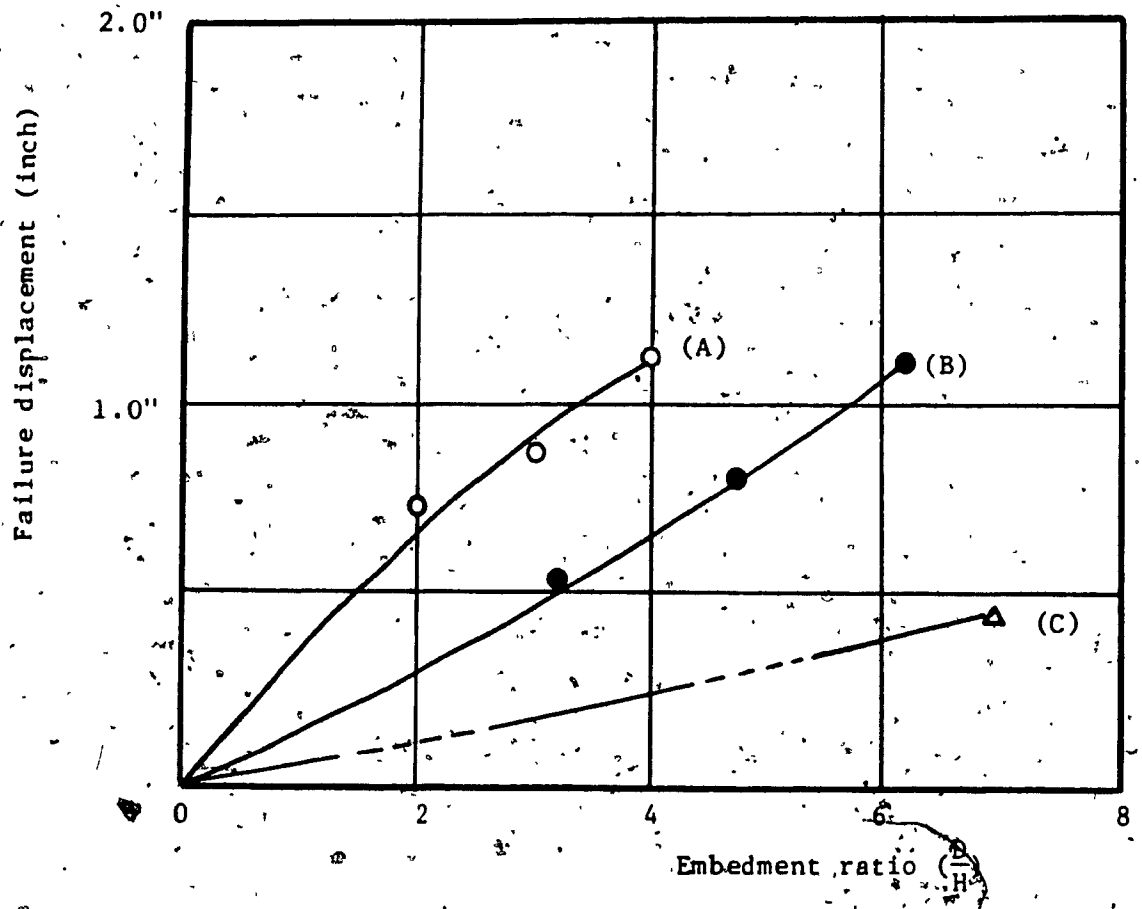

Figure 5.4-b: Failure displacement versus embedment ratio for α_v = 30 degrees

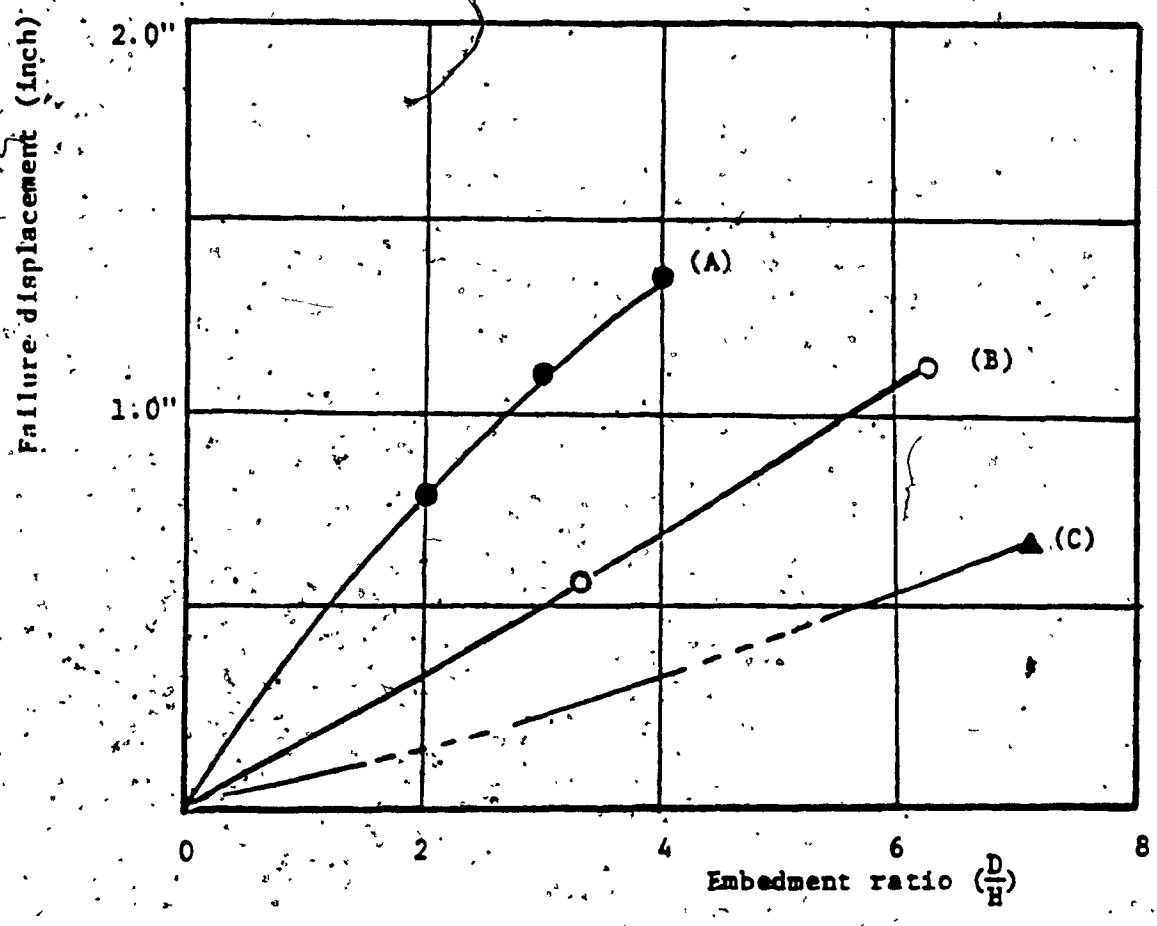

Figure 5.4-c: Failure displacement versus embedment ratio for ϕ_v = 45 degrees

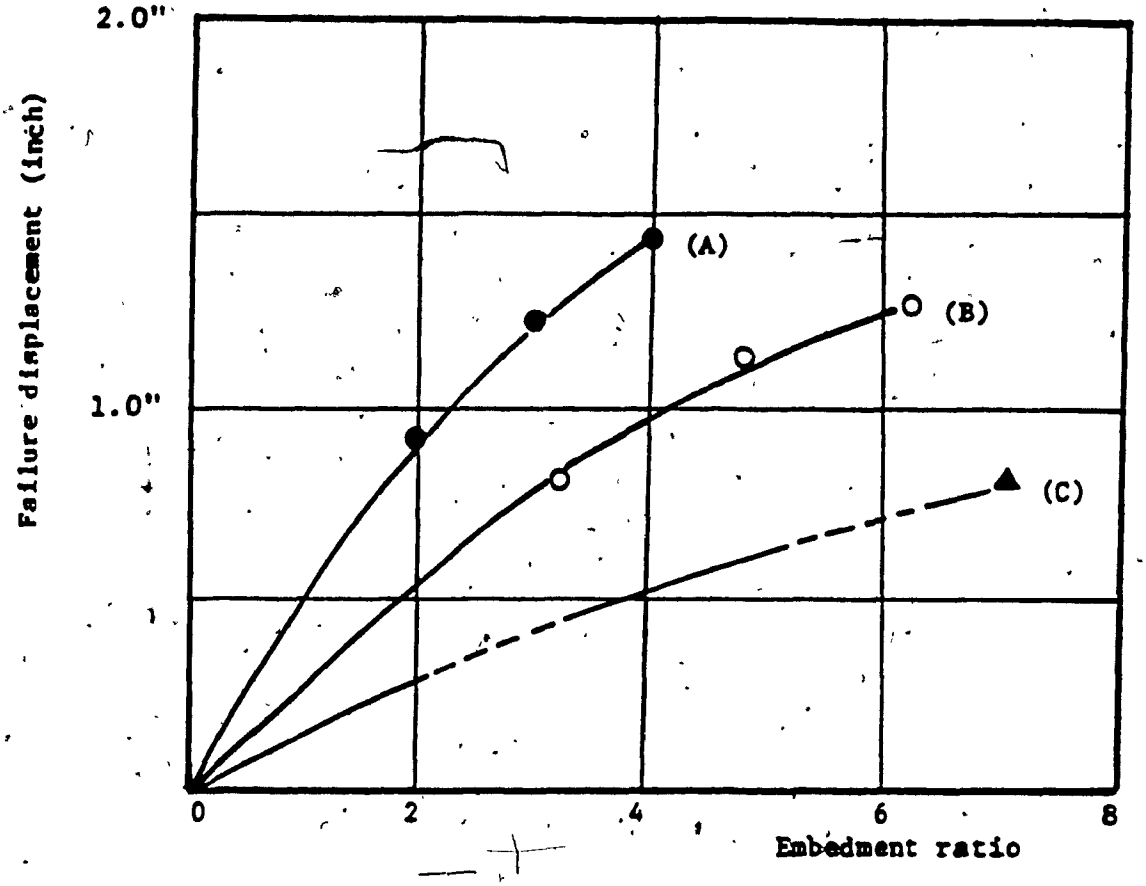

Figure 5.4-d: Failure displacement versus embedment ratio for α_v = 60 degrees

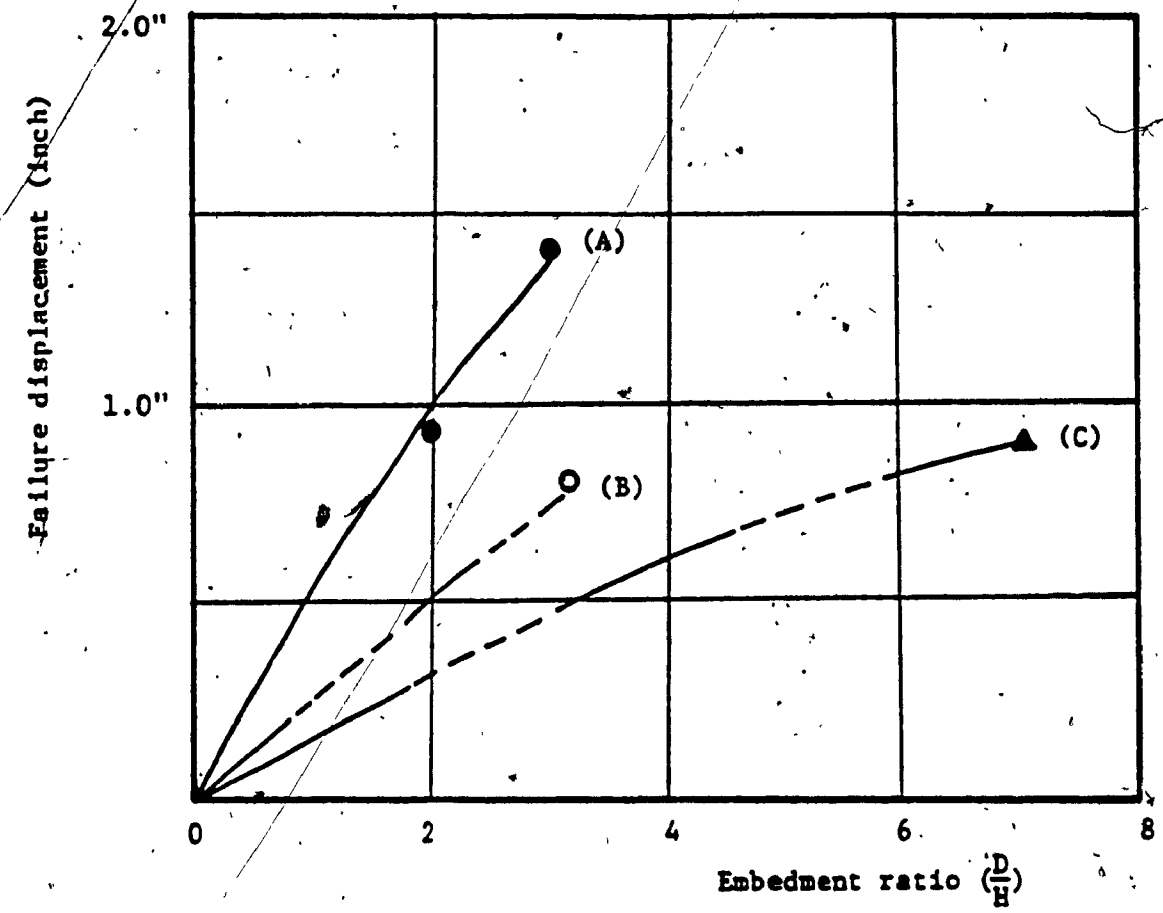

Figure 5.4-e: Failure displacement versus embedment ratio for α_v = 90 degrees

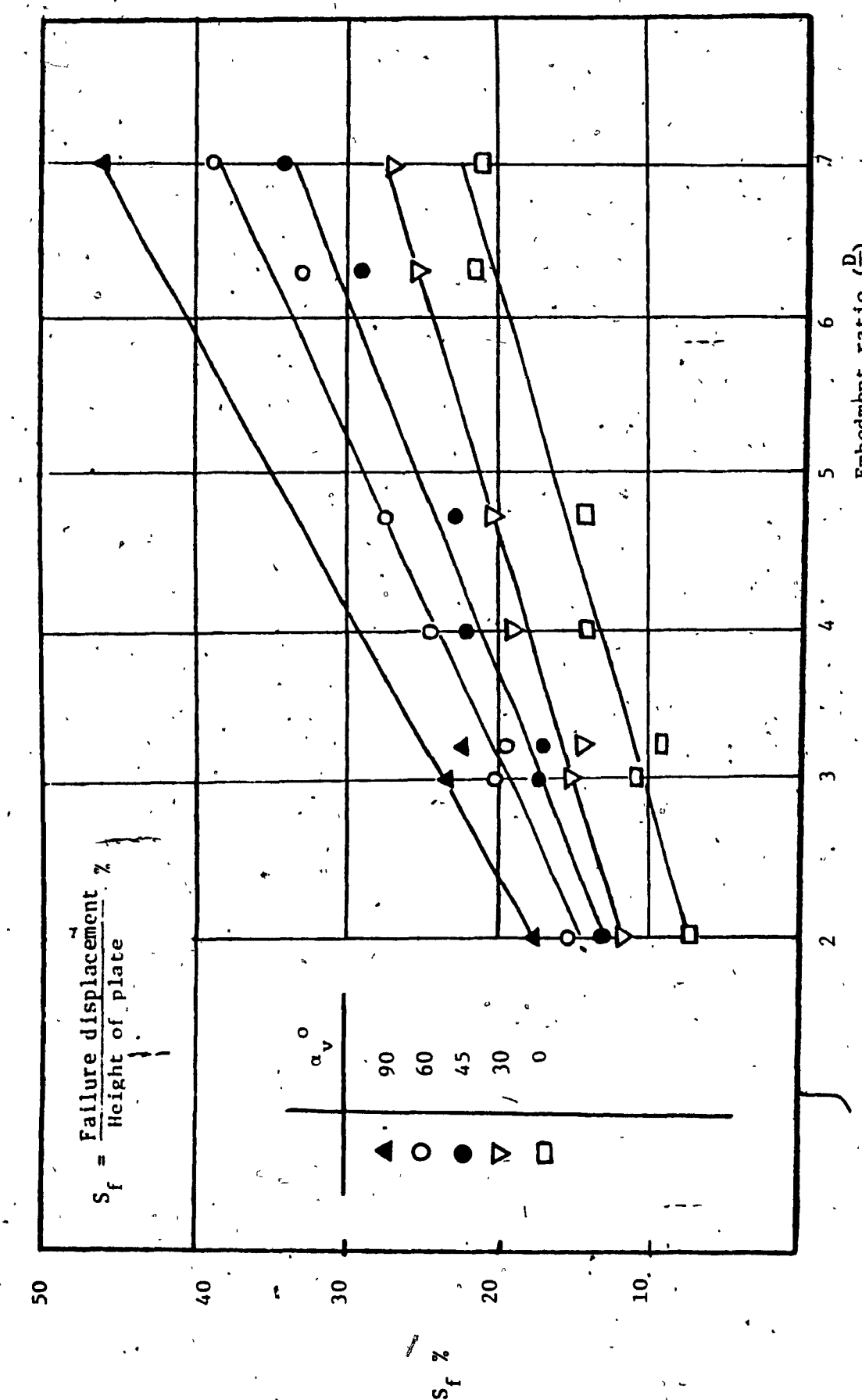

Figure 5.4-f: Variation of displacement at failure load as percentage of anchor plate height versus embedment ratio

5.5 Comparison of Test Results with the Available Theories

A. Comparison with Foriero (1985)

Foriero's theoretical investigation to predict the pullout capacity of strip anchor in sand contains two formulas, (see Chapter 2,) where the first formula of his theory is for $0 \leq \alpha_v \leq 45$ degrees, and the second formula is for $45 \leq \alpha_v \leq 90$ degrees.

The present test results agree fairly well with the first formula of the theory, where as the second formula gave very good agreement with the present test results for $\alpha_v = 60$ degrees and relatively high values for $\alpha_v = 90$ degrees (see figures 5.5-a through 5.5-g).

Accordingly, in the present investigation, it is suggested that:

once the second formula is working just for $\alpha_v = 60$ degrees according to the present test results, Figures 5.5-a to 5.5-g, and also according to the available published test results of Wang and Wu (1980), Figure 5.5-h, it is recommended to extend the first formula to be applied up to $\alpha_v = 60$ degrees instead of up to 45 degrees, because it has been found that it gives a good agreement with the present test results, as shown in Table 5.5-a, and also with Wang and Wu (1980) test results as shown in table 5.5-b. This will facilitate the application of the theory for the designers by using just one formula (the first formula) to predict the pullout capacity of strip anchor in sand for $0 \leq \alpha_v \leq 60$ degrees.

B. Comparison with Wang and Wu (1980)

As shown in Figure 5.5-i the comparison of the present test results with Wang and

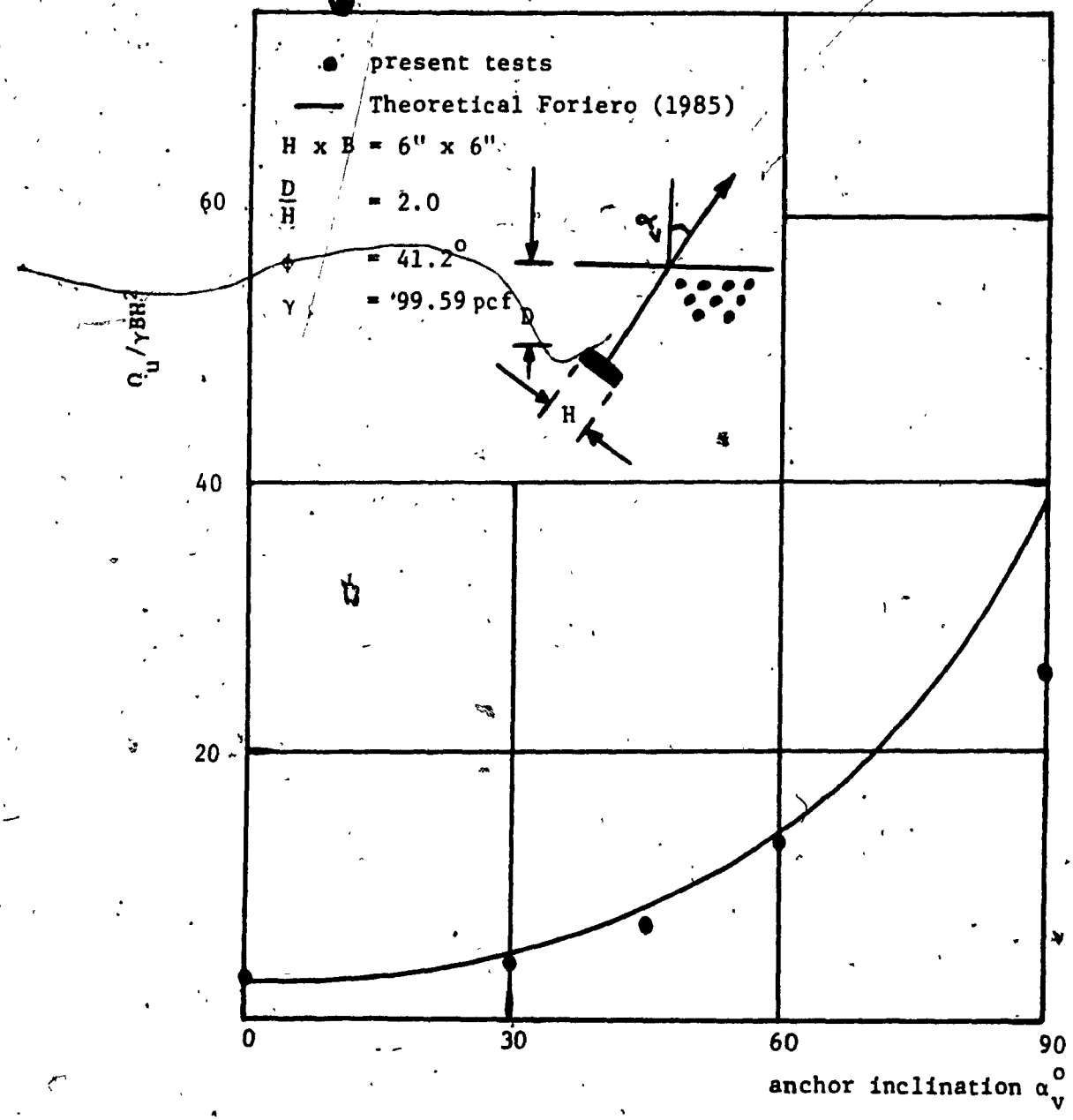

Figure 5.5-a: Comparison of present test results with Foriero Theory (1985) for embedment ratio ($\frac{D}{H}$ = 2)

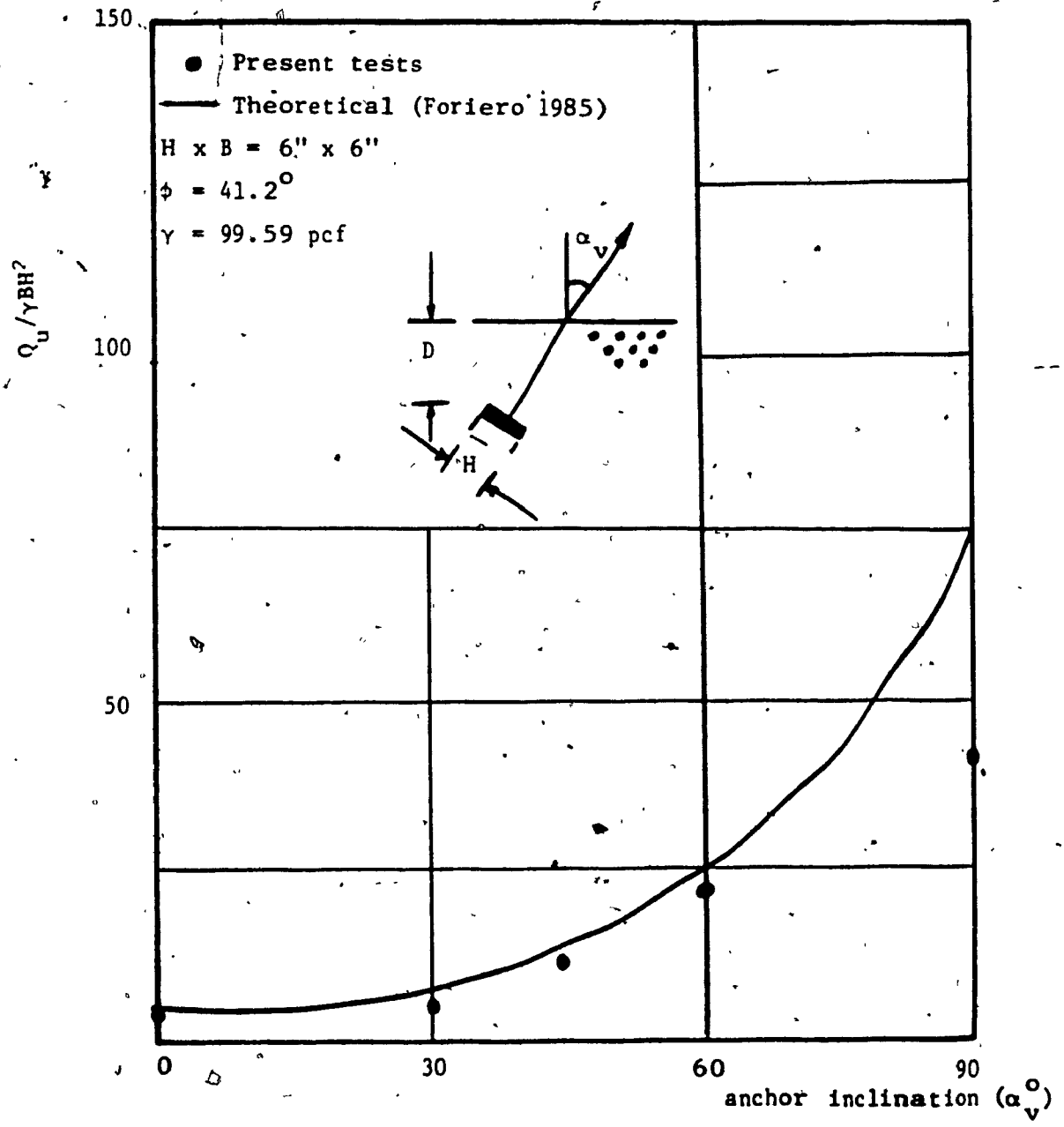

Figure 5.5-b: Comparison of present test results with Foriero Theory (1985) for embedment ratio ($\frac{D}{H}$ = 3)

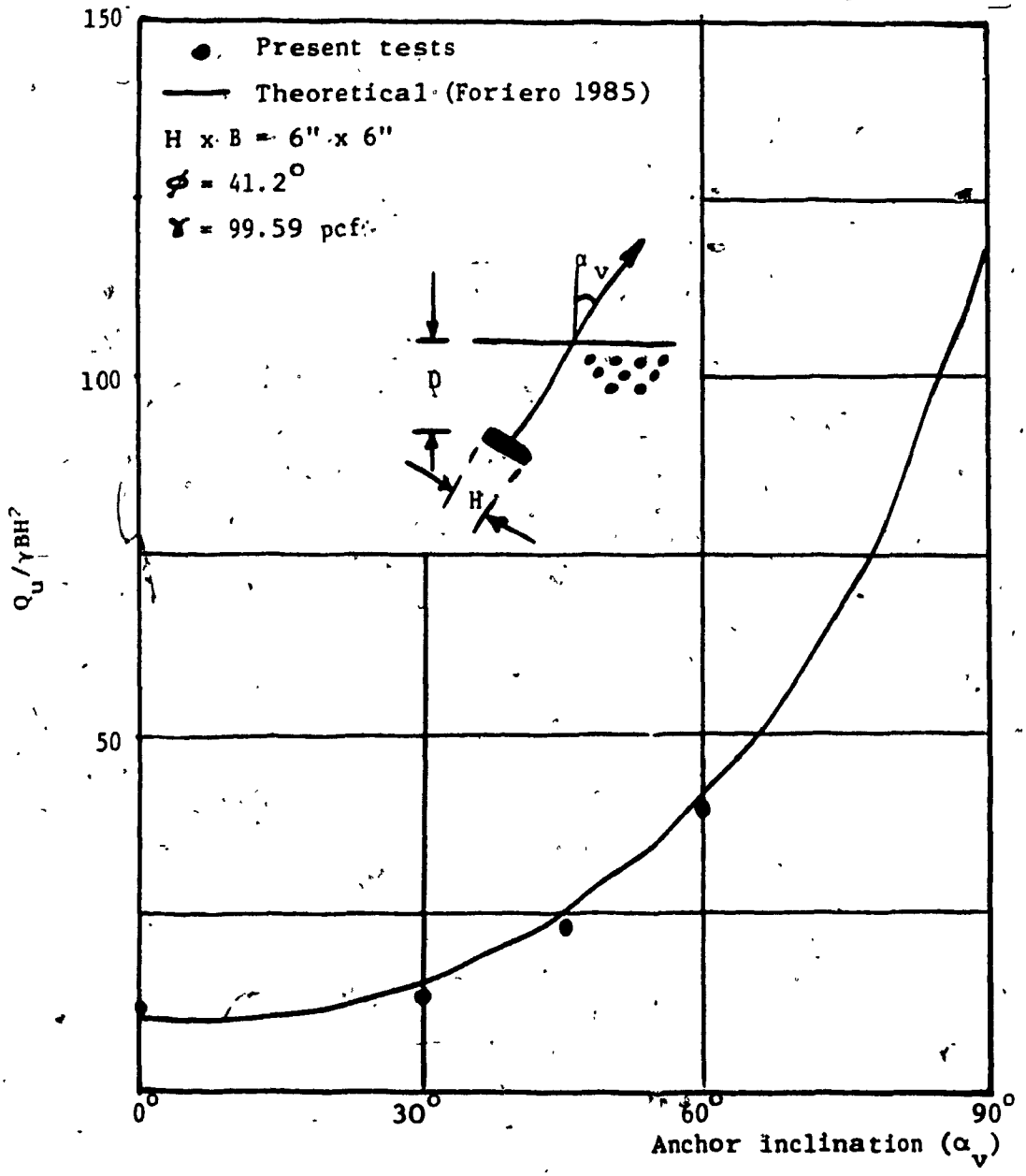

Figure 5.5-c: Comparison of present test results with Foriero Theory (1985) for embedment ratio ($\frac{D}{H}$ = 4.0)

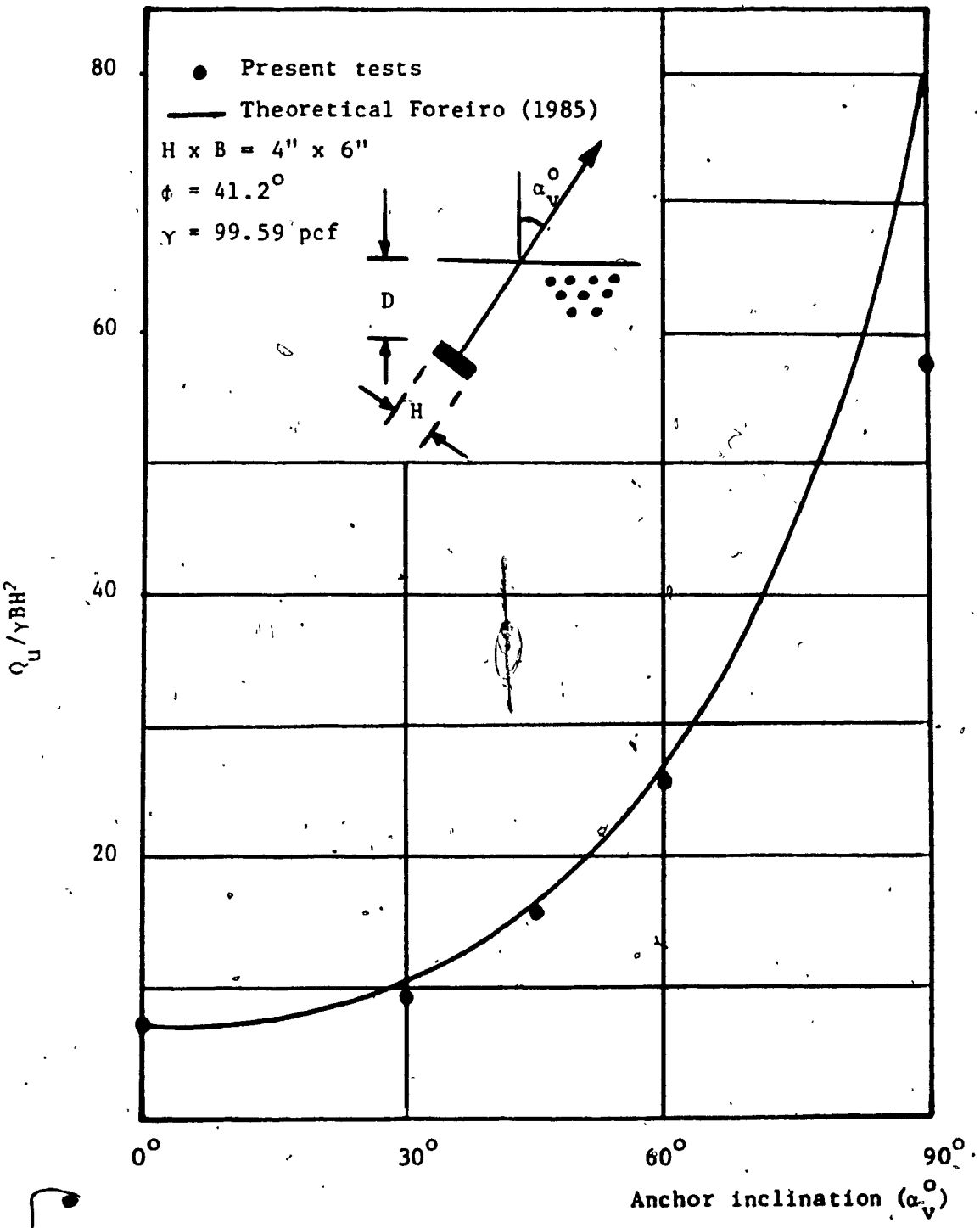

Figure 5.5-d: Comparison of the present test results with Foriero Theory for embedment ratio ($\frac{D}{H}$ = 3.25)

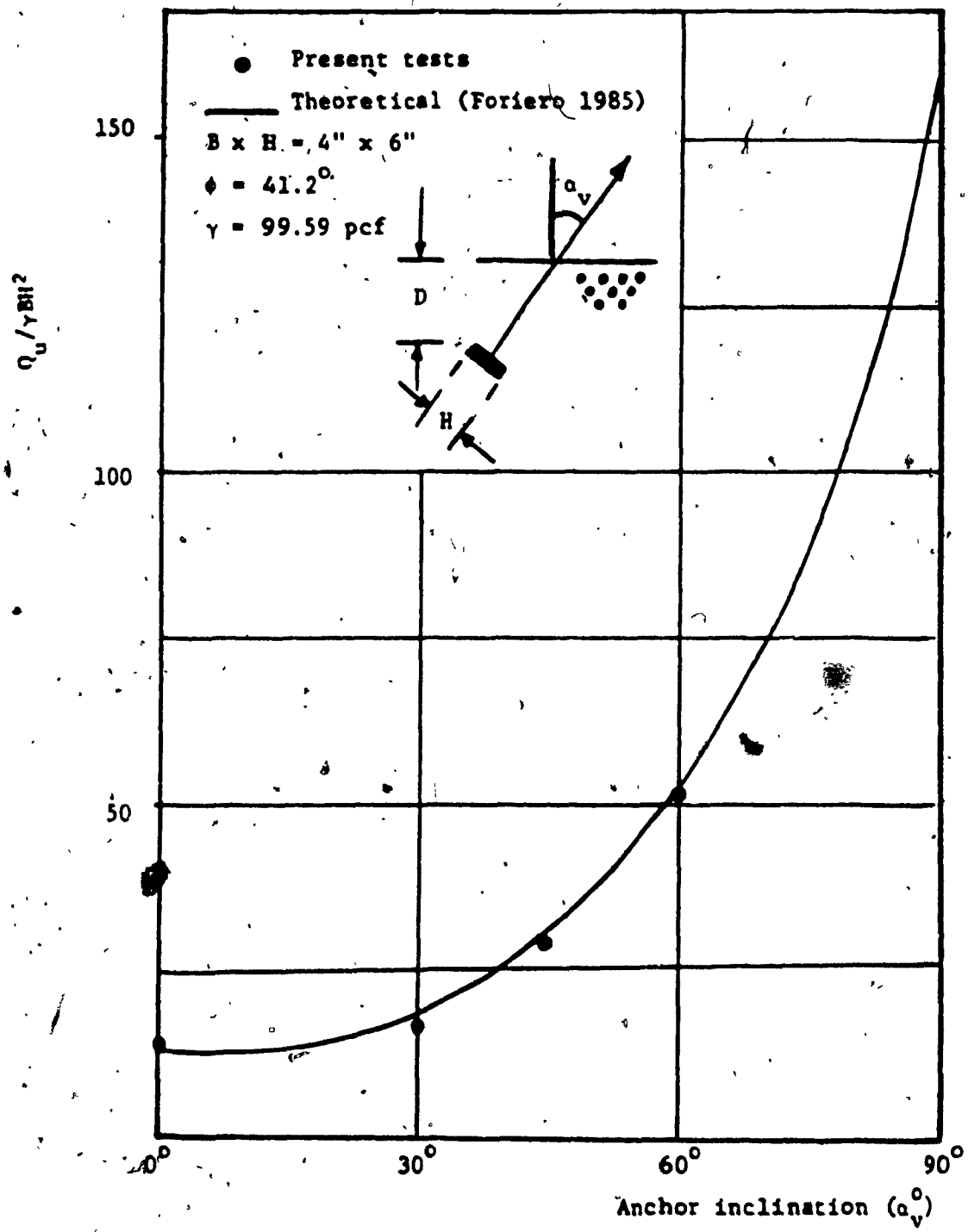

Figure 5.5-e: Comparison of the present test results with Foriero Theory for embedment ratio ($\frac{D}{H}$ = 4.75)

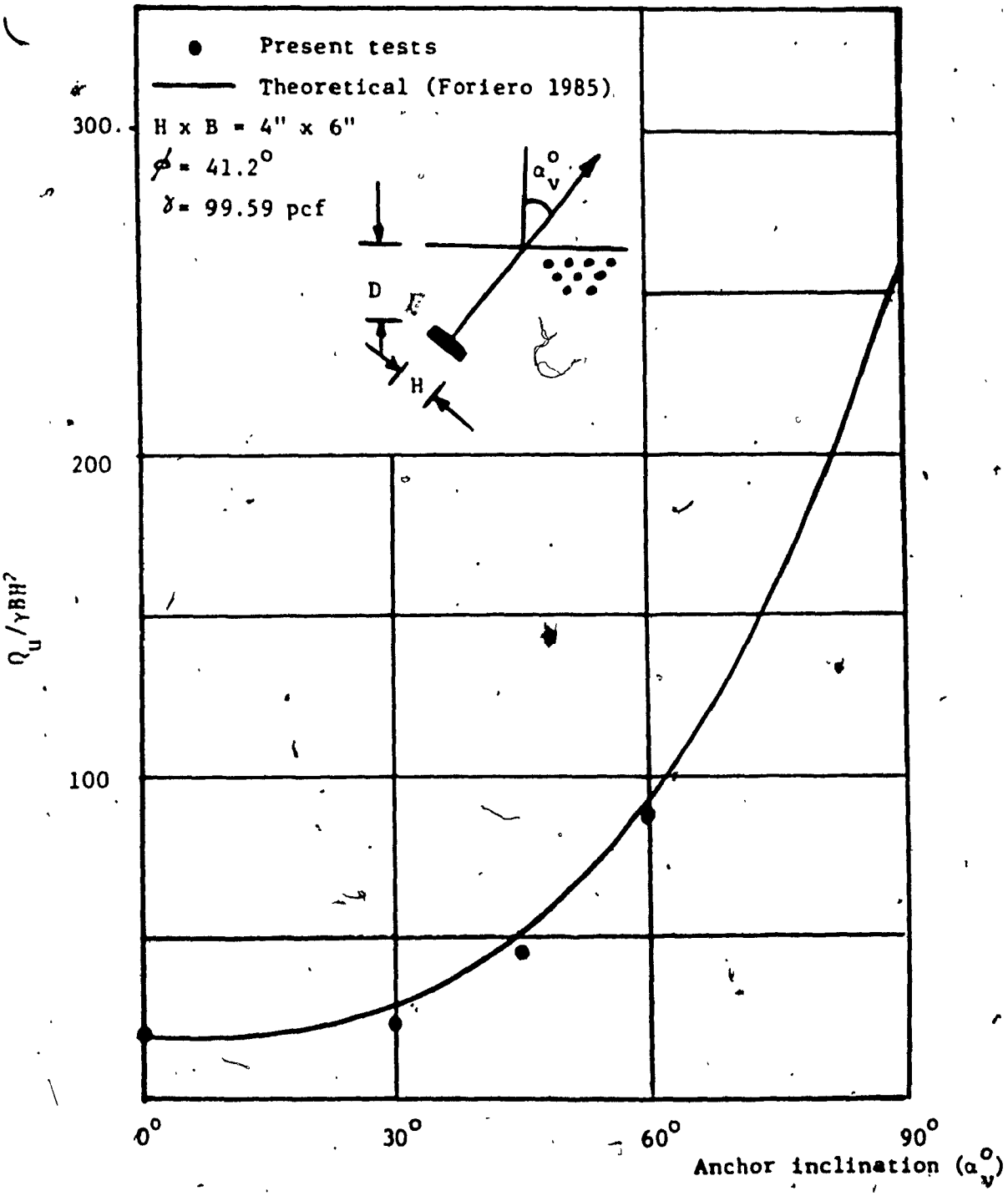

Figure 5.5-f: Comparison of the present test results with Foriero Theory for embedment ratio ($\frac{D}{H}$ = 6.25)

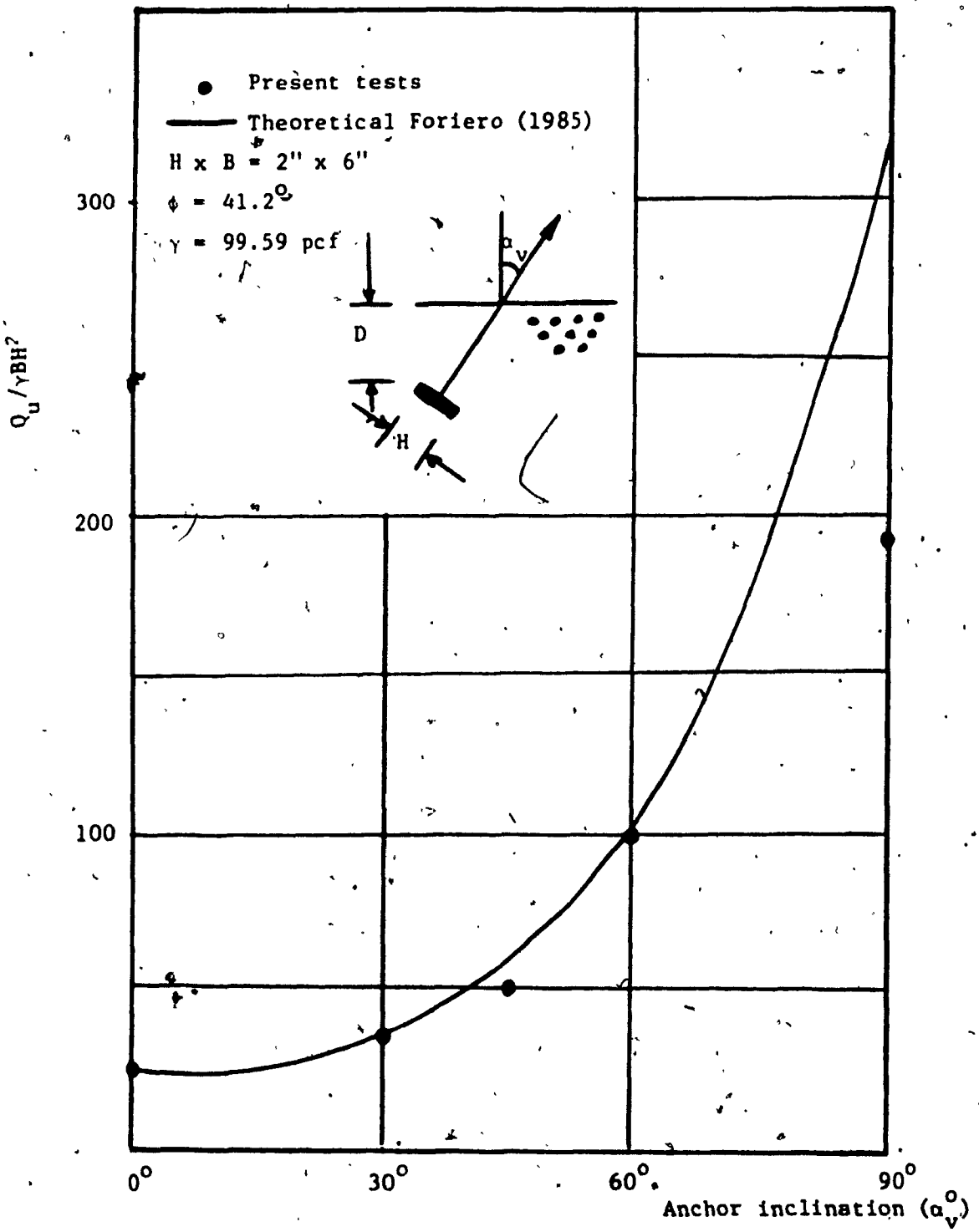

Figure 5.5-g: Comparison of the present test results with Foriero Theory 1985 for embedment ratio ($\frac{D}{H}$ = 7)

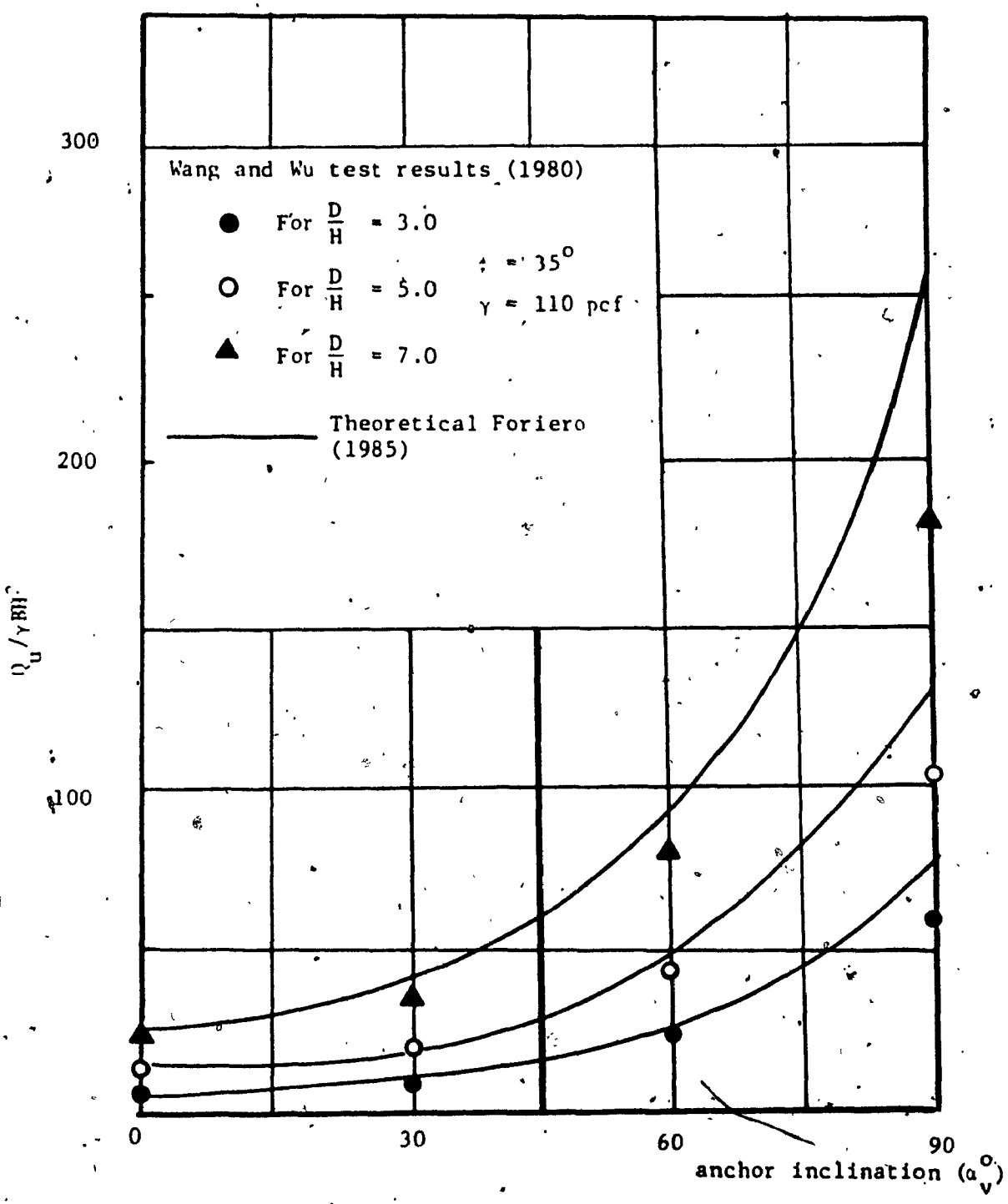

Figure 5.5-h: Comparison of Wang and Wu test results with Foriero Theory (1985)

						Q_u* (First Formula)	Q_u** (Second Formula)		
Series	Test No.	α_v Degrees	Depth D Inch	Plate Height H Inch	$\frac{D}{H}$	Experimental Q_u net lb (kg)	Theoretical Q_u* lb(kg)	Theoretical Q_u** lb(kg)	Difference in percentage between Q_u exp. and Q_u*
A	4	60	12.00	6.0	2	168.430 (76.399)	156.551 (71.011)	170.200 (77.202)	7 %
	9	"	18.00	"	3	242.736 (110.105)	295.185 (133.896)	317.050 (143.814)	
	14	"	24.00	"	4	478.890 (217.224)	478.071 (216.853)	509.720 (231.209)	0.17 %
B	18	"	13.00	4.00	3.25	157.208 (71.309)	149.600 (67.858)	160.319 (72.720)	4.8 %
	23	"	19.00	"	4.75	299.830 (136.002)	286.140 (129.793)	303.908 (137.852)	4.5 %
	27	"	25.00	"	6.25	489.907 (222.221)	454.440 (206.134)	493.541 (223.870)	7.2 %
C	31	"	14.00	2.00	7.0	149.824 (67.960)	143.744 (65.202)	151.576 (68.754)	4. %

Table 5.5-a: Calculation of the difference in the ultimate pullout capacity between the present test results and Foriero First formula (1985) for α_v = 60 degrees

$$Q_u^* = 0.5\,\gamma K_s \sin\phi\,(L_1^2 + L_2^2) + 0.5\,(L_1 + L_2)\,\gamma H \cos\alpha_v$$

(Formula 1)

α_v°	Depth D inch	Plate height H inch	(D/H)	Expermeintal Q_u lb(kg)	Theoretical Q_u^* lb (kg)	The difference in percentage between Q_{exp} and Q_u^*
60	4.5	1.5	3.0	7.00 (3.175)	6.922 (3.139)	1.1 %
60	4.5	1.5	5.0	22.50 (10.206)	24.047 (10.907)	6.8 %
60	4.5	1.5	7.0	41.25 (18.711)	44.310 (20.099)	6.9 %

Table 5.5-5: Calculation of the difference in the ultimate pullout capacity between Wang and Wu test results (1980) and Foriero First Formula (1985), for α_v = 60 degrees

Wu theory (1980) gave very good agreement for anchor inclinations with respect to the vertical of $\alpha_v = 0$ and 30 degrees.

For $\alpha_v = 45$ degrees the agreement was fair up to an embedment ratio (D/H) = 3, while for (D/H) > 3 the test result values were slightly higher than the theoretical values. However, generally the slight disparities between the present experimental results and Wang and Wu theory appears as the depth of embedment increases, and as the angle of inclination with respect to the vertical (α_v) increases. That could be due to the fact that his theory was based on testing smaller models of plate anchor and different sand of lower angle of shearing resistance (ϕ). Moreover he assumed that (ϕ) is constant, where in reality for sand that is not the case because it was very well established by many investigators that the Mohr-Coulomb relationship for cohesionless soils is non-linear i.e. for a given porosity (ϕ) varies with stress level. [DeBeer, E.E., (1963) and Ponce and Bell (1971)].

C. Comparison with Meyerhof (1973)

Figure 5.5-j shows the comparison of the present test results with Meyerhof theory of pullout capacity of inclined shallow anchors in sand [represented in dimensionless form ($Q_u/\gamma BH^2$)].

The comparison indicates that Meyerhof theory gives higher values of pullout capacity of shallow strip anchor in sand for $0 \leq \alpha_v \leq 45$ degrees, and very conservative values for $\alpha_v > 45$ degrees. This broad discrepancy could be due mainly to

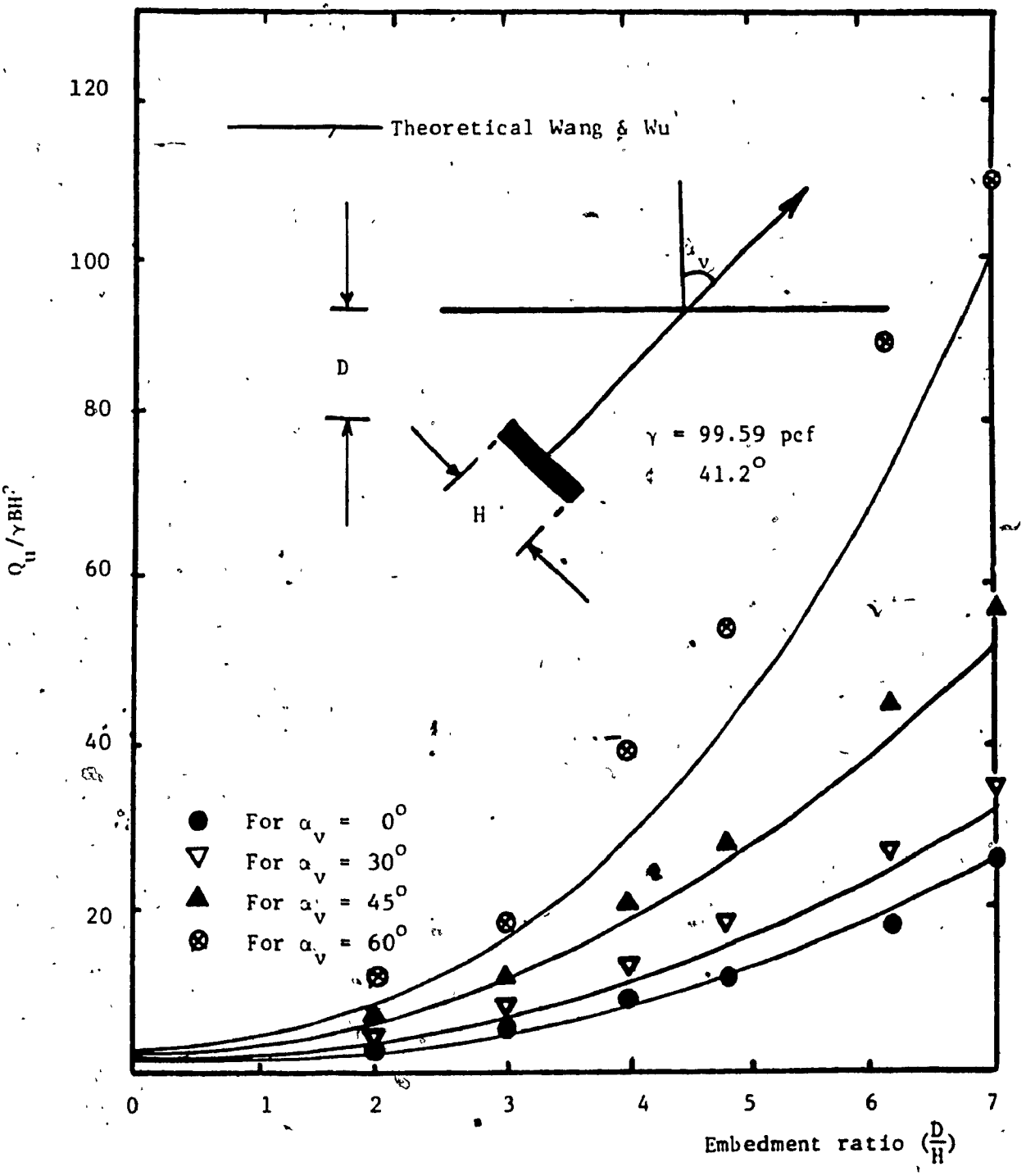

Figure 5.5-i: Comparison of present test results with Wang and Wu Theory (1980)

the following reasons:

i. The comparison is made based on Meyerhof's available data which are interpolated from published design curves that have been considerably reduced in size.

ii. His theory is based on very small anchor model of H = 1 inch. While the present experimental investigation was carried out in bigger anchor models.

iii. Generally most of the theoretical estimations of pullout capacity are conservative. This may be attributed to the fact that they are primarily based on the angle of shearing resistance. Since the envleope in Mohr-Coulomb strength of cohesionless soils is curved, the angles of mobilized shearing resistance are therefore likely to be different at different points in any individual failure zone and also different at corresponding points in the failure zones for different sized plates. This scale effect is quite important and could very much influence the comparison, however, this phenomenon is obviously more pronounced in the case of field test data.

D. Comparison of the present test results on vertical anchors with the available theories

As shown in Figure 5.5-k, the present test results for vertical anchor (α_v = 90 degrees) was compared with the theories developed by Terzaghi 1943, Ovsen 1964 Neely, Stuart and Graham 1973 and Meyerhof 1973. Nevertheless, the theory developed by Neely, Stuart and Graham, 1973 and Meyerhof, 1973 show better agreements. Therefore, interpolation between the two theories is recommended to predict the ultimate pullout capacity of continuous vertical anchors in sand.

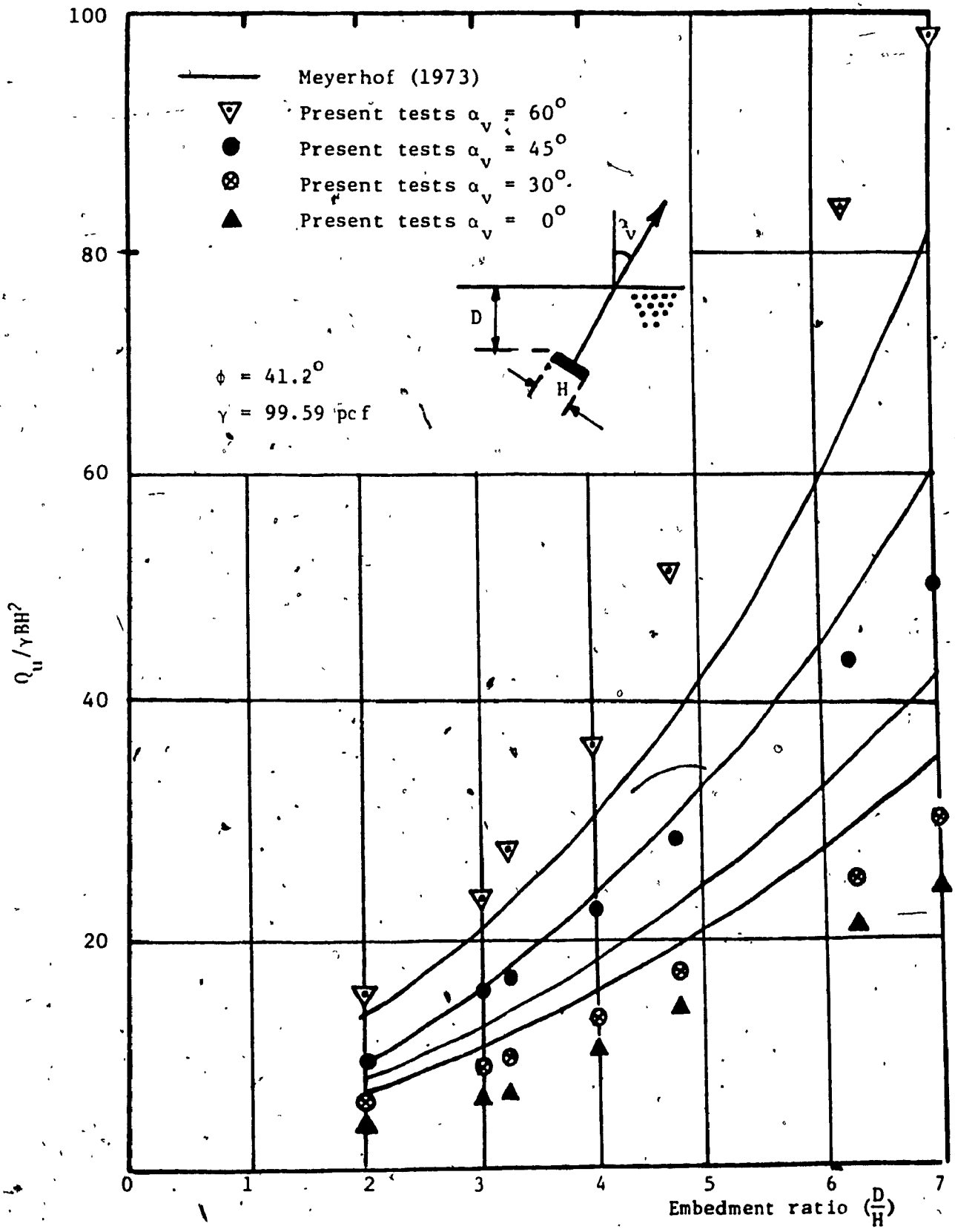

Figure 5.5-j: Comparison of present test results with Meyerhof Theory (1973)

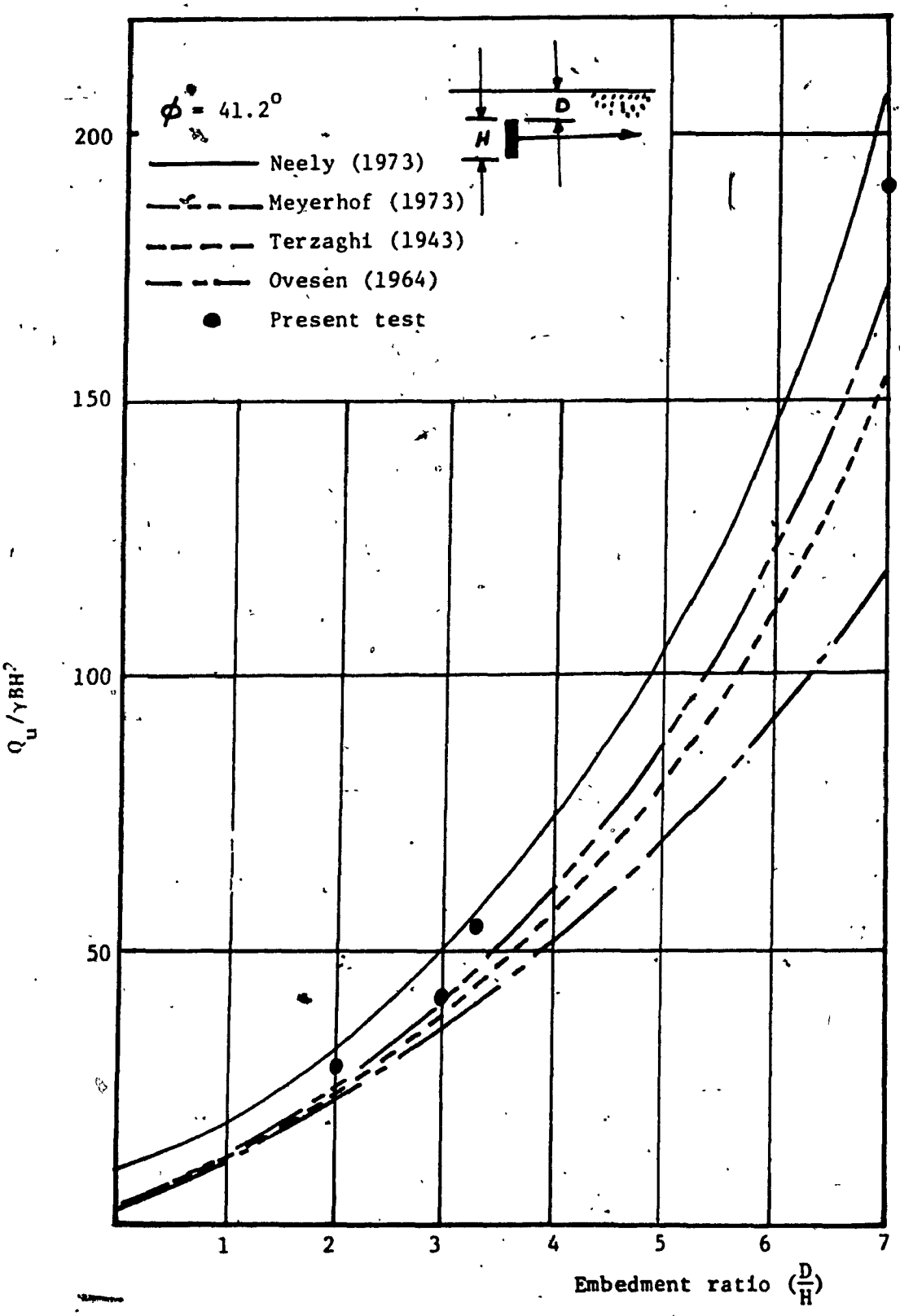

Figure 5.5-k: Comparison of present test results ($\alpha_v = 90^{o}$) with the available published theories.

CHAPTER 6

CONCLUSIONS

The behaviour of shallow strip plate anchors in sand was investigated experimentally with a great deal of reliability. Each test was carried out twice in order to check the repeatability of the experimental procedure and the degree of density control. The maximum difference between two repeat tests did not exceed 7% and average overall difference was only 3.2%. In this investigation side friction was taken into consideration.

The variables analyzed in this investigation were anchor inclination, depth of embedment, and size. The effect of each of these variables on anchor pullout capacity was carefully examined. On the basis of this research the following conclusions are drawn:

1. The study shows that the anchor failure mechanism is a progressive phenomenon. The failure surface originates from the top and bottom of the anchor plate, progressing towards the surface of the fill.
2. For a given anchor plate size at any angle of inclination from the vertical axis (α_v), the anchor pullout capacity increases with an increase in embedment ratio (D/H)
3. The anchor pullout capacity increases with an increase in the inclination (α_v), the minimum pullout capacity is when α_v = 0 degrees and the maximum pullout capacity is when α_v = 90 degrees. The rate of increase is greater as the

inclination angle becomes larger, where it is less significant when $\alpha_v \leq 30$ degrees, than when $\alpha_v > 30$ degrees.

4. The anchor capacity increases with the increase in the size of the anchor plate.
5. The displacement at failure increases with the increase in the size of the anchor plate and also with the increase in depth of embedment.
6. Based on the comparison of the present test results with the available published theories to predict the ultimate pullout capacity of strip anchor plates in sand for the range of anchor inclination at angles (α_v) vary between zero to 60 degrees, Foriero Theory, 1985 is recommended. While for anchor inclined at 90 degrees (i.e. vertical plates) interpretation between Meyerhof, 1973 theory and Neely et al theory may be used.
7. Dilation of soil, dense sand in particular, during plastic deformation tends to cause the soil in front of anchors to lock up and it is necessary for an extensive plastic region to develop before there is sufficient freedom for failure to occur (Row and Davis 1982). Hence, dilancy could increase the anchor capacity as the depth of embedment increases. Therefore, it is suggested that further research be carried out to investigate this phenomenon especially for deep anchors. Also model tests on anchor plates over a wide range of sand densities should be conducted.

REFERENCES

1. Adams, J.I. and Hayer, D.C. (1967), "The uplift capacity of shallow foundation", Ontario Hydro Research Quarterly, 19, 1.

2. Afram, A. (1984), "Pullout capacity of battered piles in sand", M. Eng. Thesis, Concordia University, Montreal, Canada.

3. Balla, A. (1961), "The resistance to breaking out of mushroom foundation for pylons", Proc. 5th International Conference on Soil Mechanics and Foundation Engineering, Paris, France, Vol. 1.

4. Buchholz, W. (1930), "Erdwiderstand auf aukerplatten", Jahrbuch Hafenbaulechnischen Gesellschaft, Vol. 12, pp. 300.

5. Bishop, A.W. (1958), "The requirements for measuring the coefficient of earth pressure at rest", Proc. Conference Earth Press., Brussels, Vol. 1.

6. Bishop, A.W. (1966), "The strength of soil as engineering materials" Geotechnique, London, England, Vol. 16, No. 2, pp. 89 - 130.

7. Casbarian, A.D.P. (1967), "Ultimate Lateral resistance of anchor plates in cohesionless soils", 3rd Pan-American Conference on Soil Mechanics and Foundations, Caracus, Venezuela, Vol II, Div. 4.

8. Chen, W.F. (1975), "Limit analyses and soil plasticity", Elsevier Scientific Publishing Company, New York, N.Y.

9. Das, B.M. (1975), "Pullout resistance of vertical anchor", Journal of Geotechnical Engineering, Div., Proc. ASCE Vol. 101, No. GT 1, pp. 87 - 91.

10. DeBeer, E.E., (1963), "The Scale affect in the transposition of the deep sounding tests on the ultimate bearing capacity of piles and caisson foundations", Geotechnique, Vol. 13, No. 1, London, England, pp. 39-75.

11. Das, B.M. and Seeley, G.R. (1977), "Ultimate resistance of deep vertical anchor in sand", Soil and Foundation, Japanese Eng. Soc. pp. 52 - 56.

12. Debeer, E.E. (1970), "Experimental determination of the shape factors and the bearing capacity of sand", Geotechnique, London, England, Vol. 20, No. 4, pp. 387 - 411.

13. Dickin, E.A. and Leung, C.F. (1979), "Discussion on horizontallay loaded vertical plate anchor in sand", Journal of Geotechnical Engr. Division, Proc. ASCE Vol. 105, No. GT 3, pp. 442 - 443.

14. Dickin, E.A. (1980), "The effect of size, shape and embedment on the ultimate resisance of vertical anchors in dense sand", Euromech. Colloquium 134; Design Against Failure in Soils, Technical University of Denmark, Copenhagen.

15. Foriero, A. (1985), "Pullout capacity of inclined strip anchor plates in sand", Master of Engineering Thesis, Concordia University, Montreal, Canada.

16. Graham, J. (1968), "Plane plastic failure in cohesionless soils", Geotechnique, London, England, Vol. 18, No. 1, pp. 301 - 316.

17. Hanna, A.M. (1978), "Bearing capacity of footings under vertical and inclined loads on layered soils", Doctor of Philosophy Thesis, Nova Scotia Technical College, Halifax, Nova Scotia, Canada.

18. Hanna, A.M., Foriero, A. and Abumengel, M. (1986), "Pullout capacity of shallow continuous anchors in sand", presented to Canadian Geotechnical Journal.

19. Hanna, T.H., (1980), "Design and construction of ground anchors", Construction Industry Research and Information Association Report 65, 2nd Edition, London.

20. Hansen, J.B., (1953), "Earth pressure calculation", Danish Tech. Press, Copenhagen, Denmark.

21. Hueckel, S. (1957), "Model tests on anchoring capacity of vertical and inclined plates", Proc. 4th International Conference on Soil Mechanics and Foundation Engineering, Canada, Vol. 2.

22. Kostyukou, V.D. (1967), "Distribution of the density of sand in the sliding wedge in front of anchor plates", Soil Mechanics and Foundation Engineering, No. 1, pp. 12 - 13.

23. James, R.G. and Bransby, P.L. (1970), "Experimental and theoretical investigation of a passive earth pressure problem", Geotechnique, London, England, Vol. 20, No. 1 pp. 17 - 37.

24. Kanayan, A.S. (1966), "Experimental investigation of the stability of bases of foundations", Soil Mechanics and Foundation Engineering, Moscow, U.S.S.R., Vol. 3, No. 6, p. 9.

25. Khosla, V.K., and Wu, T.H. (1976), "Stress-strain behavior of sand" Journal of Geotechnical Engineering Division, ASCE, Vol. 102, No. GT 4, Proc. paper 12079, pp. 303 - 321.

26. Ko, H.Y. and Scott, R.F. (1968), "Deformation of sand at failure" Journal of The Soil Mechanical and Fondation Division, ASCE, Vol. 94 , No. SM 4 Proceeding paper 6028, pp. 883 - 898.

27. Matsuo, M. (1975), "Study on the uplift resistance of footing", Soil and Foundations, Tokyo, Japan, Vol. 7, No. 4, pp. 1 - 37.

28. Meyerhof, G.G. (1951), "The ultimate bearing capacity of foundations", Geotechnique, London, England, Vol. 2, No. 4, pp. 301 - 332.

29. Meyerhof, G.G. and Adams, J.I. (1968), "The ultimate uplift capacity of foundations", Canadian Geotechnical Journal, Ottawa, Canada Vol. 5, No. 4, pp. 225 - 244.

30. Meyerhof, G.G. (1973), "Uplift resistance of inclined anchors and piles", Proceedings of the 8th International Conference on Soil Mechanics and Foundations Engineering, Moscow, Vol. 2, Part 1, pp. 669 - 686.

31. Meyerhof, G.G. (1973), "Uplift capacity of foundations under oblique loads", Canadian Geotechnical Journal, Vol. 10, No. 1, pp. 64 - 70.

32. Neely, W.J., Stuart, J.G. and Graham, J. (1973), "Failure loads of verical anchor plates in sand", Journal of Soil Mechanics and Foundations Division, Proc. ASCE, Vol. 99, No. SM 9, pp. 669 - 685.

33. Ovensen, N.K. (1964), "Anchor slabs calculation methods and model tests", Bulletin No. 16, Danish Geotechnical Institute, Copenhagen, Denmark.

34. Ponce, V.M. and Bell, J.M., (1971), "Shear strength of sand at extremely low pressures", Journal of Soil Mechanics and Foundation Division, ASCE, Vol. 97, No. SM4, pp. 625-638.

35. Tschebotarioff, G.P. (1962), "Retaining structures", Chapter 5, Foundation Engineering, edited by Leonards, G.A., McGraw-Hill, New York, pp. 438 - 524.

36. Wang, M.C. and Wu, A.H., (1980), "Yielding load of anchor in sand", paper presented to ASCE annual meeting, Geotechnical Engineering Division, Miami, Florida.